

Cardioprotective potential of miR-92a inhibition in large animal models

von Katharina Nadin Klett

Inaugural-Dissertation zur Erlangung der Doktorwürde
der Tierärztlichen Fakultät der Ludwig-Maximilians-Universität München

Cardioprotective potential of miR-92a inhibition in large animal
models

von Katharina Nadin Klett

aus Tübingen

München 2019

Aus dem Veterinärwissenschaftlichen Department der Tierärztlichen
Fakultät der Ludwig-Maximilians-Universität München

Lehrstuhl für Molekulare Tierzucht und Biotechnologie

Arbeit angefertigt unter der Leitung von

Univ.-Prof. Dr. Eckhard Wolf

Angefertigt im Klinikum rechts der Isar
der Technischen Universität München

Mentor: Prof. Dr. med. Christian Kupatt

Gedruckt mit der Genehmigung der Tierärztlichen Fakultät
der Ludwig-Maximilians-Universität München

Dekan: Univ.-Prof. Dr. Reinhard K. Straubinger, Ph.D.

Berichterstatter: Univ.-Prof. Dr. Eckhard Wolf

Korreferent: Prof. Dr. Marlon Schneider

Tag der Promotion: 25. Februar 2019

Meiner Familie in Liebe und Dankbarkeit

TABLE OF CONTENTS

I.	INTRODUCTION	1
II.	REVIEW OF LITERATURE	3
1.	Coronary artery disease	3
1.1.	Diabetes mellitus as a major risk factor for coronary artery disease.....	4
1.2.	Animal models for diabetes research	6
2.	Entities of coronary artery disease	8
2.1.	Hibernating myocardium.....	8
2.1.1.	Induction of hibernation in large animals for research matters.....	10
2.2.	Myocardial infarction	11
2.2.1.	Induction of myocardial infarction in large animals for research matters.	12
3.	Therapeutic options for CAD	13
3.1.	Gene therapeutic angiogenesis	13
4.	Micro RNAs	15
4.1.	The miR- 17~92 cluster.....	16
4.2.	Strategies of miRNA modulation in vivo.....	17
5.	Modes of therapeutic agent application	19
6.	Aim of this study	20
III.	MATERIAL AND METHODS	21
1.	Material	21
1.1.	Drugs	21
1.2.	Medical consumables	22
1.3.	Medical devices	22
1.4.	Lab devices.....	23
1.5.	Chemicals and reagents	23
1.6.	Cell culture consumables.....	24
1.7.	Software.....	25
2.	Methods	26
2.1.	In vitro experiments.....	26
2.1.1.	Migration assay	26

2.1.2.	Ring formation assay	27
2.2.	In vivo experiments	27
2.2.1.	Legal background	27
2.2.2.	Laboratory animals	27
2.2.3.	Preparation of animals for the interventions	28
2.2.4.	Anesthesia and preliminary for catheterization	28
2.2.5.	Functional assessment	29
2.2.6.	Setup of the ischemia/reperfusion model	29
2.2.7.	Setup of the stent implantation trial	30
2.2.7.1.	Day 0	30
2.2.7.2.	Day 28	30
2.2.7.3.	Day 56	31
2.2.7.4.	Peri- and post-operative anticoagulation regime	31
2.2.8.	Heart function measurements	33
2.2.8.1.	Invasive blood pressure measurement	33
2.2.8.2.	Global left ventricular heart function measurements	34
2.2.8.3.	Sonomicrometry for regional heart function	35
2.2.8.4.	Staining for infarction size determination	36
2.2.8.5.	Post mortem angiography and capillary filling	36
2.3.	Histology	37
2.3.1.	PECAM-1/NG2 staining	37
2.3.2.	HE Staining	38
2.3.3.	Sirius Red for fibrosis detection	39
2.3.4.	Apoptosis stain	40
2.4.	Statistics.....	40
IV.	RESULTS.....	41
1.	Cell culture data	41
1.1.	Migration assay	41
1.2.	Ring formation assay	43
2.	Data from the 24h model	45
2.1.	Post mortem assessment of infarct size	45
2.2.	Microscopic assessment of capillary network	47
2.3.	Assessment of apoptosis.....	49

2.4.	HE staining for inflammation	51
2.5.	Global heart function	52
3.	Data from the stent model	54
3.1.	Blood glucose levels.....	54
3.2.	Microscopic assessment of capillary network.....	55
3.3.	Collateral and Rentrop classification.....	57
3.4.	Assessment of apoptosis.....	59
3.5.	Sirius red stainings for fibrosis.....	61
3.6.	Global heart function data	63
3.7.	Regional heart function	66
V.	DISCUSSION	67
1.	Ameliorating hallmarks of myocardial ischemia	67
1.1.	Mechanism of induced capillarization via miR-92a inhibition	67
1.2.	Positive effect on fibrosis development	69
1.3.	Reduction of apoptosis	69
1.4.	Stabilization of cytoskeleton	70
1.5.	Improving myocardial performance	71
2.	Clinical relevance of miRNA for cardiac issues and beyond.....	72
2.1.	Comparison of miR-92a inhibition to other therapeutic approaches.....	73
2.2.	Longtime effect of miR-92a inhibition.....	75
3.	Limitations of present study	76
4.	Conclusion and outlook.....	78
VI.	SUMMARY.....	79
VII.	ZUSAMMENFASSUNG	81
VIII.	INDEX OF TABLES AND FIGURES	83
1.	Index of tables	83
2.	Index of figures	83
IX.	REFERENCES	85
X.	ACKNOWLEDGEMENT	105

INDEX OF ABBREVIATIONS

A.	Arteria	ERK	extracellular signal- regulated kinase
AAV	adeno-associated virus	et al.	et alii
AF	Alexa Fluor	F	French (catheter scale; 1F=1/3mm)
AGE	advanced glycation end product	g	gram
Ang	angiopoietin	G	Gauge
ANOVA	analysis of variance	h	hour
atm	standard atmosphere	H ₂ O dest	distilled water
ATP	adenosine triphosphate	HAES	hydroxyethyl starch
bEnd.3	brain-derived endothelial cells.3	HDL	high-density lipoprotein
bpm	beats per minute	hpf	high power field
bw	bodyweight	I/R	ischemia/reperfusion
CAD	coronary artery disease	ICAM-1	intercellular adhesion molecule -1
CD	cluster of differentiation	INS	insulin
con	control	IU	international units
CVD	cardiovascular disease	iv	intravenous
DAPI	4',6-diamidino-2- phenylindole	KCl	potassium chloride
d	day	kg	kilogram
db	diabetic	KLF2	Krüppel-like factor 2
DM	Diabetes mellitus	KLF4	Krüppel-like factor 4
DMEM	Dulbecco's modified Eagle's medium	LAD	left anterior descending artery
DNA	deoxyribonucleic acid	LDL	low density lipoprotein
e.g.	exempli gratia	LMU	Ludwig- Maximilian University of Munich
EC	endothelial cells	LNA	locked nucleic acid
ECG	electrocardiography	lncRNA	long non-coding ribonucleic acid
EF	ejection fraction	LV	left ventricle
eNOS	endothelial nitric oxide synthase		
ER	endoplasmic reticulum		

LVEDP	left ventricular end diastolic pressure	PTCA	percutaneous transluminal coronary angioplasty
MAPK	mitogen-activated protein kinase	PV	pressure-volume
mg	milligram	RAGE	receptor for advanced glycation endproducts
MI	myocardial infarction	RCX	Ramus circumflexus
miR	micro ribonucleic acid	resp.	respectively
miRNA	micro ribonucleic acid	RISC	ribonucleic acid-induced silencing complex
MKK4	mitogen-activated kinase 4	RNA	ribonucleic acid
ml	milliliter	ROS	reactive oxygen species
mmHg	millimeters of mercury	scr	scrambled
mPTP	mitochondrial permeability transition pore	SEM	standard error of the mean
mRNA	messenger ribonucleic acid	SERCA 2	sarco/endoplasmic reticulum Ca ²⁺ -ATPase
NaCl	sodium chloride	SES	subendocardial segment
NF-κB	nuclear factor kappa-light-chain–enhancer of activated B cells	shortening	
NG2	neuron- glial antigen 2	siRNA	small interfering ribonucleic acid
P/S	penicillin/streptomycin	Sirt-1	sirtuin-1
p	probability value	SOCS 5	suppressor of cytokine signaling 5
PAK4	p21 activated kinase 4	SSR	synchronized suction and retroinfusion
PBS	phosphate buffered saline	T1DM	type 1 Diabetes mellitus
PCI	percutaneous coronary intervention	T2DM	type 2 Diabetes mellitus
PECAM-1	platelet endothelial cell adhesion molecule 1	TIE-2	tyrosin kinase
PET	positron emission tomography	TNF-α	tumor necrosis factor
pH	power of hydrogen	tRNA	transfer ribonucleic acid
PNDM	permanent neonatal Diabetes mellitus	TUM	Technical University of Munich
PTFE	polytetrafluoroethylene	TUNEL	Terminal desoxynucleotidyl transferase dUTP nick end labeling

UK	United Kingdom
USA	United States of America
V.	Vena
VEGF	vascular endothelial growth factor
vWf	von Willebrand factor
w/v	weight per volume
WHO	World Health Organization
wt	wildtype

I. INTRODUCTION

Cardiovascular diseases (CVD) are number one cause of death and disabilities worldwide with almost “pandemic” extent [1]. CVD are accountable for 31 % of global deaths [2]. Numbers of premature deaths worldwide will even further grow in the future. This fact is indebted by changing societal demography like an ageing society and tremendous prevalence of diabetes mellitus. Despite cardiovascular therapy has made enormous progress, the risk of developing cardiovascular disease as well as impaired outcome after cardiovascular events is enhanced in patients presenting with risk factors for CVD. Frequently, current therapeutic strategies like catheter angioplasty are not sufficient in those patients due to impaired coronary and capillary overall status. Limitations of existing therapy in a vast and growing patient population have fueled research for alternative therapeutic strategies. Advanced understanding of the human genome and the continuous discovery of target genes have prompted gene therapeutic attempts for the fight against heart failure. Particularly, microRNA (miRNA) provide new therapeutic possibilities because of their regulatory functions in the development of CVD on a molecular basis. Few microRNAs have entered the preclinical and clinical stage since they are promising candidates for therapeutic approaches. Findings from prior studies have uncovered the role of miR-92a in angiogenesis. Overexpression of miR- 92a was demonstrated to hamper vessel formation in vitro, whereas therapeutic approaches to inhibit miR-92a in vivo had beneficial effects on the heart. Aim of this preclinical study was to analyze the potential of miR-92a inhibition via locked nucleic acid (LNA) in a wildtype (wt) and transgenic diabetic swine model of chronic ischemia (hibernating myocardium). In addition, this study focuses on the effect of the LNA application in an acute ischemia/reperfusion model in transgenic diabetic pigs.

II. REVIEW OF LITERATURE

1. Coronary artery disease

CVD encompass vascular disorders of the brain (cerebrovascular), heart and blood vessels (coronary artery diseases (CAD), rheumatic heart disease and congenital heart disease), peripheral artery disease and deep vein thrombosis. The majority of deaths (4 out of 5) caused by CVDs are due to heart attacks and strokes [3]. Within the group of CVDs, CAD are the most common event. CAD describes a progressive chronic disease reflecting the manifestation of atherosclerosis. In the onset of CAD, plaques, lining coronary vessels, lead to hemodynamic stenosis and thereby shortage of blood supply to the cardiac muscle. Atheromatous plaques consist of mainly macrophages or debris of calcium, lipids and cholesterol [4]. Particularly, rapid growth of plaques is hazardous because they may become vulnerable and rupture causing sudden thromboembolic events. With the formation of debris, the elastic inside lining of coronaries becomes atherosclerotic and begins to harden and stiffen. If the vessel lumen is narrowed by 50 – 70 %, the arteries' elastic dilative capacity shrinks. In case of narrowing by 80 – 90 %, blood supply to the tissue is restricted at rest [5]. This malnutrition of myocardial tissue evokes reduction of heart function [6] and, when prolonged, sustained tissue damages and even everlasting tissue necrosis [7]. The term CAD refers to several entities of different origin, localization and duration:

- myocardial infarction
- angina pectoris (stable/ unstable)
- cardiac arrhythmias
- sudden heart death.

Risk factors contribute to the buildup of deposits narrowing the vessels throughout the body. The individual risk to come down with CAD increases with behavioral patterns that narrow vessels and coronaries such as tobacco smoking, physical inactivity, fatty diet, obesity and alcohol abuse. Men are generally at greater risk than women [8]. After menopause, risk of CAD increases in women with the drop of estrogen.

1.1. **Diabetes mellitus as a major risk factor for coronary artery disease**

Diabetes mellitus is one of the 5 major Framingham factors for developing CAD. To date an estimate of 425 million of diagnosed patients globally renders diabetes mellitus (DM) one of the most common widespread diseases [9]. According to the WHO's global report on diabetes, the global burden of diabetes has almost doubled from 4.7 % to 8.5 % in the world's adult population since 1980 [10]. The forecast trend is believed to further drastically increase until 2030 [11].

DM describes a metabolic disorder resulting from inadequate insulin secretion or insulin action characterized by chronic hyperglycemia and impaired carbohydrate, fat and protein metabolism. Symptoms of DM may present as polyuria and subsequent thirst, visual impairment and loss of weight. In its severe phases, ketoacidosis may cause stupor and coma. Long-term effects of DM can result in retinopathy and blindness, nephropathy and renal failure, risk of ulcers and amputation.

Due to its heterogenic pathogenesis, there are different types of DM: Type 1 DM (T1DM) results from an autoimmune destruction of the insulin-producing β -cells in the pancreas mediated by the expansion of CD4+ and CD8+ T- helper cells and the activation of autoantibody-producing cells [12]. T1DM is an autoimmune and auto inflammatory disease [13]. T1DM can occur at any age, but since it is more often diagnosed in children and young adults, it was traditionally termed as "juvenile diabetes" due to its early onset [14]. A variety of explanatory theories for the cause of T1DM have been put forward: genetic causes, environmental influence and drug effects. More than 50 genes seem to play a role in the development of T1DM [15], the locus IDDM1 in the MHC Class II, however, has shown to be the strongest mediator. Environmental factors as triggers such as dietary agents (gluten) [16], gut microbiota [17] and viral infections [18] are discussed.

As a disorder of multifactorial origin, DM type 2 (T2DM) encompasses impaired insulin secretion, its resistance and failing in insulin processing. In case of insulin resistance - which renders cells unable to take in glucose- pancreatic β -cells increase insulin output to maintain normal blood glucose levels [19]. Insulin resistance and the insulin overproduction influence each other in a vicious cycle [20]. The causes for developing T2DM are mainly western lifestyle and genetic

factors. Obesity [21], sedentary lifestyle, fatty diet, smoking [22], stress, aging and insomnia [23] are jeopardizing drivers for developing diabetes. More than 30 genes contributing to the development of T2DM are described [24]. Rare forms of diabetes arise from monogenic abnormalities of single genes: maturity onset diabetes of the young (MODY) among others [25]. While T1DM is only diagnosed in 5 % [26] of the patient population, mainly young patients, T2DM makes up the vast majority of all diabetes diagnoses.

Gestational diabetes is a disorder in which a woman develops diabetes during pregnancy arising from insulin resistance. Although, its precise pathologic mechanism is yet unknown, pregnancy hormones might contribute. Risk factors for developing gestational diabetes are maternal obesity and age at pregnancy [27], ethnicity [28] and polycystic ovary syndrome [29] and family burden for DM per se. After delivery, maternal gestational diabetes resolves in most cases; however, mothers, who developed gestational diabetes once, possess a higher likelihood of recurrence in further pregnancies and of developing T2DM. Offspring from pregnancies with gestational diabetes are at higher risk of developing congenital heart diseases, T2DM and CVD in later life [30].

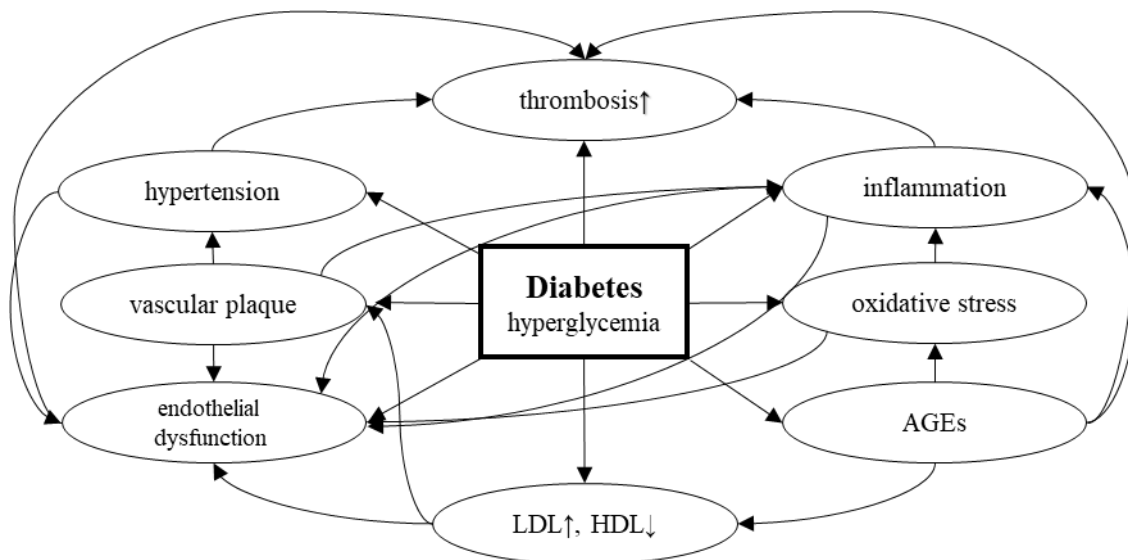


Figure 1: Vicious circle of DM

Mechanisms by which DM facilitates and enhanced the progression of CAD and vessel narrowing and damage

DM is a major risk factor for stroke, cardiovascular disease, heart failure, peripheral artery disease and atrial fibrillation. The metabolic abnormalities in DM (e.g. insulin resistance, hyperglycemia) force a vicious circle of pathophysiologic

vascular changes impairing endothelial function. Thereby, mechanisms are so intertwined that one aspect might not be pivotal alone:

Oxidative stress (reactive oxygen species = ROS), inflammation and platelet aggregation are fostered by hyperglycemia. In DM, inflammation is driven by pro-inflammatory cytokines as tumor necrosis factor TNF- α or interleukin-6 activating the nuclear factor NF- κ B by upregulation of adhesion molecules [31]. This leads to an increased binding of platelets and leukocytes enhancing thrombogenesis. Increased leukocyte migration promotes inflammation and plaque instability. Advanced glycation end products (AGEs) arise from sugars non-enzymatically glycosylated to proteins due to high glucose levels. Their contribution to the progression of vessel damage is paramount. The mechanisms of AGEs comprise inflammation by binding to RAGE receptors driving inflammation via NF- κ B and other signals. Oxidative stress and increased glycation of low-density lipoproteins and of the platelet derived growth factor (PDGF) activate the proliferation of monocytes and macrophages [32]. Dyslipidemia goes along with DM since glucose and fat play a role in energy metabolism.

Atherosclerosis arises from high levels of LDL cholesterol which accumulate in fat-laden macrophages (foam cells) thereby promoting thrombosis, inflammatory cytokines and apoptosis. The pro-angiogenic potential of HDL (high density lipoproteins) is lost in DM due to structural changes [33].

The production of reactive oxygen species (ROS), mainly as a byproduct of cellular energy metabolism is altered, in DM due to mitochondrial dysfunction. ROS are implicated in cellular pathways such as cell proliferation, apoptosis and mitogen-activated protein kinase (MAPK) signaling [34]. Serving as signaling molecules, ROS influence vasodilatation and vessel constriction as well as their permeability [35]. Their harmful effect lies in membrane damage and oxygenation of proteins. Due to their high reactivity, ROS can damage DNA, RNA and lipids.

1.2. Animal models for diabetes research

Being a global health burden renders Diabetes in the focus of ongoing research. For the sake of understanding and clarifying pathology and development of DM, animal models are indispensable. The induction of animal models is mainly based on either impaired insulin production and lack of insulin (T1DM) or insulin resistance

(T2DM). A convenient model should combine two features: simple implementation of DM induction and a realistic mimicry of the disease, its pathways and complications in the human setup. Currently, a broad range of models and different species is available [36].

Chemically diabetes can be induced through streptozotocin (STZ) application in rodent or large animal models [37]. It causes specific pancreatic β -cell necrosis and thereby induces an insulin dependent DM and combines alterations in carbohydrate and amino acid metabolism [38]. STZ administration is a cheap method to initiate DM but is hampered by variable outcomes. Many factors like gender, strain or circadian rhythm influence STZ sensitivity [39]. Symptoms of STZ induced DM are mild to severe depending on the dose and the application interval.

The Coxsackie B virus has been described to induce β -cell destruction in non-human primates [40]. Viral application is complicated since those viruses can cause either autoimmunity or its prevention, depending on the condition [41].

In pigs, pancreatectomy leads to constant DM and hyperglycemia [42]. Yet, it is a highly invasive approach which requires a skilled surgeon. Livelong supplementation of exocrine pancreas enzymes is obligatory in animals undergoing pancreatectomy. Blood insulin was shown to disappear already 30 min after total pancreatectomy, whereas blood glucose levels were demonstrated to massively increase which might lead to ketoacidosis [43].

Thanks to genetic engineering, it is possible to design animal models which mimic the characteristics of diabetes in the human patient. With the Akita mouse, there is a non-obese rodent model of permanent neonatal diabetes mellitus (PNDM) and consistent hyperglycemia [44]. A point mutation in the insulin gene 2 (*Ins2*) causes misfolded proinsulin production. Thus, its progressing is impaired which leads to insulin accumulation in the endoplasmic reticulum (ER) and thereby ER stress [45]. Diabetes in Akita mice is taken after that of human MODY with regard to the pancreatic β -cell loss and the early onset of the disease [46]. Hyperglycemia in Akita mice and MODY patients arises secondary from hypoinsulinemia. Even though Akita mice are non-obese and have low circulating lipid levels, they develop insulin resistance. Akita mice show a clinically manifest DM 3 to 4 weeks post-partum signed by hyperglycemia and hypoinsulinemia. However, rodent models hold little translationality.

Renner et al. designed a swine model of PNDM carrying the mutated porcine insulin gene INS^{C94Y} [47], [48]. This mutation is mimicking the INS^{C96Y} mutation in humans and the Akita mouse. INS^{C94Y} transgenic pigs show elevated blood glucose levels compared to wildtype from birth on. Blood insulin concentration is significantly decreased in INS^{C94Y} transgenic pigs at an age of 4.5 month. The alterations in blood insulin are due to the reported loss of β -cell mass in the pancreas. Secondary changes are an abnormal body growth (41 % lower compared to wildtype littermates) and reduction of organ weights (except kidneys). Furthermore, cataract development starts from day 8 and affects the whole lens at 4.5 month as a result of high blood glucose. The cardiac phenotype of INS^{C94Y} transgenic pigs was described by Hinkel et al. in 2017 [49]: porcine diabetic hearts present with capillary rarefaction accompanied by increased fibrosis even without ischemic challenge. Those alterations go along with a deterioration in heart function. Core measures for heart performance such as ejection fraction (EF), an important value for cardiac volume output, and left ventricular end diastolic pressure (LVEDP), a prognostic marker for the progression of left sided heart failure, were altered in these animals indicating an impaired cardiac performance. Similar patterns of vessel degeneration were seen in specimens procured from hearts of diabetic end-stage heart failure patients. Regarding the similarities in human DM patients and the INS^{C94Y} transgenic pig, this model is a suitable tool for cardiovascular research because it mimics realistically cardiac changes in diabetes and allows for pre-clinical testing of novel therapeutic approaches.

2. Entities of coronary artery disease

2.1. Hibernating myocardium

In zoology, hibernation deriving from the Latin *hibernus* (*wintry*), defines a phase of lowered metabolism and inactivity in endotherms enabling the organism to stay vital in times of poor energy availability.

In cardiology, the term hibernation as proposed by Diamond [50] and later demonstrated by Rahimtoola, describes a condition of impaired cardiac function at rest because of reduced blood flow and nutrition supply [51]. PET studies revealed that acontractile hibernating myocardium is still alive even though its arterial perfusion is poor [52]. Prerequisite for developing myocardial hibernation is resting

blood supply to the tissue. Pig trials unveiled that the myocardium tolerates a reduction of blood flow (sub endocardial: 0.17 ml/min/g and transmural: 0.25 ml/min/g) [53]. If blood supply further decreases, it leads to induction of infarction and tissue necrosis. Brief intermittent periods of ischemia might have a cumulative effect leading to necrosis [54]. So, hibernating may be acute, sub-acute or chronic, occurring in stable or unstable angina [55], myocardial infarction [56] and left ventricular dysfunction [57] due to severe coronary artery stenosis.

As an adaptive mechanism to maintain viable, myocardial function and metabolism are both reduced to deal with a concomitant reduce in blood flow. The reduction in microvascular blood flow is directly proportional to the reduction in myocardial function [58, 59, 60] as postulated in the term ‘perfusion-contraction-matching’ by Ross in 1991 [61]. If blood flow is restored, hibernating myocardium can partially or totally recover.

Chronic hibernation presents with a variety of tissue and microbiological changes such as myofibrillar lysis [62], increase of reparative fibrosis, accumulation of extracellular matrix proteins desmin and tubulin [62], loss of cytoskeletal integrity and a reduction of sarcoplasmic reticula and mitochondria. However, these changes existing in the presence of artery stenosis may not cause cell necrosis as long as there is resting perfusion [63]. The pathomechanisms underlying these phenomena have not yet been entirely understood, but some factors seem to contribute:

- changes in calcium handling in the sarcoplasmic reticula
- malfunction of connexin43 gap junctions contributing to arrhythmogenicity [64]
- changes in calcium sensitivity of myofibrils
- shift from aerobic to anaerobic metabolism [65].

Hibernation must be distinguished from *stunned* myocardium, even though they may coexist [66]. As proposed by Kloner, stunning is a state of viable myocardium salvaged after coronary reperfusion, yet showing signs of post ischemic dysfunction but eventually returning to normal [67]. Heyndrickx et al. showed in canine trials that the myocardium stays ischemic, but not irreversibly damaged, long after its reperfusion [68]. The pivotal difference between stunned and hibernating

myocardium lies in the tissue perfusion, which is near normally perfused in stunning, but reduced in hibernating myocardium. However, there is a considerable overlap of both symptoms since they share the same features: the prerequisite of reduced blood supply and wall motion abnormalities which improve after reperfusion.

2.1.1. Induction of hibernation in large animals for research matters

Hibernation as chronic ischemia offers advantages for research. Hibernating hearts show hallmarks of CAD, like left heart insufficiency reflected in poor cardiac performance and output as well as shortage of blood supply at rest. Since the tissue is not necrotic, it is accessible to neovasculatory stimuli.

Implantation of an ameroid constrictor is widely used for the induction of a hibernating myocardium in large animals for the sake of research [69]. Ameroid constrictors are circular steel constructs coated with an inner swellable casein membrane. Circumferential implantation of the constrictor ring around a vessel requires thoracotomy and a skilled surgeon. Vessel occlusion is achieved due to hygroscopic swelling of the casein membrane. Ameroid constrictor implantation is traumatic for the endothelium and is entailed by platelet aggregation and thrombogenesis [70]. Hence, extent of infarction development is unpredictable in this method. This method is further complicated by inflammation due to the surgery access. More controlled induction of hibernation in the sense of infarction size development is offered by the ligation of vessels via occluder implantation [71]. Hydraulic occluders provide best possible control but requires intense care of the animal due to externalized hardware for the hydraulic pump [72]. Von Degenfeld et al. established a catheter- based method of hibernation induction in swine [73]. Within 28 days, total occlusion of the vessel via implantation of an hourglass shaped polytetrafluoroethylene (PTFE) - covered stent via catheterization, causing significant decrease of regional myocardial blood supply at rest, is achieved. The PTFE membrane hampers blood side flow through the meshes of the stent. Like in the ameroid model, exact time point of vessel occlusion is unpredictable after stent implantation but occurs between day 7 and 28 post operationem. Infarction size is < 5 % of left ventricular tissue mass. Catheter-based stent implantation does not require thoracotomy and is highly reproducible (see chapter III.2.2.7. for the procedure of stent implantation as used in this studies).

2.2. Myocardial infarction

Myocardial infarction (MI) is a sudden, possibly life-threatening pathologic event caused by a lack of oxygen supply to the myocardium. It is mostly due to thrombotic vessel occlusion [74] followed by the occurrence of tissue necrosis. The pathogenesis of MI is strongly associated with inflammatory events of coronary arteries, leading to rupture of a coronary atherosclerotic plaque [75].

In the first stage of acute MI, the myocardium is injured owing to anoxia and the cessation of supply with metabolic substrates leading to cell death and scar formation in the long run. The mismatch between energy supply and demand underlies pathologic processes:

- reduced production of adenosine triphosphate (ATP) [76]
- a shift from aerobic to anaerobic metabolisms
- accumulation of byproducts from the anaerobic metabolism
- calcium and sodium overload [77]
- reduced pH.

Thirty minutes after infarction, tissue damage is irreversible. For the sake of infarct size reduction, reperfusion is the striven therapeutic approach. Paradoxically, reperfusion itself can have a pathologic impact; this phenomenon is called myocardial ischemia/reperfusion (I/R) injury [78]. I/R is featuring vascular, myocardial or electrophysiological malfunction. During reperfusion, ion flux changes rapidly leading to a quick pH change which is cytotoxic [79]. Mechanisms underlying I/R injury are complex due to the interplay of several biochemical pathways. During ischemia, minerals such as sodium, calcium or hydrogen accumulate peaking in acidosis. The “calcium paradox” describes a phenomenon of excess intracellular calcium influx arising from membrane leakages in the sarcolemma due to lack of ATP and from sarcoplasmic reticulum dysfunction. Intracellular calcium overload leads to tissue damage [80]. As cellular power plants, mitochondria play a crucial role in I/R injury. During I/R, leakages in their mitochondrial permeability transition pore (mPTP) lead to release of reactive oxygen species (ROS). Additionally to damaging nuclear components, ROS can provoke the opening of mPTP themselves [81]. This reaction is the positive

feedback loop of “ROS-induced ROS release” [82].

Another complication occurring during I/R, is the “no flow phenomenon”. Even though there is no angiographic evidence for a vessel obstruction, adequate reperfusion is not achieved in some patients post MI [83]. Microvasculature spasms, oxidative stress, inflammation, adhesion of thrombocytes and neutrophils, as well as swelling of myocytes and endothelial cells seem to be the main culprits for the etiology [84]. Infarction size can vary depending on the location of vessel occlusion and individual inflammatory response. After 24 - 48 h post MI, coagulation necrosis begins with the infiltration of neutrophil granulocytes. Necrotic myocytes are phagocytosed by macrophages; intracellular cascades and neuro humeral activation are triggered by granulocytes. Due to myocyte loss, left ventricle contractility shrinks and diameter increases. These processes seem to drive infarct expansion and remodeling of the remote myocardium, i.e. leading to hypertrophy of cardiomyocytes and interstitial fibrosis [85, 86].

2.2.1. Induction of myocardial infarction in large animals for research matters

Appropriate animal models of MI induction seek for an adequate assembly of the human infarcted heart. In pigs, permanent LAD occlusion with silk is a very reproducible method, however, requiring thoracotomy [87]. This model creates a myocardium in form of “no flow”. Coronary artery embolization through microspheres, polystyrene beads or agarose is performed via PTCA but lacks the control of the exact infarction location. I/R is most reliably induced by balloon occlusion causing MI (see chapter III.2.2.6 for the procedure of MI induction).

3. Therapeutic options for CAD

Cardiomyocyte number remains constant during lifespan because the heart represents an organ of poor parenchymal turnover [88]. Aim of the treatment of myocardial ischemia is the restoring of blood flow to the myocardium. Ischemia can evoke permanent myocyte loss leading to tissue replacement with less contractile fibrotic fibers, chronic dysfunction of heart performance (ejection fraction (EF) decrease and left ventricular end diastolic pressure (LVEDP) increase (Frank-Starling-law)) [89]. On the one hand, therapy in ischemia is directed to lyse thrombi pharmacologically. Antianginal medications are aspirin, nitrates, beta blockers, calcium channel blockers and ranolazine [84]. Invasive mechanical blood flow restoration is performed via percutaneous coronary intervention (PCI) like balloon angioplasty, stent implantation or coronary bypass surgery. Reperfusion within the ‘golden hour’ after infarction might enable a complete recovery of the myocardium. The longer the infarcted areal remains halted from perfusion, the more it is exposed to already mentioned changes and the less a tissue recovery can be warranted [90]. In patients lacking reperfusion therapy in time, absence of viable myocardium is a prognostic marker for their mortality [91].

3.1. Gene therapeutic angiogenesis

Even though therapeutic strategies made great progress within the last decades, some patients are not amenable to conventional approaches. PCI fails in those “no-option” patients in whom outcome remains poor. Advanced CAD in small distal vessels, chronic total occlusion and comorbidities preclude them from angioplasty. Insofar, it has been a goal of therapeutic approaches besides others to promote angiogenesis and arteriogenesis for the sake of evoking compensatory blood vessels [92, 93]. Even though the term angiogenesis is widely used for all forms of postnatal vessel growth, it describes the process of vessel building from pre-existing vessels and their sprouting ending in new capillary networks [94, 95, 96, 97]. Angiogenesis is driven by tissue hypoxia [96]. At the beginning of angiogenesis, NO-mediated vessel dilatation and VEGF (vascular endothelial growth factor) increase vessel permeability. Lured by proangiogenic signals, endothelial cells (EC) migrate and protrude filopodia. These “tip cells” guide new sprouts, “stalk cells” advance further into environmental tissue sprouting filopodia. They establish a lumen to

further enable sprout elongation. Anastomoses between neighboring sprouts are shaped by tip cells [95]. After sprouting, pericytes can migrate and support vessel maturation [97]. Regulating role in angiogenesis is attributed to Notch-signaling and VEGF [98]. Conversely, arteriogenesis defines the formation of “natural bypasses” through the growth of collateral arteries out of existing anastomoses [99]. Unlike angiogenesis, which is promoted by hypoxia, physical force drivers like shear stress can induce arteriogenesis [100]. Changes in shear stress, like postischemic vasodilatation, cause secretion of NO and excess expression of adhesion molecules, one of them MCP-1 [101]. Lymphocytes and mononuclear cells are recruited [102]. Smooth muscle cells begin to proliferate due to the presence of mononuclear cells which leads to an increase in vessel lumen. Some authors surmise that only the collaboration of angio- and arteriogenesis can lead to a clinical relevant vessel growth in ischemia [102]. In contrast, vasculogenesis is the de novo development of vessels stem cell driven [103]. Vasculogenesis occurs mainly during embryo development, but it is also seen in adults in terms of tumor vascularization and during tissue repair [104]. Some molecules were identified to have a proangiogenic effect like the vascular endothelial growth factor (VEGF), HIF-1, thymosin β 4, PDGF, among others [105, 106, 107]. Besides mentioned proteins, many microRNAs seem to be involved in vessel development.

4. Micro RNAs

Only 1-2 % of the human genome is translated into proteins, for a long time the vast rest was believed to be “junk” DNA [108]. Among other molecules like tRNA, siRNA or lncRNA, microRNA (miR, miRNA) belong to the abundant group of non-coding RNAs. These are not translated into proteins. MiRNA are present in plants, animals and humans and are located in almost every organ system. As the name reveals, miRNAs are molecules of ~ 22 nucleotides in length only and modulate gene expression at a posttranscriptional level [109]. It is believed that miRNA regulate more than 60 % of human protein coding genes [110]. Being generated in the cell nucleus, primary miRNAs are processed into hairpin shaped precursor miRNAs by the RNase-III enzyme “Drosha” [111] and further proceeded by the ribonuclease “Dicer” into microRNA complexes, after their exportation into the cytoplasm by XPO5. There, miRNA are incorporated in RNA-induced silencing complexes (RISC) regulating gene expression by targeting messenger RNA (mRNA) [112] leading in their degradation or inhibition. Not only targeting mRNA but also complete networks of related transcripts, miRNA are inevitably involved in many cardiovascular diseases [113, 114, 115, 116]. MiRNA expression patterns are changed in terms of CVD [117, 118]. Their down- or upregulation can inhibit or enhance pathological responses in CVD.

4.1. The miR- 17~92 cluster

The miR-17~92 cluster encompasses miR-17, miR-18a, miR-19a, miR-19b-, miR-20a and miR-92a [119]. The miR-17~92 cluster was observed in tumors [120] in which its overexpression promotes tumor angiogenesis [121]. The angiogenic effect is traced back to miR-18a and miR-19a by effecting endothelial cells (EC).

Bonauer et al. showed that human ECs express the miR17~92 cluster member miR92a [122]. Unlike the proangiogenic effect of miR-18a and miR-19a in tumors, the authors revealed that forced overexpression via precursor molecule (termed pre92) of miR-92a impedes angiogenesis in vitro. It inhibits sprout formation in human EC, reduces their migration and their adhesion to fibronectin. Further, they investigated whether inhibition of miR-92a via antagomir could promote vessel growth in a murine hind limb ischemia model. Mice injected with the antagomir-92a showed a reduction in toe necrosis due to improved neovascularization in the ischemic limb. This study indicates that the inhibition of the overexpressed miR-92a has a proangiogenic effect. A porcine infarction model gave evidence that miR-92a inhibitions protects from I/R injury and is capable of reducing infarct size [123]. The study further showed that miR-92a was consistently upregulated in infarcted hearts. These data suggest that miR-92a negatively regulates endothelial function.

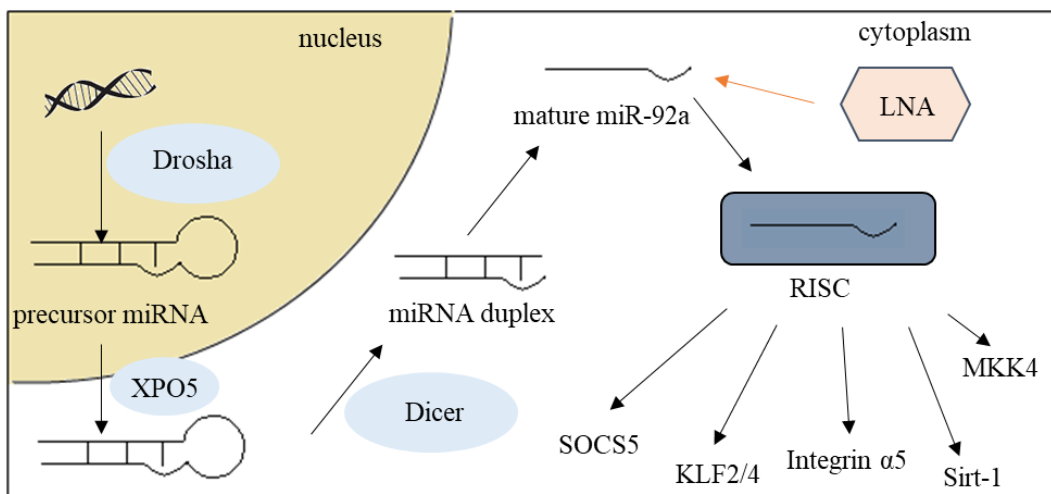


Figure 2: Processing of miR-92a

From its origin in the nucleus to its impact on target molecules and the possibility of its inhibition via LNA application (red arrow).

The effect of miR-92a is based on targeting protective endothelial molecules. The involvement of miR-92a in regulating developmental processes and (patho)physiological responses has been shown to be ample: integrin α -5 was

shown as direct target of miR92a [124, 126]. It plays a critical role in blood vessel development [125]. The class III histone deacetylase sirtuin-1 (Sirt-1) was demonstrated to promote corneal epithelization [126] and proliferation in dermal repair [117].

KLF2 and KLF4 which are crucial for maintaining endothelial function are regulated by miR-92a [129, 130]. Upregulation of mir-92a lowers the expression of its target KLF4 which was shown to be arteroprotective [129]. Further studies have proven that suppressor of cytokine signaling 5 (SOCS5) is a putative target of miR-92a. SOCS5 impedes inflammation and endothelial activation [130].

Furthermore, overexpression of miR-92a decreases levels of sphingosine-1-phosphate receptor 1 (S1P1) and mitogen-activated kinase kinase 4 (MKK4) [122]. Even though eNOS is not a direct target but influenced by integrin α -5 and KLF2, it is dysregulated by miR-92a in the broadest sense [131].

4.2. Strategies of miRNA modulation in vivo

Numerous studies prove that down- or up regulated miRNAs expression can be modulated in vivo. Therapeutic approaches in miRNA modulation aim to “normalizing” miRNA levels. Via miRNA-transfection (e.g. via adeno-associated viruses (AAV) [110]) an increase in miRNA levels can be reached. AAV are an effective means of delivering agents because of their diverse tropism to different tissues.

For the inhibition of miRNAs, complementary oligonucleotides (~8-25nt in length) against the target miRNAs’ seed region have been designed, so called “antimiRs”. The prerequisites for antimiRs to silence an upregulated miRNA are several: it needs to be able to penetrate the cell, it should be safe and stable against degradation and it should bind to the target miRNA with high efficacy and specificity [132]. Chemical modifications of antimiRs include locked nucleic acid (LNA)-modified oligonucleotides. These are 2’-O-methyl group-modified oligonucleotides, where the 2’-O-oxygen is bridged to the 4’ position via methylene linker forming a rigid bicycle locked into a sugar confirmation. The mechanism underlying the LNA uptake into the cell is still unclear, but their factual cellular transfection was proven [133]. After cellular uptake, the LNA binds to its complementary miRNA. In a non-human primate study, antimiR application significantly reduced levels of miR-122

[134]. Its applicability and therapeutic potential was further proven in primates with chronic hepatitis C [135].

Cholesterol-conjugated modifications of oligonucleotides (“antagomirs”) are easily up taken because of cholesterol’s lipophilic ability to bind to surface membrane receptors. Krützfeldt et al. [136] proved miR silencing using an antagomir against the liver specific miR-122 showing that a high dose systemic injection was capable of efficiently reducing miR-122 levels. Compared to antagomirs, antimiRs have some advantages. Due to their high affinity, they require lower doses to achieve the same efficacy. Moreover LNA based therapeutic miRNA inhibition was already tested in human patients [137, 138]. AntimiRs have shown greater promise from a clinical therapeutic perspective. In pigs, evidence for a working heart catheter-based regional LNA-92a delivery was already given [123]. Antegrade and retrograde application of the LNA-92a into the target zone leads to higher enrichment of the agent compared to systemic iv injection.

5. Modes of therapeutic agent application

In principle, there are different ways of applying therapeutic agents: per os, subcutaneous in the blood system, systemic or regional application can be differentiated.

Systemic applications are easy to perform, but a sufficient accumulation of an agent in a certain target region cannot be guaranteed by dint of its wide distribution in the body. While the systemic application can be done via any peripheral venous access, the regional application to the heart requires a percutaneous sheath introducer and heart catheterization. Regional application can be further differentiated in catheter based intra-muscular, antegrade or retrograde application as well as surgical direct injection. The decision on the route of application aims at reaching the best possible accumulation of the agent in the target zone.

Antegrade application takes a percutaneous access to the coronary artery of the heart. If combined to a balloon, the antegrade catheter's lumen is reduced so that the dwell time of an agent in the target territory is prolonged due to reduced blood flow.

For the retrograde application, the synchronized suction and retro infusion (SSR), a modification of the synchronized retro perfusion described in 1976, might be utilized [139]. The principle of selective suction and pressure-regulated retroinfusion has been reported previously [140, 141, 142]. In a preclinical trial in pigs, the feasibility of reperfusing ischemic tissue via coronary vein was proven [142]. The evidence for safety and efficacy of retro perfusion via SSR was provided in a human patient cohort [143]. Boekstegers et al. could show that a noninvasive, regional application of a drug is possible cathetering from the collateral vein of the target vessel via selective pressure regulated retroinfusion [144]. It enables a retrograde infusion of ischemic tissue coming from the "backdoor entrance" – the coronary vein. Another advantage is the long dwell time up to 10 minutes of the agent in the target area. SSR is a valuable means for the delivery of agents into cardiac regions inaccessible for antegrade catheterization, for example due to vessel occlusion. Retroinfusion was shown to be more effective than antegrade when applying gene therapeutic agents [145].

6. Aim of this study

Human EC were noted to express miR-92a [122]. In conditions of hyperglycemia, expression of miR-92a is even further exacerbated. Inhibition of miR-92a has traceable effect on miR-92a expression in vivo and in vitro. Therefore, a first in vitro set of experiments pursues the question of a potential positive effect on sprouting of bEnd.3 cells in culture under normal (low glucose) and hyperglycemic conditions (high glucose).

Prior studies have noted that miR-92a inhibition has a cardio-protective effect and is capable of alleviating myocardial infarction [123, 124]. As stated above, a catheter based delivery of the antimiR LNA-92a to porcine hearts is feasible [123]. Its cardioprotective effect in wildtype pigs was demonstrated after acute myocardial ischemia. In consideration of large numbers of CAD patients presenting with DM, the hypothesis that LNA-92a is cardioprotective in INS^{C94Y} transgenic pigs compared to controls was tested. The time course of 24 h was selected to answer the question concerning a potential preservation and protection of preexisting vessels and myocytes after miR-92a inhibition.

In addition, longtime outcome after miR-92a inhibition remains unknown. In consideration of increasing patients suffering from chronic ischemia and myocardial hibernation, the focus of this preclinical study was on the question whether the inhibition of the overexpressed miR-92a can promote angiogenesis in chronic ischemia in wildtype and diabetic pigs. The stent implantation model picked for this study unites relevant entities occurring in chronic ischemia such as reduced heart performance and capillary rarefaction. In this model, inducing chronic ischemia without considerable infarction and tissue necrosis renders the reduction stent implantation adequate for the analysis of a potential longtime effect of therapeutic agents [73], in this case LNA-92a.

III. MATERIAL AND METHODS

1. Material

1.1. Drugs

acarbose	Glucobay [®] , Bayer (Leverkusen, Germany)
acetylsalicylic acid	Aspirin [®] , Bayer (Leverkusen, Germany) Aspisol [®] , Bayer (Leverkusen, Germany)
adrenaline	Infectopharm (Heppenheim, Germany)
amiodarone	Cordarex [®] Sanofi Aventis (Frankfurt am Main, Germany)
atropine	B.Braun (Melsungen, Germany)
azaperone	Stresnil [®] , Elanco (Indianapolis, USA)
carprofen	Rimadyl [®] , Pfizer (New York, USA)
cefuroxime	Hikma (London, UK)
clopidogrel	Plavix [®] , Sanofi (Frankfurt am Main, Germany)
fentanyl	Fentadon [®] , Albrecht (Aulendorf, Germany)
glyceroltrinitrate	Nitrolingual [®] , Pohl-Boskamp (Hohenlockstedt, Germany)
HAES	B.Braun (Melsungen, Germany)
heparin	Ratiopharm (Ulm, Germany)
iopromide	Ultravist [®] 370, Bayer (Leverkusen, Germany)
ketamine	Narcetan [®] , Vetoquinol (Ismaning, Germany)
magnesium sulfate- heptahydrate	Inresa (Freiburg, Germany)
midazolam	Ratiopharm (Ulm, Germany)

pancuronium	Inresa (Freiburg, Germany)
potassium chloride	B.Braun (Melsungen, Germany)
propofol 2 %	Propofol Lipuro [®] , B.Braun (Melsungen, Germany)
saline (0,9 %)	B.Braun (Melsungen, Germany)

1.2. Medical consumables

catheter: Cournard, Judkins, Pigtail	Cordis (Miami, USA)
coronary guide wire	Galeo, Biotronik (Berlin, Germany)
endotracheal tube acc. to Magill	Dahlhausen (Cologne, Germany)
inflator	Merit Medical Systems (South Jordan, USA)
percutaneous sheath introducer	Cordis (Miami, USA)
PTCA-dilatation catheter	Maverick Monorail, Boston Scientific (Marlborough, USA)
PTFE- stent	Abbott (Chicago, USA)
PV-loop catheter	Scisense [®] , Transonic (Ithaca, USA)
retroinfusion catheter	PTC Pro- Med Technology Consult GmbH (Mödling, Austria)
surgical ligations	Resorba Medical GmbH (Nuremberg, Germany)
surgical sutures	Ethicon, Somerville (New Jersey, USA)

1.3. Medical devices

Ambo bag	B.Braun (Melsungen, Germany)
blood gas analyzer	Rapidlab 1265, Siemens (Berlin, Germany)
ECG/ Defibrillator	Lifepak 20 [®] , Medtronic (Minneapolis, USA)
laryngoscope	B.Braun (Melsungen, Germany)
mobile C- Arm	OEC Privo [®] , General Electric (Boston, USA)

Perfusor [®] space	B. Braun (Melsungen, Germany)
pressure monitoring system	Logical [®] , Smith Medicals (Dublin, USA)
puls oximeter	Datex Onmeda, General Electrics (Boston, USA)
PV Loop pressure control unit	Scisense [®] , Transonic (Ithaca, USA)
rib shears	Aesculap (Tuttlingen, Germany)
rib spreader	Aesculap (Tuttlingen, Germany)
sonomicrometer	Triton Technology Inc. (San Diego, USA)
sonomicrometric crystals	Sonometrics (Ontario, Canada)
temporary pacemaker	Osyпка Pace 110 [®] , Osypka (Freiburg, Germany)
ventilator	Julian [®] , Draeger (Lübeck, Germany)

1.4. Lab devices

confocal microscope	Leica TCS SP5 X, Leica (Wetzlar, Germany)
cryostat	Microm HM 560, Thermo Fisher Scientific (Waltham, USA)
fluorescence microscope	Leica DMI 6000B, Leica (Wetzlar, Germany)
minus 80 freezer	VWR (Darmstadt, Germany)

1.5. Chemicals and reagents

2,3,5 triphenyltetrazolium chloride	Sigma Aldrich (St. Louis, USA)
α -actinin antibody (host: rabbit)	Santa Cruz Biotechnology (Santa Cruz, USA)
acetone	Carl Roth GmbH (Karlsruhe, Germany)
antifade mounting medium with DAPI	Vectashield, Vector Laboratories (Burlingame, USA)
bovine serum albumin	Sigma Aldrich (St. Louis, USA)

Entellan [®]	Merck Millipore (Burlington, USA)
eosin	Carl Roth GmbH (Karlsruhe, Germany)
horse serum	Gibco, Invitrogen (Carlsbad, USA)
in situ cell death detection kit	Sigma Aldrich (St. Louis, USA)
isopropanol	Carl Roth GmbH (Karlsruhe, Germany)
Mayer's hemalum solution	Carl Roth GmbH (Karlsruhe, Germany)
methylene blue	Sigma Aldrich (St. Louis, USA)
NG2 antibody (host: rabbit)	Biorbyt (San Francisco, USA)
paraffin for histology	Sigma Aldrich (St. Louis, USA)
PBS tablets	Gibco, Invitrogen (Carlsbad, USA)
PECAM-1 antibody (host: mouse)	Santa Cruz Biotechnology (Santa Cruz, USA)
secondary antibodies (all)	Thermo Fisher (Waltham, USA)
triton X-100	Sigma Aldrich (St. Louis, USA)
xylol	Carl Roth GmbH (Karlsruhe, Germany)

1.6. Cell culture consumables

bEnd.3 cells	ATCC (Manassas, USA)
culture-insert 2 well in μ- dish 35 mm	Ibidi GmbH (Martinsried, Germany)
DMEM	Gibco, Invitrogen (Carlsbad, USA)
D- (+) – glucose solution	Sigma Aldrich (St. Louis, USA)
FBS	Gibco, Invitrogen (Carlsbad, USA)
incubator	HERAcell [®] , Heraeus, Thermo Fisher (Waltham, USA)
matrigel [®] matrix	Corning (Wiesbaden, Germany)
PBS	Gibco, Invitrogen (Carlsbad, USA)
pen/ strep	Gibco, Invitrogen (Carlsbad, USA)

1.7. Software

Conduct 2000 V.0150.9	Cardiodynamics (San Diego, USA)
Image J	Java, Sun Microsystems (Santa Clara, USA)
Leica LAS X software	Microscope Software, Leica (Wetzlar, Germany)
sonomicrometry software	SonoSoft, Sonometrics (Ontario, Canada)
SPSS Statistics	IBM corporations (Armonk, USA)

2. Methods

2.1. In vitro experiments

Endothelial cells hold the capacity for migration and angiogenesis in vivo. In in vitro approaches of low and high glucose media, the potential effect of an LNA-92a application compared to a scrambled LNA resp. untransfected cells on migration and angiogenesis was analyzed. The cell culture experiments were performed using bEnd.3 cells. This acronym stands for brain endothelial cells deriving from BALB/c mice, a highly inbred murine strain. BEnd.3 cells were cultured in DMEM medium in an incubator at 37 °C and 5 % CO₂ until their amount was sufficient for the experiments. Prior to the start of both experiments, the cells were equally distributed for the incubation in either low glucose medium (DMEM + 10 % FCS + 1 % Pen/Strep + 4,5 g/l glucose) or high glucose medium (DMEM + 10 % FCS + 1 % Pen/Strep + 9,0 g/l glucose) for 36 h. Thereafter, 3 x 10⁵ bEnd.3 cells were seeded onto each well of a 6-well plate in 3 ml low resp. high glucose medium. After 24 h, the medium was changed and reduced to 2 ml/well. Following, the cells from each condition were transfected according to the scheme showed in Table 1 and then distributed either to the angiogenesis resp. migration assay.

condition	LNA-92a	scrambled LNA (scr)	control (con)
low glucose	12,5 µg/ml	12,5 µg/ml	none
high glucose	12,5 µg/ml	12,5 µg/ml	none

Table 1: Overview on cell culture approaches for assays

2.1.1. Migration assay

Four hours after their transfection, 35,000 cells in 70 µl DMEM + 10 % FCS + 1 % Pen/ Strep were plated into each of the two wells of an ‘‘ibidi culture insert µ-dish 35’’ (see figure 6, A) and cultured for 24 h. Then the culture dish insert was removed forming a gap between both wells, the dish was filled with 2 ml DMEM + 1 % Pen/ Strep. Serving as baseline value, the gap was microscoped in polarized light microscopy at 4-fold magnification. After 22 h, all dishes were microscoped. Remaining uncovered area of the gap was measured using Image J and calculated from the baseline gap area in %.

2.1.2. Ring formation assay

Ibidi μ -slides for angiogenesis were prepared with 10 μ l matrigel/well. Four hours after their transfection, 15,000 cells/well in 35 μ l Huvec-medium + 5 % FCS + 1 ng/ml VEGF were transferred. After 22 h, all wells were microscopied and ring formations were counted per well.

2.2. In vivo experiments

2.2.1. Legal background

The interventions were performed according to the approval of the District Government of Upper Bavaria (registered under the numbers: 62-13, 141-11). The animal housing was accomplished sticking to the guidelines of the “German Animal Welfare Act”. The pigs were kept in groups up to six individuals throughout the whole experiment. The animal experiments took place at “Zentrum für Präklinische Forschung” (Klinikum rechts der Isar, TUM, Munich, Germany) and at “Walter-Brendel-Zentrum” (Klinikum der Universität, LMU, Munich, Germany).

2.2.2. Laboratory animals

Pigs of either sex were purchased from the “Chair for Molecular Animal Breeding and Biotechnology” (Ludwig Maximilian University, Munich, Germany) one week prior to the start of the experiments. The animals were INS^{C94Y} transgenic pigs showing a diabetic phenotype as described previously and landrace wildtype pigs.

The animals (wildtype (wt) and diabetic (db)) either underwent chronic ischemia (stent implantation) or acute infarction (24h model). All animals received either an application of the LNA-92a or a scrambled LNA (LNA scr), which is a non-sense LNA not binding to miR-92a, as controls (con). At the first intervention of the stent model, the pigs were about 10 weeks old and had a body weight of ~25 kg, on day 28 the weight was about 45 kg and 60 kg on day 56. Pigs undergoing acute infarction, were about 10 weeks old and weighed about 25 kg. The animals were nourished rationed with a conventional pig feed and tap water ad libitum. The distribution of animal into groups was randomly selected. Group distribution can be taken from Table 2.

acute (ischemia/reperfusion)		
group	feature	animals (=n)
MI db con	diabetic, LNA scr	4
MI db LNA-92a	diabetic, LNA-92a	4
chronic (stent implantation)		
group	feature	animals (=n)
con	wildtype, LNA scr	5
LNA-92a	wildtype, LNA-92a	4
db con	diabetic, LNA scr	3
db LNA-92a	diabetic, LNA-92a	4

Table 2: Animal groups for the stent and MI model

2.2.3. Preparation of animals for the interventions

The protocol of anesthesia and for heart function measurements was the same for stent implantation and ischemia/ reperfusion, differences in medicament regime can be taken from the congruent paragraphs. All transgenic diabetic pigs from all groups did not receive insulin to maintain their diabetic phenotype. Prior to feeding, they received 50 mg acarbose as anti-diabetic medication. At the beginning of each intervention, blood glucose levels were measured from venous blood with a blood gas analyzer.

2.2.4. Anesthesia and preliminary for catheterization

Prior to each intervention, all pigs were deprived of food for 8 hours. At the beginning of each intervention, the animals were sedated with an intramuscular injection of 2 mg/kg bw azaperone, 15 mg/kg bw ketamine as well as 0.02 mg/kg bw atropine.

Via venous catheter placed in the Vena auricularis caudalis the anesthesia was deepened applying 5 mg midazolam and 0.05 mg fentanyl. For securing the airways, the pigs were intubated with an endotracheal tube according to Magill with cuff and then volume-regulated ventilated. Anesthesia was maintained through the perfusion of 2 % w/v propofol at a rate of 10 mg/kg bw/h over the course of the intervention. For the substitution of volume and stabilization of heart rhythm, HAES and 0.9 % saline containing 150 mg amiodarone and 5 g magnesium sulfate-heptahydrate were transfused.

Vital parameters were monitored with pulse oximetry, capnography, ECG lead

according to Einthoven and invasive arterial blood pressure measurement. After percutan incision of around 3 cm in medial direction of the Musculus sternocleidomastoideus, an 8 or 9 F percutaneous sheath introducer was implanted into the Arteria carotis communis respectively an 11 F introducer into the Vena jugularis externa after the vessels were ligated cranially, serving as ports for the catheters. Prior to ligation of the vessels, 10,000 IU heparin were applied intravenously. Iopromid served as a contrast agent in all interventions for the exact positioning of the stent and angiography. A mobile C-arm X- ray was made use of as imaging device. After the intervention, the percutaneous sheath introducers were removed ligating the vessel caudally and the wound was adapted. Thanks to good collateralization of the A. vertebralis the vessel ligation is not lethal to pigs since the brain is still supplied with blood. Stopping the perfusion of propofol ended the anesthesia. 4 mg/kg bw carprofen (Rimadyl) daily served as oral analgesic for 72 h after the intervention. As infection prophylaxis, 750 mg cefuroxime was injected.

2.2.5. Functional assessment

After repeating global heart function measurements, regional heart function was obtained, therefore a sternotomy was necessary. Thereafter, the animals were sacrificed via injection of saturated KCl in the left ventricle, after application of fentanyl and propofol. For further immunohistological and molecular biological investigations, the heart was sampled and stored at -80°C .

2.2.6. Setup of the ischemia/reperfusion model

Hour 0: After preparation according to the described procedure, basal measurements for global heart function were obtained. For the induction of ischemia, a 7 F Judkins right catheter, an inflator, an over- the- wire balloon (3,0 x 12 mm) and a coronary guide wire (14 mm) are prepared. The 7 F Judkins right catheter was advanced into the LAD and attached to a Y-Connector. Before the balloon was driven through the Judkins, the coronary guide wire was thread onto the over the wire balloon. Balloon and coronary guide wire were pushed forward in the LAD, resting eventually distally of the first side branch. Ischemia was then induced via balloon inflation at a pressure of 6 atm using the inflator. The provoked infarction was maintained for 60 min. Before balloon occlusion, 0.05 mg fentanyl served as analgesic and its application was repeated every 20 minutes, 150 mg amiodarone were injected for rhythm stabilization. After 30 min of ischemia, the

position of the catheter was double checked. Briefly before the balloon was deflated, the LNA-92a resp. the scrambled LNA was injected. Twenty-four hours later, after global and regional heart function measurement, the animals were sacrificed, hearts were explanted and sampled.

2.2.7. Setup of the stent implantation trial

2.2.7.1. Day 0

The animals were instrumented as described previously. A 9 F Judkins right coronary catheter, a 0.018"/180 cm and a 0.014"/190 cm coronary guide wire, a PTCA dilatation catheter (3.0x12mm), a 6 F Pigtail catheter, a 6 F Cournard Catheter as well as an inflator were prepared. Before implantation, the stent was prepared according to following procedure: the stents are fabricated from medical stainless steel and an ultra-thin layer of expandable polytetrafluoroethylene (PTFE) [73]. The stent (13 mm lengths, 3 mm diameter) is mounted on a 16 G cannula. A notch was formed via ligation in the middle of the stent with a thread (USP 0). After the thread had been removed, a 5-0 sized thread was knotted five times into the notch. Thereby, a stent with a central lumen of 1.77 mm² was created. Then the stent was removed from the cannula and fixated on a PTCA- balloon with a pressure of 1atm. The stent was then positioned into the RCX using a 9 F Judkins, a PTCA dilatation catheter and an inflator. The implantation of the reduction graft stent leads to a vessel stenosis of around 75 %. Total occlusion of the LAD was achieved after 28 days.

2.2.7.2. Day 28

Global myocardial function was obtained via conductance- catheter; measurements for ejection fraction (EF) and left ventricular end diastolic pressure (LVEDP) were performed. For the retroinfusion of the LNA-92a resp. the LNA scr for control groups, a Swan-Ganz Catheter modified by Boekstegers with four lumens was implanted into the Vena interventricularis anterior, after a 6 F-Cournard catheter was placed in the coronary sinus, through witch a 0.018"- coronary guide wire was pushed forward in the anterior vein. The application was performed pressure regulated. For this purpose, two of the lumens of the SSR catheter were connected to the high-pressure reservoir, filled with saline. The agent was connected to the infusion lumen directly after the high-pressure reservoir separated by a valve

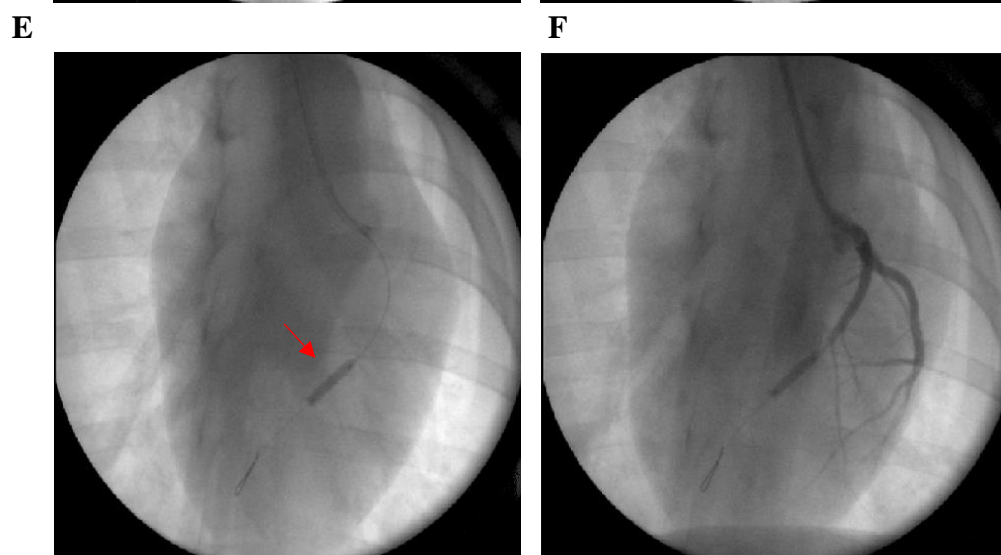
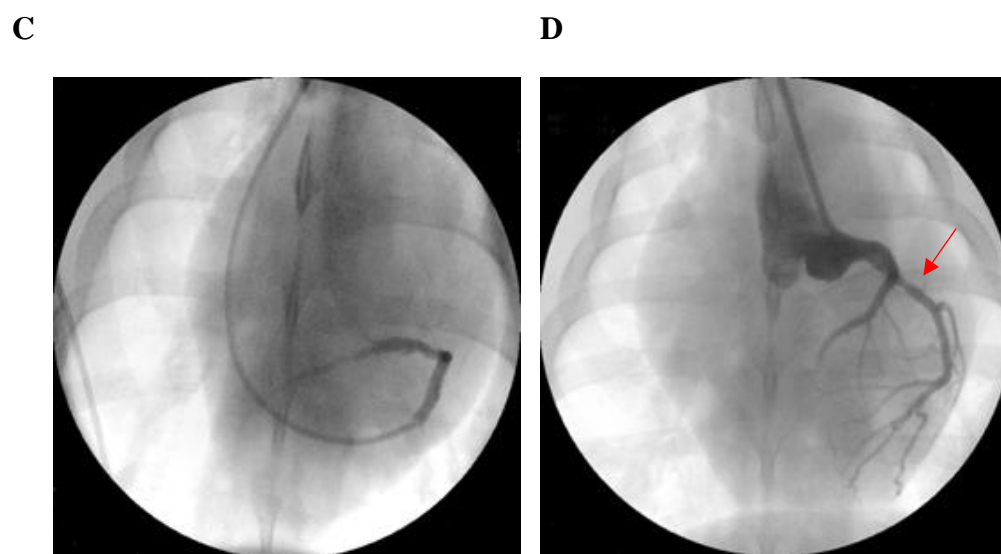
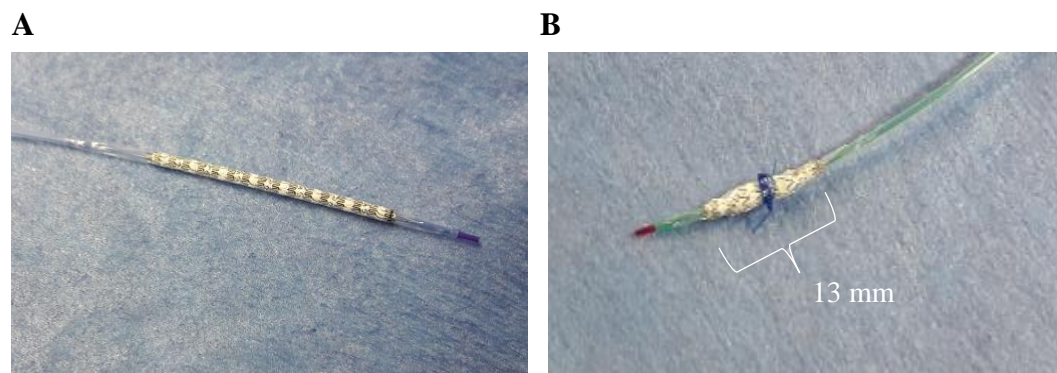
stopcock. The third lumen served as a port for coronary venous pressure, the forth was used to inflate the balloon at the catheter's tip. Before retroinfusing the agent, the coronary venous occlusion pressure was ascertained by 20 sec balloon occlusion of the coronary vein, the present retroinfusion pressure was set 20 mmHG higher. With the start of retroinfusion, the valve stopcock was opened providing the agent driven by the high pressure in the reservoir together with the saline until the preset retroinfusion pressure was reached in the coronary vein. 0.75 mg LNA-92a were applied (= 5 mg/kg heart weight).

2.2.7.3. Day 56

Under analgesia and muscle relaxation with 4 mg pancuronium, the sternum was opened with a rib shears and rib spreaders starting from the xiphoid up to the manubrium, after global heart function measurements as described previously were repeated. Myocardial contractility can be obtained via sonomicrometry. Therefore, two sonomicrometric, ultrasonic crystals were implanted subendocardial either into the ischemic RCX area or as control in the non-ischemic LAD-region in a distance of circa 1 cm to each other. The measure was performed under baseline and atrial pacing up to 150 bpm. To demonstrate collateralization, a post mortem coronary angiography was performed injecting contrast agent into the left coronary main trunk.

2.2.7.4. Peri- and post-operative anticoagulation regime

The occlusion of the stent within the first 7 days after implantation needs to be avoided. The thrombogenic surface of the stent as well as the accompanied changes in blood flow in the vessel require an adequate platelet aggregation inhibition. As an anticoagulant 75 mg clopidogrel per os were applied the day before the surgery. During the first intervention 20,000 IU heparin as well as 500 mg acetylsalicylic acid were venously injected to achieve full anticoagulation. Up to day 7 after intervention the pigs were treated with 75 mg clopidogrel and 100 mg acetylsalicylic acid as oral administration.



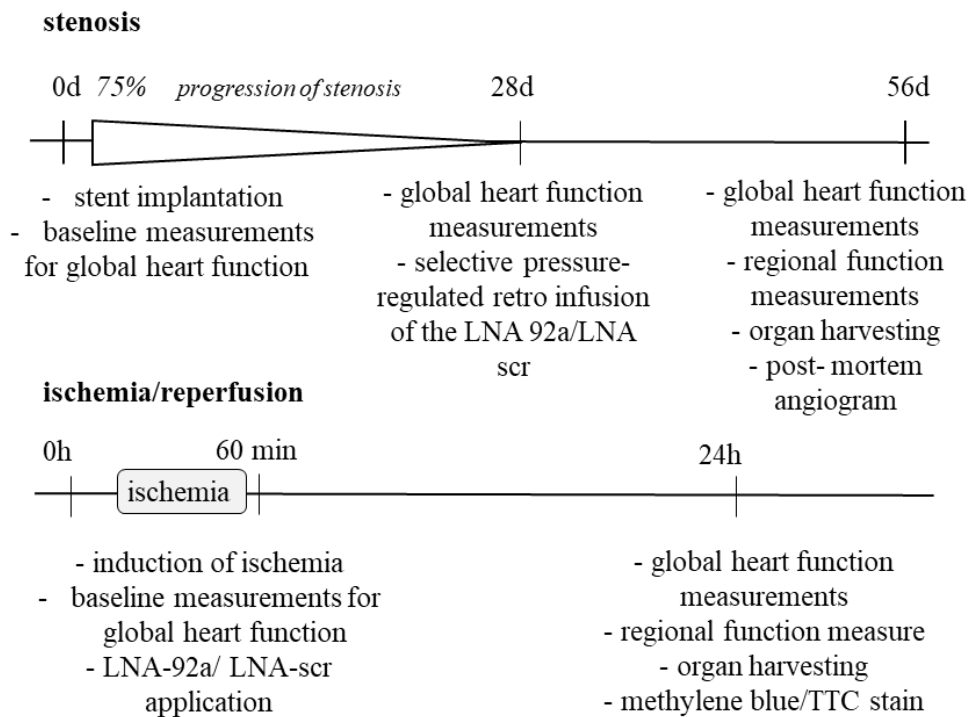
G

Figure 3: Experimental setup for the chronic and acute ischemia model

A) Reduction stent before preparation with the PTFE-membrane (white) to avoid blood flow through the meshes. B) Ligation of the PTFE-stent creates an hourglass shaped tapering. Prepared stent for implantation is crimped on a PTCA balloon. C) Retrograde catheterization coming from the venous branch into the target areal. D) Angiogram showing a PTFE-stent (arrow) in the RCX right after implantation. E) A coronary guide wire and a dilatation balloon (arrow) are driven in the LAD via Judkins catheter for induction of infarction. F) Contrast agent application verifies shortcut of blood flow distally from the occluded balloon. G) Timeline of experimental setup displaying interventions and their main procedures from day 0 to day 56 in the stent implantation model and the I/R model.

2.2.8. Heart function measurements

2.2.8.1. Invasive blood pressure measurement

A constant physiologic blood pressure is crucial for the maintenance of organ perfusion. For the monitoring, the central arterial pressure was assessed from the arterial percutaneous sheath introducer connected to a fluid-filled electronic pressure transducer. The advantage of invasive blood pressure measure is the continuous record from beat to beat.

2.2.8.2. Global left ventricular heart function measurements

Ejection fraction (EF) is an important measure for the determination of cardiac performance. EF describes the volume of blood ejected from the ventricle of the heart into the systemic circulation with each heartbeat. It delineates the ratio between the volume of the effectively pumped blood fraction to the volume of blood in the ventricle indicating the heart's pumping efficiency (left ventricular ejection fraction). It is calculated as per following formula:

$$EF(\%) = \frac{SV}{EDV} \times 100$$

The stroke volume (SV) is defined as the difference between the end-diastolic and end-systolic (ESV) volume. Hence the EF results in:

$$EF(\%) = \frac{EDV - ESV}{EDV} \times 100$$

A healthy heart's EF should be > 55 %, in adults usually around 60 – 70 %.[146]

EFs under 35 % identify an insufficient cardiac output as it is seen in heart failure, heart infarction or hypertrophic cardio-myopathy, to name only a few. EF is commonly measured via transthoracic echocardiography according to Simpson's rule or MR imaging.

In this study, LV angiography was recorded in anterior-posterior position for the quantification of EF at baseline heart rates and right ventricular pacing of 130 bpm. Therefore, the minimal, end-systolic and the maximum, end-diastolic ventricle volume were determined planimetrically in Image J Software. The left ventricular end-diastolic pressure (LVEDP) [mm HG] was obtained via conductance catheter (Scisense, Transonic) and Sonosoft Software. LVEDP serves as a measure for heart insufficiency and left-sided heart failure; in case of impaired cardiac output, the LVEDP is increased [147]. Changes in LVEDP can be calculated as ($\Delta LVP/\Delta t$). This value indicates the velocity of pressure changes and evaluates myocardial contractility. Physiological LVEDP is < 17 mmHg.

2.2.8.3. Sonomicrometry for regional heart function

The phenomenon of piezoelectricity was discovered by Pierre Curie when he observed that crystals such as quartz generate electrical polarization under mechanic stress [148]. The term sonomicrometry describes a technique of measuring distances between piezoelectric crystals embedded in a medium (in this case heart tissue) through detection of the speed of acoustic signals. The time taken for the signal to pass through the heart tissue from one crystal (diameter 2 mm) to the other and so the muscle contractility can be quantified [149]. The faster the signal is transferred, the closer the distance between the crystals and the more contractile the myocardium. The crystals are implanted in a parallel direction to the fibers and pushed to the sub endocardial tissue.

The ECG, which is recorded during the whole procedure, is necessary to distinguish the crystal distances between end-systolic (ESP) and end-diastolic (EDP) time points. Hence using the following formula, the subendocardial segment length shortening (SES) can be calculated:

$$SES(\%) = \frac{EDP - ESP}{EDP} \times 100$$

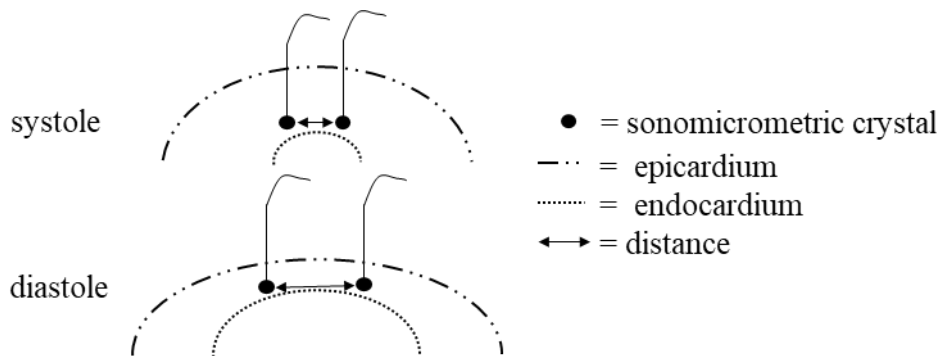


Figure 4: Scheme of sub-endocardial segment shortening

2.2.8.4. Staining for infarction size determination

For the differentiation of infarcted, non-infarcted and area at risk in the 24 h model, the explanted hearts were stained via 2 % methylene blue solution for non-infarcted tissue after ligation of the LAD. In addition, 10 ml 10 % TTC were injected in the vessel. TTC is a redox indicator for cellular respiration showing a deep red color in presence healthy viable heart from the cardiac lactate dehydrogenase, while areas of potential infarctions turn out to be paler. Thereby, the vital area at risk could be distinguished from infarcted tissue. For further analysis, the hearts were cut vertical to their axis into 5 slides (from basal (1) to apical (5)). Photographs were taken and analyzed planimetrically with ImageJ to determine infarction size.

Thereafter, transmural specimens from infarcted tissue, area at risk and control areal (RCX) were taken from those slices and stored at -80°C . Tissues from slice 2 and 3 were used for histology.

Pig heart undergoing stent implantation were stained for TTC for the sake of being able to exclude animals with an infarcted area bigger than $< 5\%$.

2.2.8.5. Post mortem angiography and capillary filling

Post- mortem angiograms were taken after heart explantation for the visualization of collaterals and classification of Rentrop scores. Therefore, a 6 F insert from a percutaneous sheath introducer was introduced into the Truncus communis and flushed with contrast agent. Rentrop scoring is a rating scale for capillary filling [150]:

Grades of vessel filling	Description
0	None
1	side branched filled via collateral channels without visualization of the epicardial segment
2	Partial filling of the epicardial segment via collateral channels
3	Complete filling of the epicardial segment of the artery via collateral channels

Table 3: Rentrop's classification scheme

2.3. Histology

All histologic stainings were performed in either cryo-conserved or paraffin embedded tissues. Analysis and quantification were implemented in a blinded manner for all tissues. For the histological assessment, tissue from the second and third heart slice from the RCX region (stent model) resp. from the LAD region (area at risk) were selected.

2.3.1. PECAM-1/ NG2 staining

Immunohistochemistry enables insights into vessel integrity and maturation. PECAM-1, also known as CD31, indicates the presence of endothelial cells, whereas NG2 is located on the cell surface of pericytes. Cryoconserved tissues were cut to a thickness of 5 μm on a cryotome, mounted on microscope slides beforehand. Tissue slices from the LAD and RCX region were stained according to following protocol. Ten representative pictures were taken with fluorescence microscopy (magnification 63-fold) from each animal and signals for PECAM-1 and NG2 were counted.

Procedure	Time
thaw tissue sections	10 min
fixate in cold acetone	10 min
encircle tissue with a hydrophobic pen to keep liquid pooled	
incubate in incubation buffer (2 % bovine serum albumin, 0.1 % Triton-X 100, 1 % horse serum in PBS) at room temperature	30 min
incubate with primary antibody for PECAM-1 (1:50, host: goat) in incubation buffer at 4°C	over night
wash in PBS	3 x 10 min
incubate with secondary antibody (donkey anti-goat, 1:50, rhodamine conjugated) in incubation buffer at room temperature	2 h
wash in PBS	3 x 10 min
incubate with primary antibody for NG2 (1:100, host: rabbit) in incubation buffer at 4°C	over night
wash in PBS	3 x 10 min
incubate with secondary antibody (mouse anti-rabbit, 1:100, AF 488) in incubation buffer at room temperature	2 h
wash in PBS	3 x 10 min
mount using cover slips and antifade mounting medium with DAPI	

Table 4: Staining protocol for Pecam-1/ NG2

2.3.2. HE Staining

As a topographic stain, hematoxylin and eosin stain (HE) is traditionally used for pathologic tissue evaluation. Hematoxylin, gained from the logwood tree, stains basophilic structures, such as nuclei, DNA and rough endoplasmic reticula, in blue color. Eosin is a synthetic acid dye staining basic tissue components in shades of red color (e.g. mitochondria, collagen and keratin). HE stains visualize tissue inflammation and cell infiltration. Paraffin embedded specimen from the 24 h model from the LAD region were stained in HE according to the protocol in Table 5. Five representative pictures were taken in light microscopy (20-fold magnification) and level of infiltration was assessed semi-quantitative by a scoring scheme from 1-3 (1 = mild infiltration, 2 = moderate, inflammatory cells visible, but connective tissue intact, 3 = severe, inflammatory cells infiltrate the tissue intensely) [151].

Procedure	Time
xylol	2 x 10 min
100 % isopropanol	2 x 5 min
95 % isopropanol	2 x 5 min
70 % isopropanol	5 min
rinse in tap water	quick
Mayer's hemalum solution	1 min
rinse in running tap water	5 min
rinse in tap water	5 min
Eosin 0,1 %	2 min
rinse in tap water	quick
rinse in 70 % isopropanol	quick
95 % isopropanol	2 x 1 min
100 % isopropanol	2 x 2 min
xylol	2 x 5min
mount with Entellan	

Table 5: HE staining protocol

2.3.3. Sirius Red for fibrosis detection

Fibrosis is characterized by the accumulation of matrix proteins like collagen and glycosaminoglycan. The development of fibrosis is an integral component of CAD and triggered by ischemia [152]. Metabolic disturbances like DM can further facilitate fibrosis [153]. Sirius red stain is a sensitive method for collagen fiber detection stained in red color, whereas the cytoplasm appears yellow in light microscopy. The tissue was embedded manually in paraffin after isopropanol dehydration according to Romeis [154]. Following they were stained according to the protocol below [155]. For the detection two specimen from the left ventricle were analyzed. Pictures were taken at a 20-fold magnification from animals undergoing stent implantation. Fibrosis quantity was determined from 10 independent images each with Image J Software.

Procedure	Time
70 % xylo	3 x 10 min
100 % isopropanol	2 min
90 % isopropanol	2 min
70 % isopropanol	2 min
H ₂ O dest	5 min
H ₂ O dest	10 min
0,1 % Sirius red solution (v/v)	60 min
H ₂ O dest	rinse
H ₂ O dest	rinse
90 % isopropanol	2 min
100 % isopropanol	2min
70 % xylo	3 x 10 min
mount with Entellan	

Table 6: Sirius Red staining procedure

2.3.4. Apoptosis stain

Apoptosis describes the programmed cell death and is seen in CAD caused by ischemia and oxidative stress. Its presence indicates proceeded myocyte destruction. For apoptosis detection the well-established terminal deoxynucleotidyl transferase dUTP nick end labeling (TUNEL) method was used. TUNEL detects DNA fragments which arise from DNA breaks during apoptosis. The staining was performed according to provided kit data sheet (in situ cell death detection kit).

2.4. Statistics

The results are given as mean \pm standard error of the mean (SEM). The results were checked for significance via ANOVA-test. When a significant difference was obtained, multiple comparison tests were performed using the Student-Newman-Keuls test. The assessment of significance was calculated via Student t test. All calculations were done with SPSS Version 20.0. A $p < 0.05$ (*) was considered significant, $p < 0.01$ (**) and $p < 0.001$ (***) highly significant.

IV. RESULTS

1. Cell culture data

1.1. Migration assay

Capacity for migration of bEnd.3 cells was assessed in a migration assay using different glucose conditions. Extent of migration was quantified from the uncovered gap area after the cell culture dish insert was removed (figure 6, B). After 22h, migration extent was retarded under normo and even more retarded in high glucose conditions which is reflected in a vast uncovered area (%) in untreated cells and when a scrambled LNA was applied. This indicates that the scrambles LNA does not positively influence migration. As can be seen in figure 5, LNA-92a application is capable of significantly enhancing migration capacity in the normo glucose dishes as well as the high glucose culture.

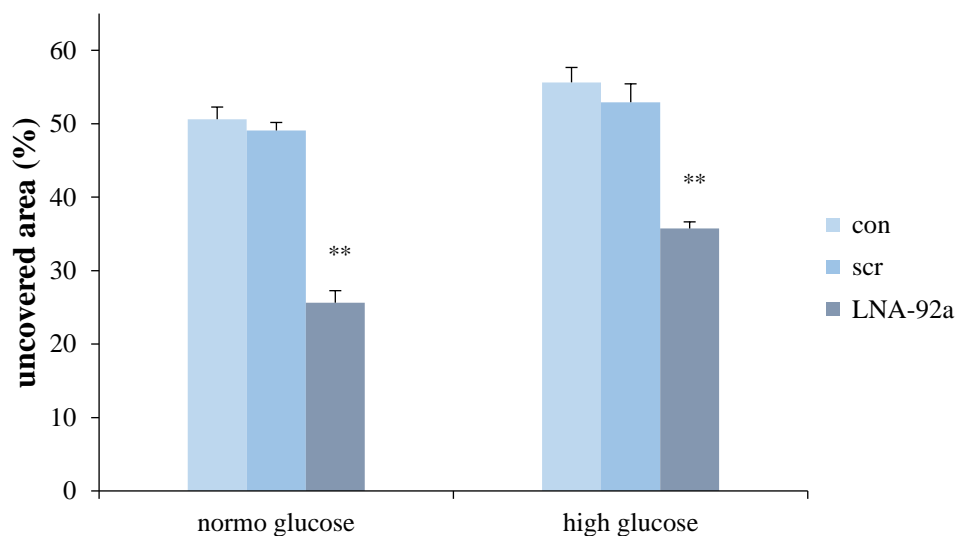


Figure 5: Migration capacity of bEnd.3 cells

Uncovered area is reduced in LNA-92a treated cells due to enhanced migration. Enhanced migration after LNA-92a transfection is seen in b.End3 cells cultured in normo and high glucose media. (Mean \pm SEM, **p<0.01)

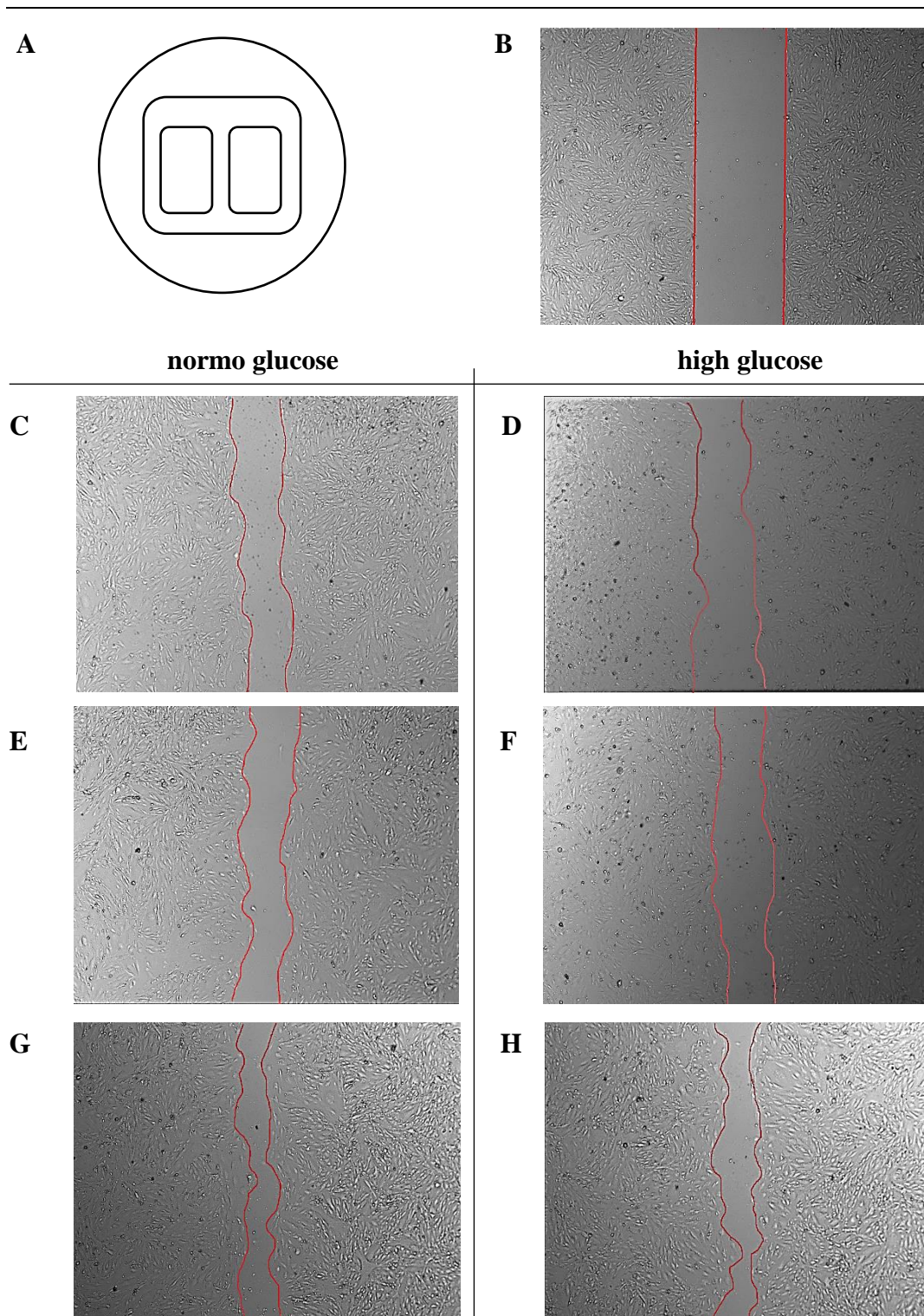


Figure 6: Representative pictures of migration assays

A) Schematic illustration of the cell culture migration dish. B) Gap after removing the insert at time point 0. C) Untreated cells in low glucose and in high glucose (D) served as negative controls. E) Cells treated with scrambled LNA in low glucose and in high glucose medium (F) show retarded migration. G) Reduction of uncovered area due to enhanced migration after LNA-92a application. H) A similar migration is seen in treated cells in high glucose conditions.

1.2. Ring formation assay

Capacity for ring formation was assessed in normo and high glucose conditions in bEnd.3 cells. Under normo glucose, ring formation is seen, but poorer compared to LNA-92a transfected cells. Treatment with scrambled LNA does not positively effect ring formation capacity, when compared to control cells. In high glucose conditions, ring formation is hampered, bEnd.3 cells accumulate forming clumps and do not tend to form rings. In LNA-92a treated cells, capacity for forming rings is recovered. When comparing control cells to scrambled LNA transfected cells in normo and high glucose conditions, there is no difference in the number of rings formed per well, indicating that the scrambled LNA does not affect tube formation capacity.

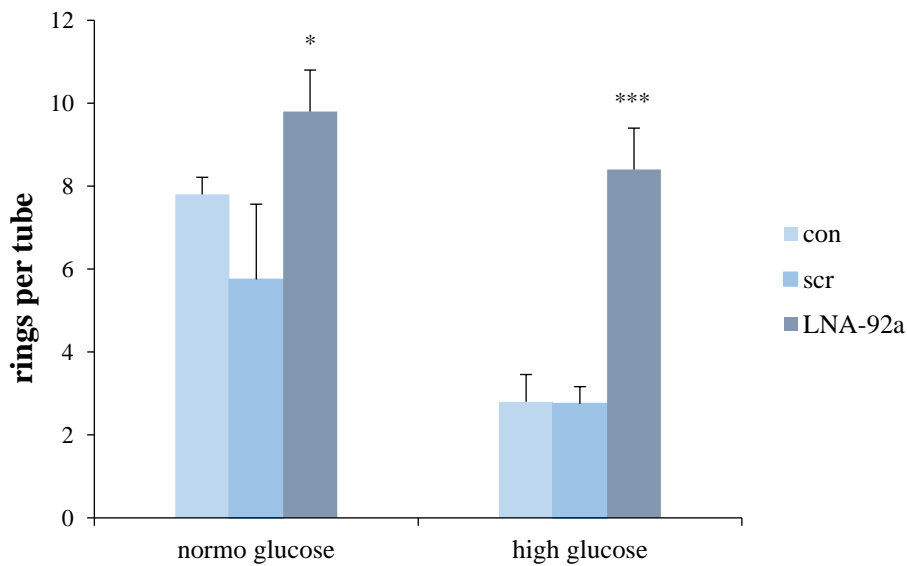


Figure 7: Rings per tube in normo and high glucose media

Cells are capable of forming significantly more rings in normo and high glucose media, when transfected with the LNA-92a. (Mean \pm SEM, * $p < 0.05$, * $p < 0.001$)**

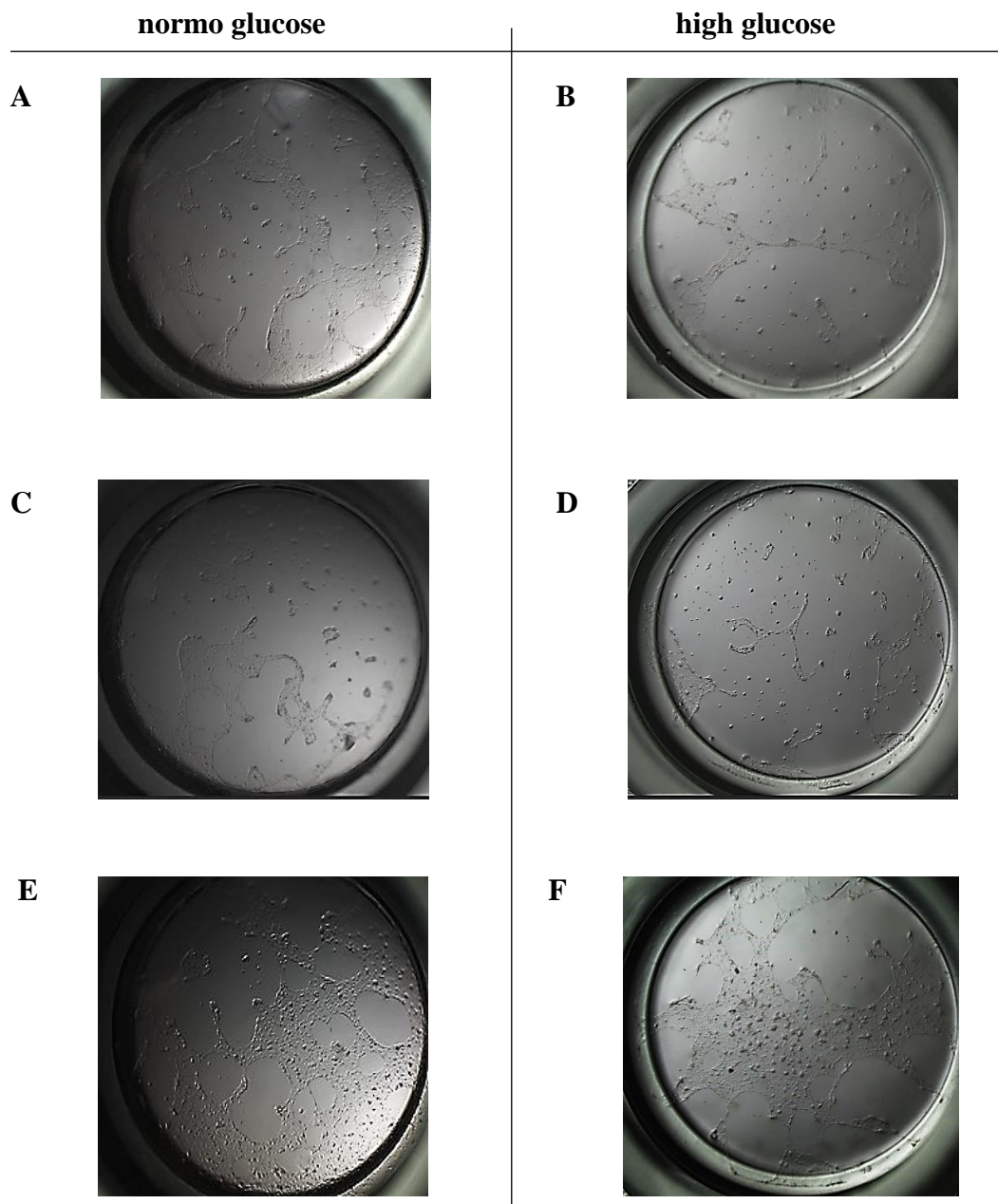


Figure 8: Ring formation assay

A) Ring formation capacity is hampered in the untransfected cells as well as cells receiving a scrambled LNA (**C**). **B)** In high glucose media, capacity for ring formation disappears in untransfected cells and in cells transfected with scrambled LNA (**D**). Cells accumulate forming clumps instead of rings. Rings are formed after LNA-92a treatment in normo glucose (**E**) and high glucose medium (**F**).

2. Data from the 24h model

2.1. Post mortem assessment of infarct size

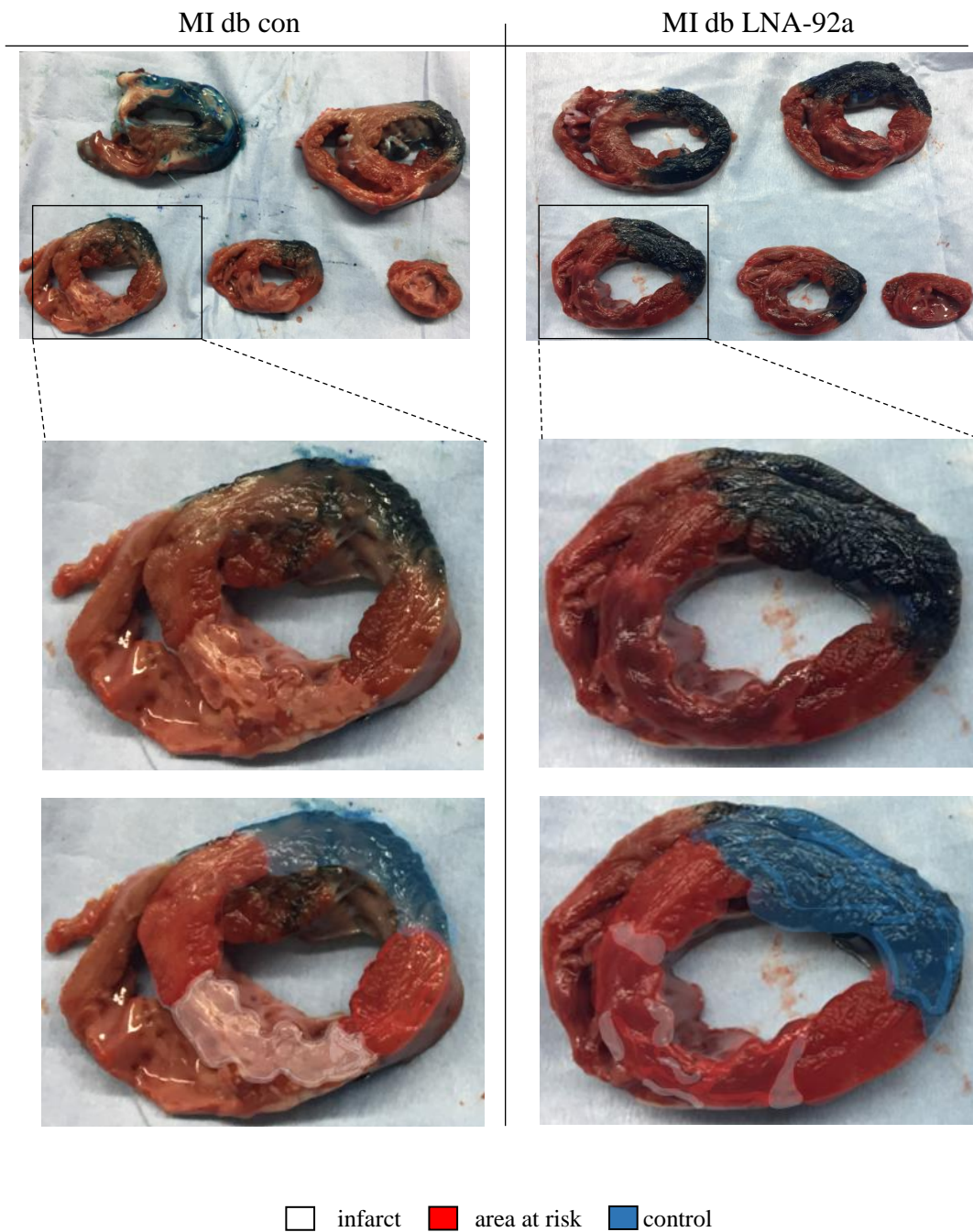


Figure 9: Post mortem myocardial TTC stainings

After explantation, hearts were cut into 5 slices after staining with TTC for vital tissue giving insights into infarction size. Upon LNA-92a application, infarction size is visibly reduced.

Assessment of infarction size was performed after explantation of the heart via injection of TTC into the coronaries. In the 24h model, LNA-92a administration could reduce infarction size after balloon occlusion. Relation of infarction size compared to the AAR was significantly reduced after LNA- 92a treatment. Size of AAR in comparison to the left ventricular mass was approximately similar between both groups.

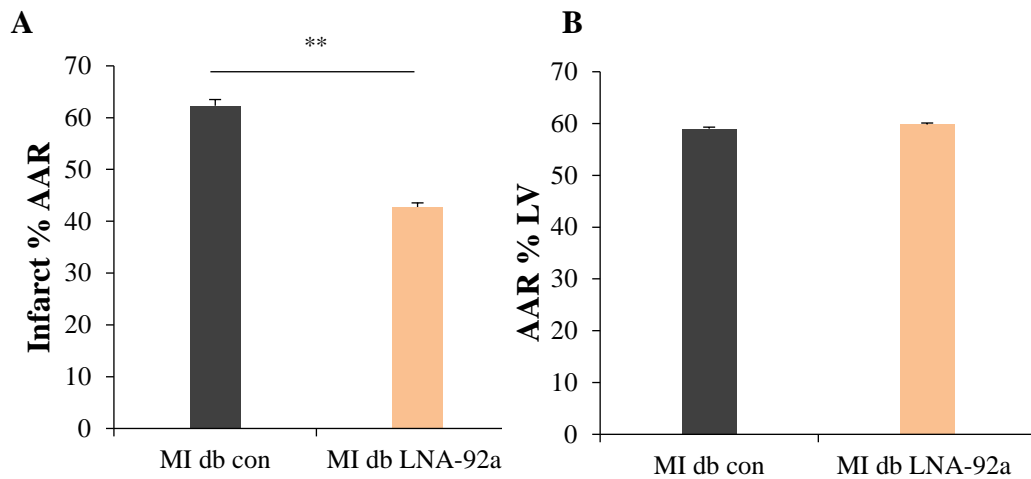


Figure 10: Infarct size

A) Infarct%AAR is significantly reduced after treatment. B) AAR%LV are similar when compared between both groups (Mean \pm SEM, **p<0.01)

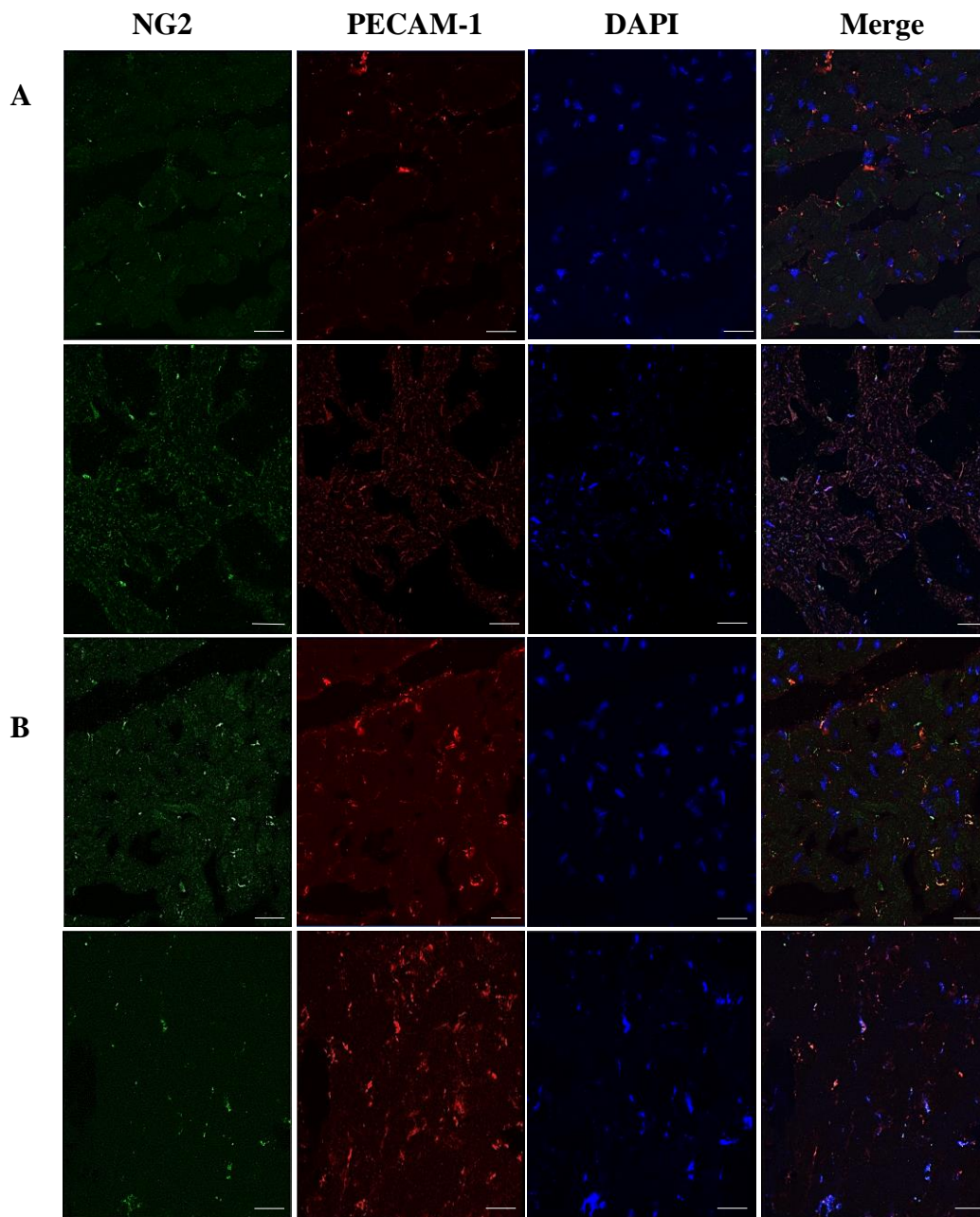
2.2. Microscopic assessment of capillary network

Figure 11: PECAM-1/ NG2 stainings

A) Capillary rarefaction is seen in the MI db con. Distribution of PECAM-1 and NG2 positive signals is poor in untreated myocardia after 24h of I/R. B) Upon LNA-92a administration, PECAM-1/ NG2 positive signals increase. Representative pictures taken in confocal microscopy display a dens capillary network (scale bar= 25 μ m).

Stainings from the 24 h model reveal that LNA-92a administration is entailed by higher levels of PECAM-1/ NG2 (MI db con PECAM-1: $338.7 \pm 18.4/\text{mm}^2$ and NG2: $248.7 \pm 11.7/\text{mm}^2$ and for MI db LNA-92a PECAM-1: $567.7 \pm 23.2/\text{mm}^2$ and NG2: $362.3 \pm 19.1/\text{mm}^2$). Compared to the db con, PECAM-1 values are increased by 40.3 % and NG2 by 31.3 %.

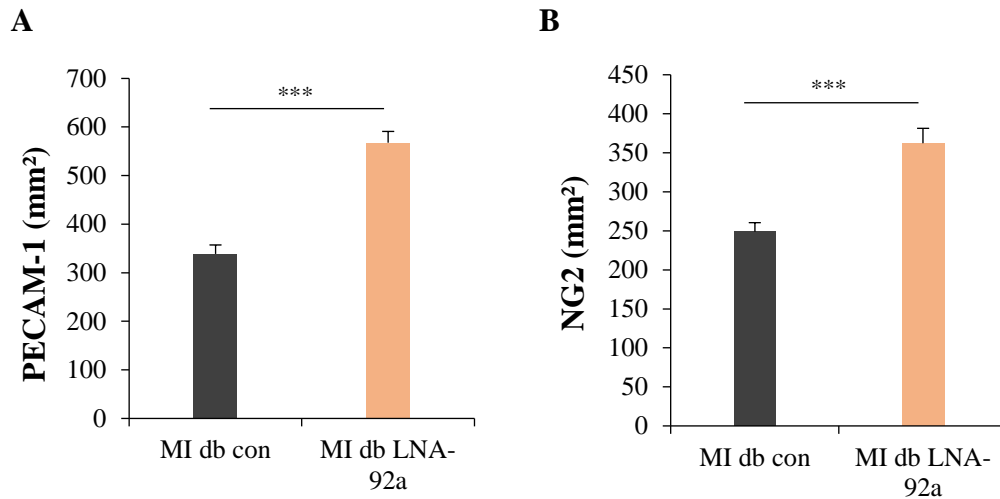


Figure 12: Assessment of capillary density in the 24h model

A) Analysis of PECAM-1 and B) of NG2 positive signals in fluorescence microscopy. While PECAM-1 and NG2 values were low in controls, capillary density upon LNA-92a increased. (Mean ± SEM, *p<0.001)**

2.3. Assessment of apoptosis

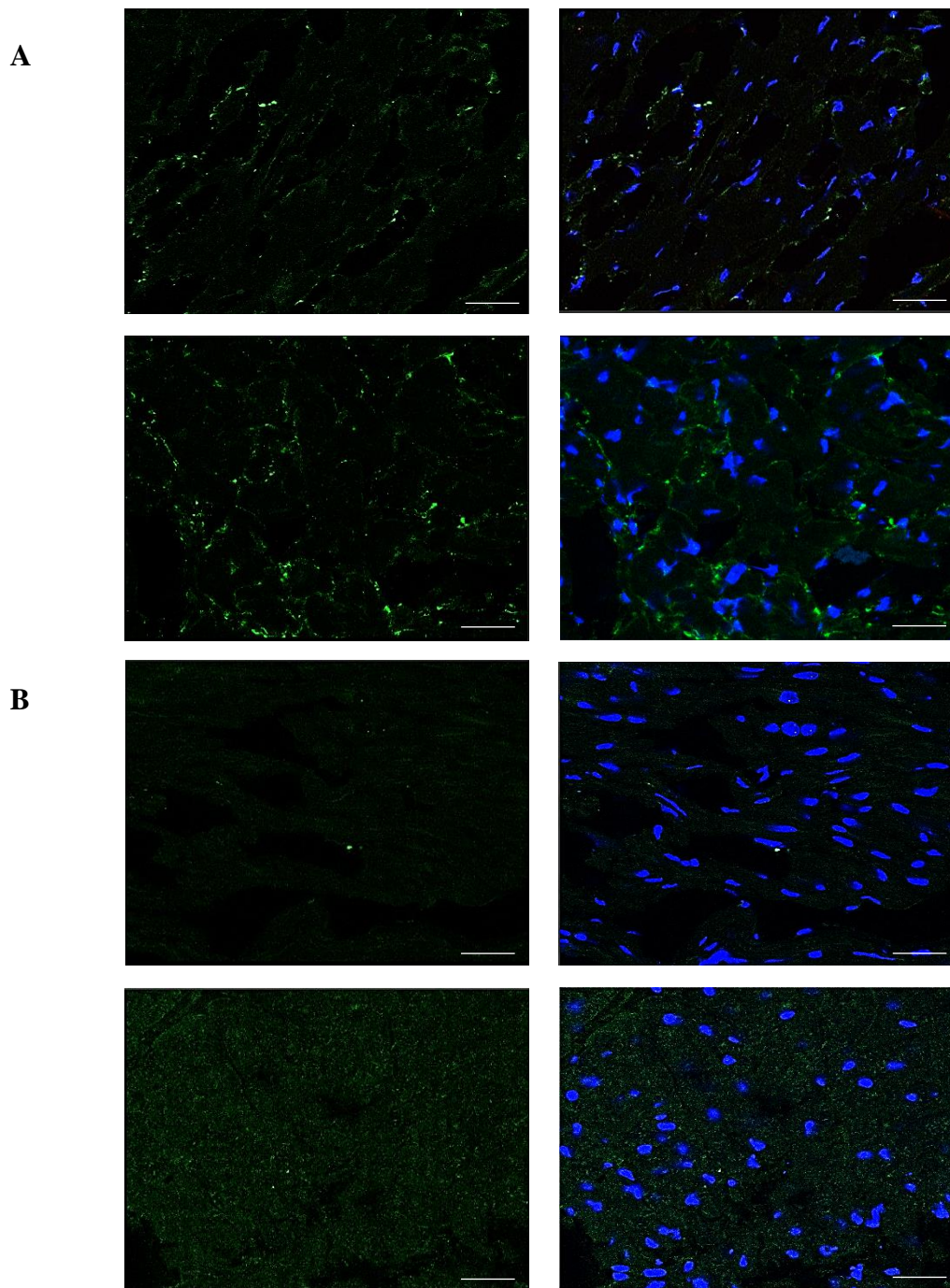


Figure 13: Representative TUNEL stainings

While increased amount of TUNEL positive signals (green) is seen in untreated animals (A= MI db con), LNA-92a administration was capable of reducing apoptosis in the MI db LNA-92a group (B) (scale bar = 25 μ m) (blue=DAPI)

Twenty-four hours after I/R, occurrence of apoptosis as seen in TUNEL stain, is drastically increased in untreated diabetic pigs (MI db con: 10.2 ± 2.88 +/hpf). LNA-92a reduced development of apoptosis also in the 24 h model (MI db LNA-92a: 4.04 ± 1.13 +/hpf). Thereby, amount of apoptosis is decreased by 60.32 % after treatment.

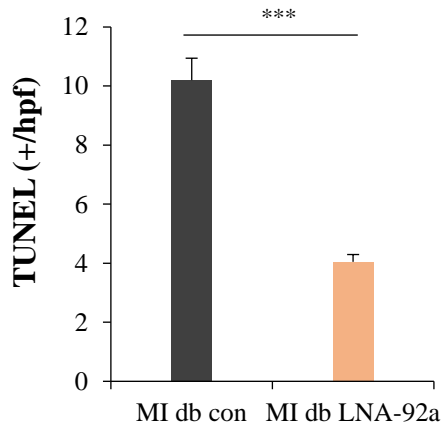


Figure 14: Quantification of TUNEL stainings

Significantly less apoptosis signals are seen after 24h of I/R upon LNA-92a treatment (Mean \pm SEM, * $p < 0.001$).**

2.4. HE staining for inflammation

Tissues gained in the 24 h model were stained in H&E for the detection of inflammation and cell infiltration. Quantification was assessed in a scoring scheme from 1 to 3 (1 = mild infiltration, 2 = moderate, inflammatory cells visible, but connective tissue intact, 3 = severe, inflammatory cells infiltrate the tissue intensely). As can be seen in the graph (figure 15, C), inflammation is severely enhanced in untreated, infarcted, diabetic animals, LNA-92a could significantly mitigate cell infiltration.

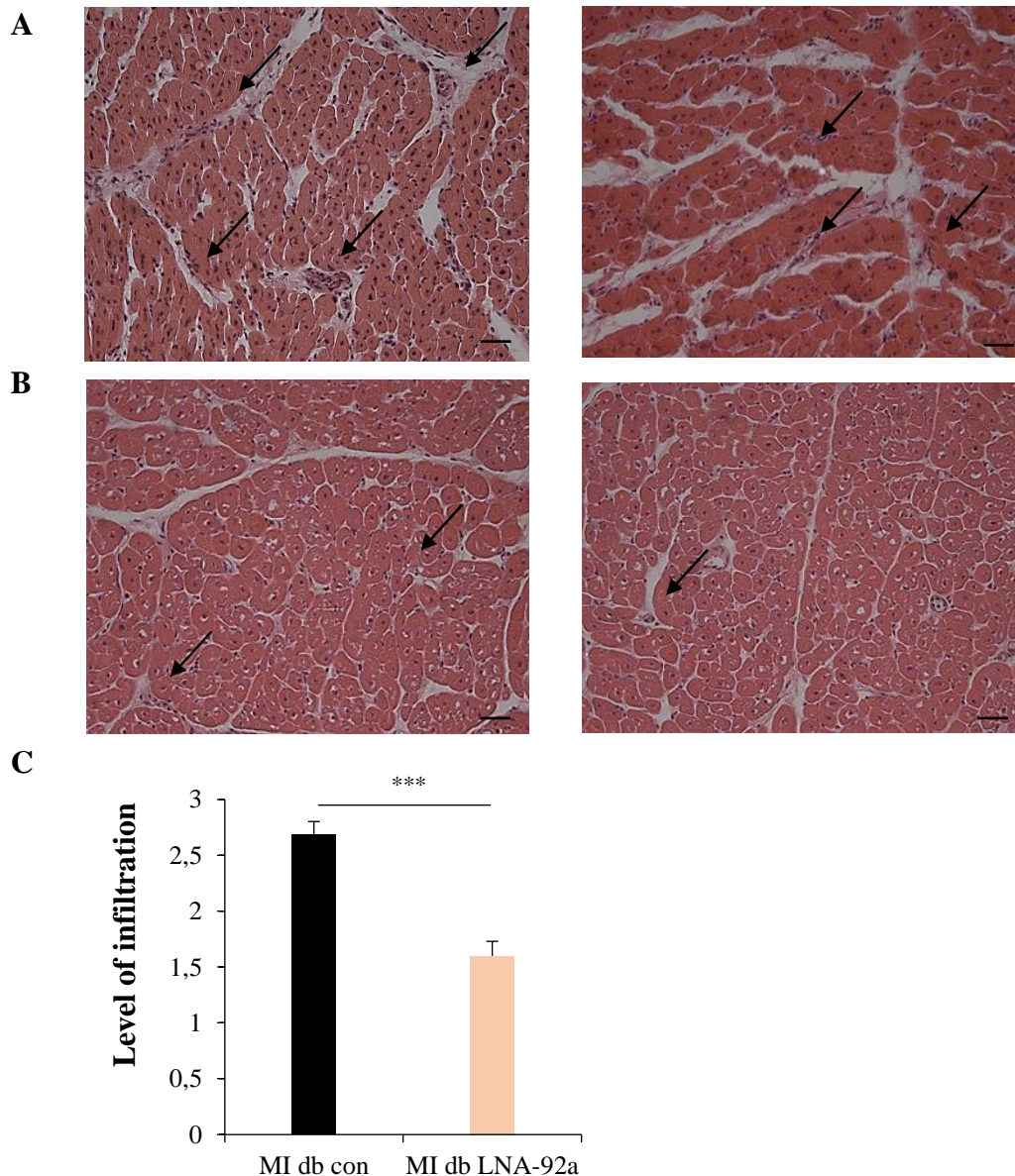


Figure 15: HE staining for inflammation

A) HE stains display pronounced inflammation (arrows) in the MI db con. B) Less cell infiltration is seen in the MI db LNA-92a group (scale bar = 50µm). C) Level of infiltration is reduced after LNA-92a treatment. (Mean ± SEM, *p<0.001)**

2.5. Global heart function

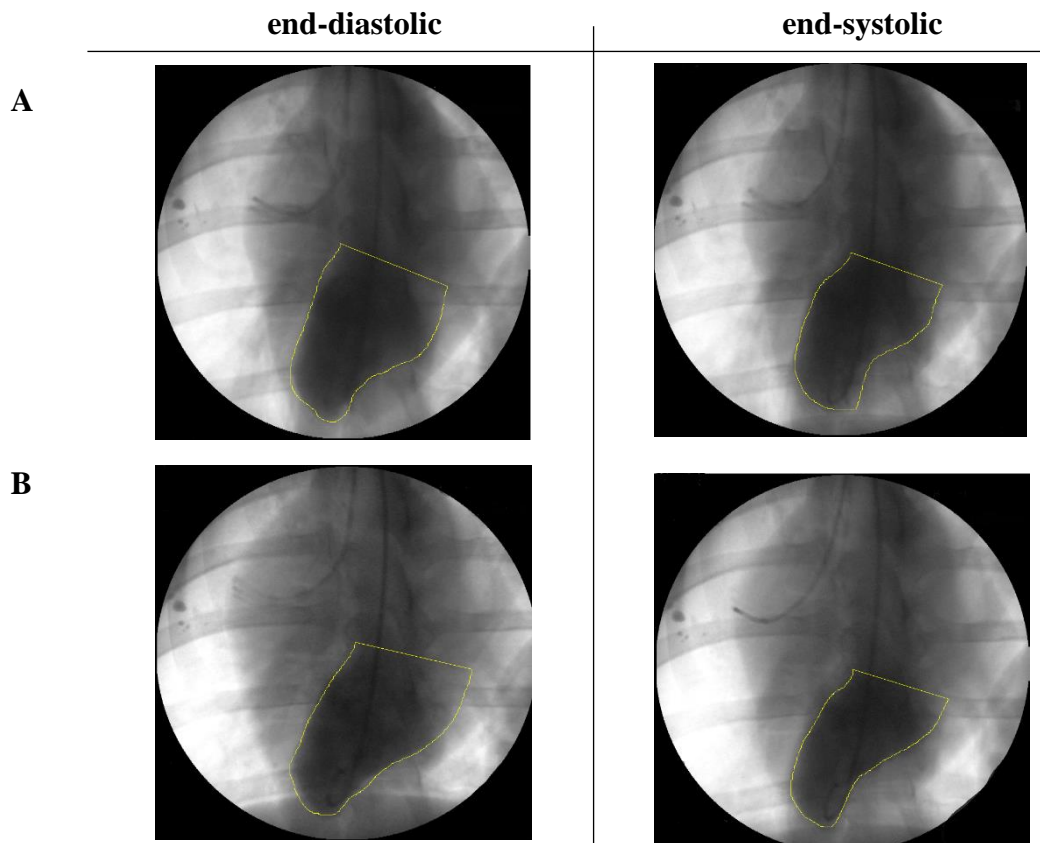


Figure 16: Angiograms (24 h post I/R)

Angiograms taken 24h after I/R via contrast agent application into the LV unveil reduced EF in the MI db con (A). Cardiac function is improved upon miR-92a inhibition. EF is increased in the MI db LNA-92a animals (B).

In the 24 h model, EF drastically decreased in untreated pigs indicating a poor cardiac output. In the treated animals, loss of EF was less pronounced (~ 13 %) as seen in figure 16 (A+B). LVEDP is high pre-ischemia in both diabetic groups, but values further increase 24 h after I/R in the MI db con group. In the MI db LNA-92a group, LVEDP (Δ LVEDP: 0.3 mmHg) barely changed from baseline measurements to the 24 h time point.

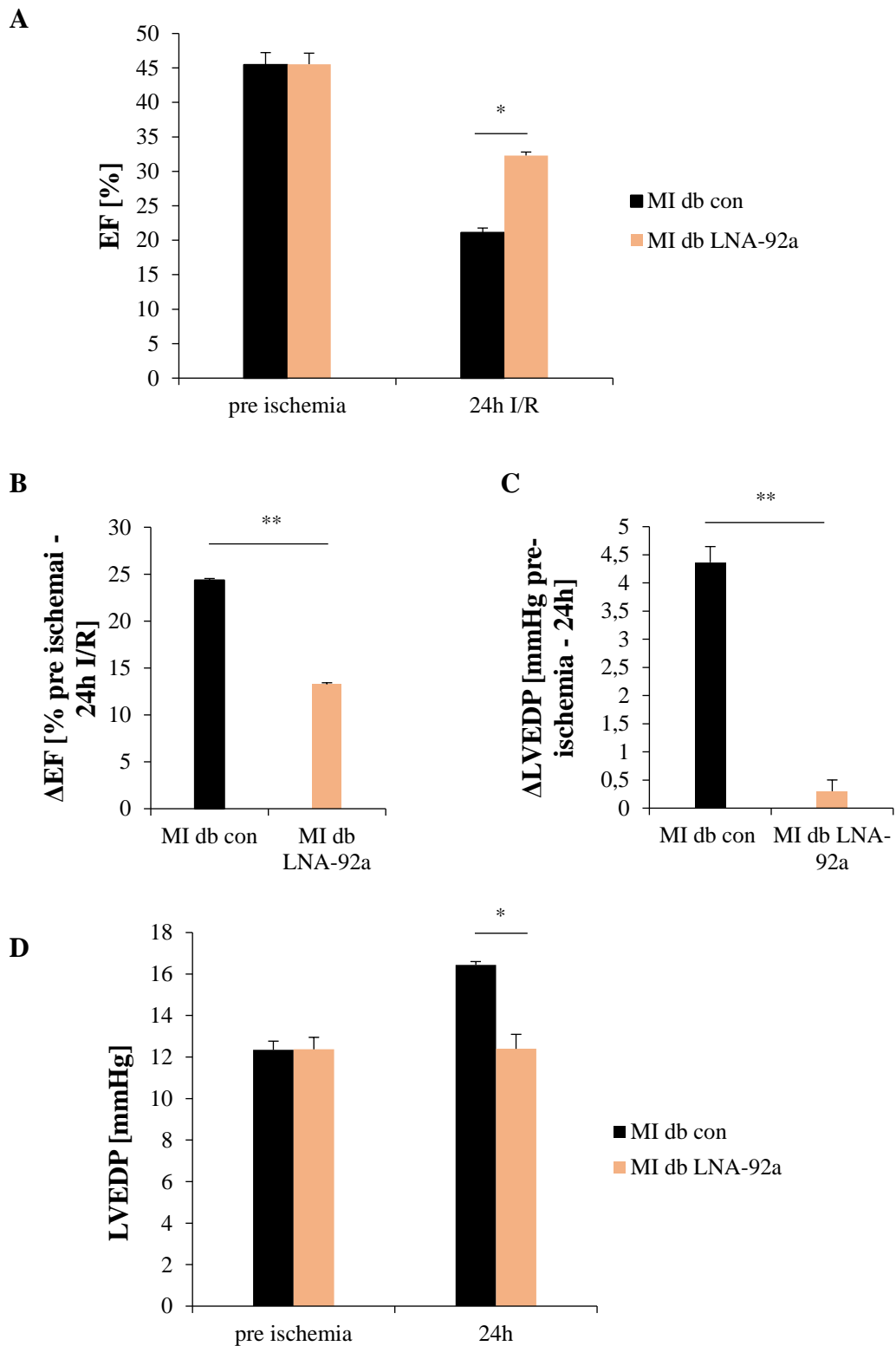


Figure 17: EF and LVEDP obtained in the 24 h model

A) EF is similar in the MI db con and MI db LNA-92a cohort. After 24 h it is significantly reduced in the MI db con compared to the treated group **B)** Loss of EF is less strong in the treated animals. **C)** Delta LVEDP shows an increase in the MI db con animals. **D)** LVEDP values obtained before and after (24 h) infarction. (Mean \pm SEM, * $p < 0.05$, ** $p < 0.01$)

3. Data from the stent model

3.1. Blood glucose levels

Blood glucose was measured from a venous blood sample gained from each pig undergoing stent implantation. As can be seen in figure 18, blood glucose levels are high in diabetic groups. Wildtype pigs show physiologic glucose levels indicating they were sober at the day of each intervention. When comparing blood glucose levels within one group, they are approximately identical regardless the day of the intervention. This finding counts for all 4 groups. Thus, regional catheter based LNA-92a administration apparently does not affect systemic blood glucose levels. In INS^{C94Y} pigs, glucose values were high throughout the experiment due to lack of insulin therapy. High glucose levels in those pigs are intended to maintain their diabetic cardiac phenotype, as described beforehand.

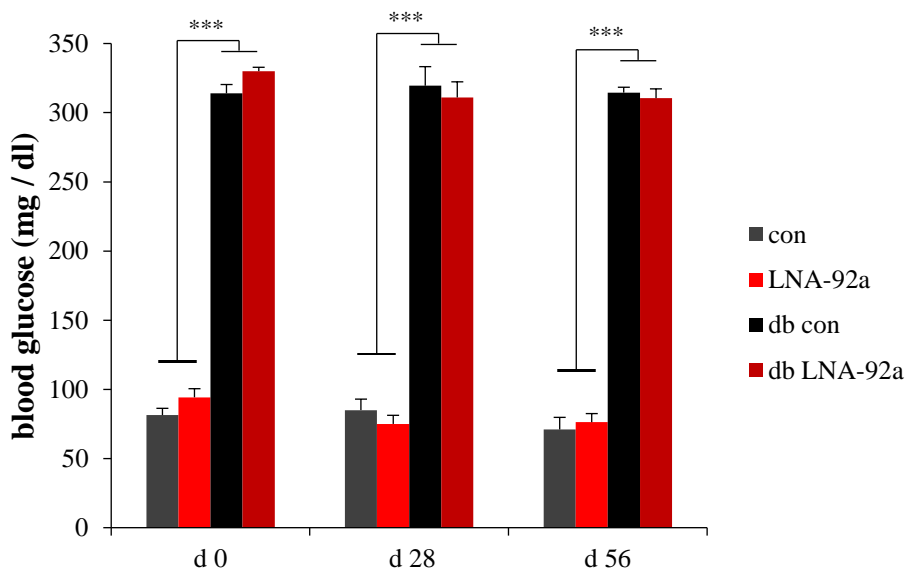


Figure 18: Blood glucose levels measured from stent implanted pigs

Blood glucose levels are high in transgenic diabetic pigs throughout the duration of the experiment. LNA-92a did not influence blood glucose values. (Mean \pm SEM, *** $p < 0.001$)

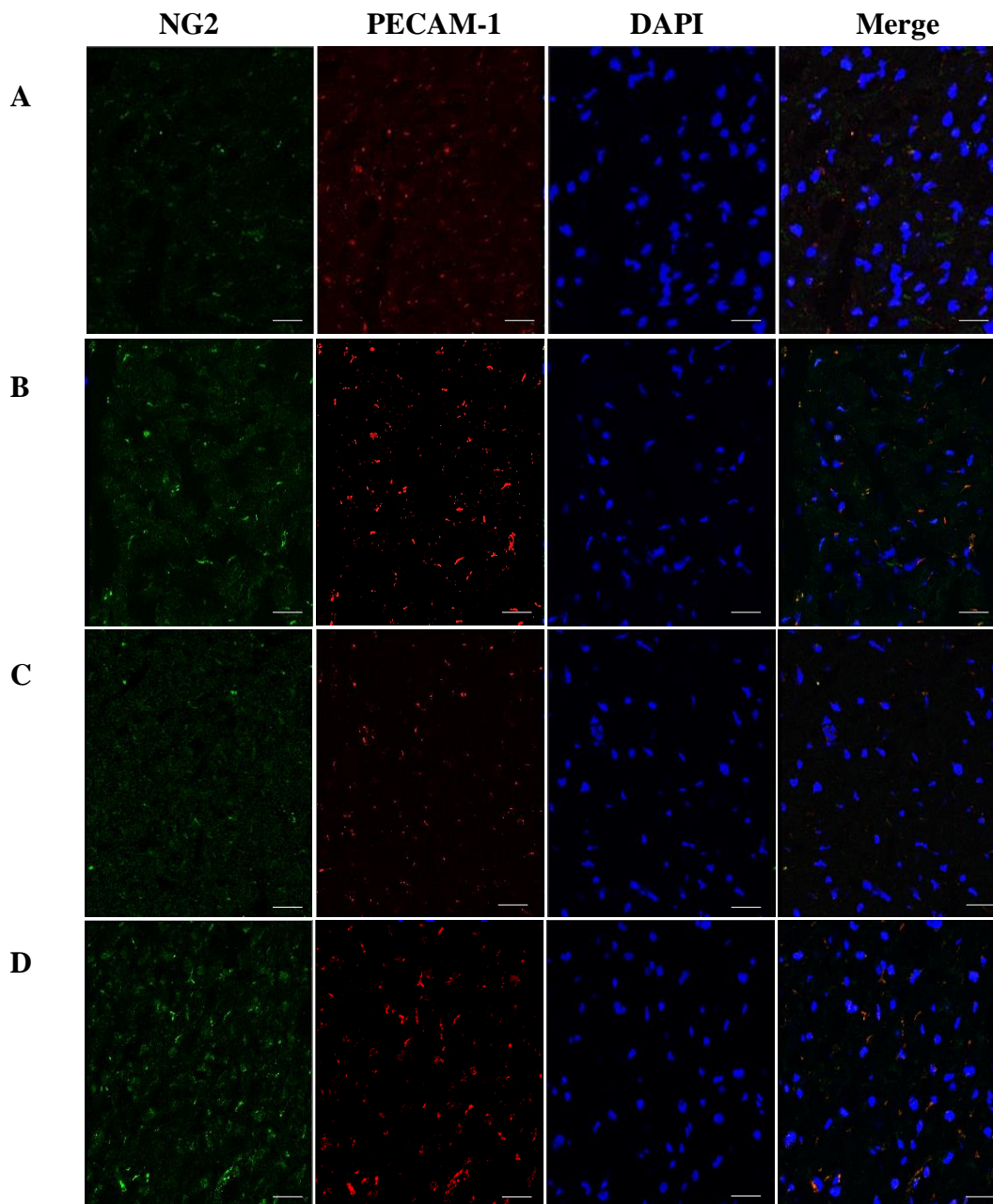
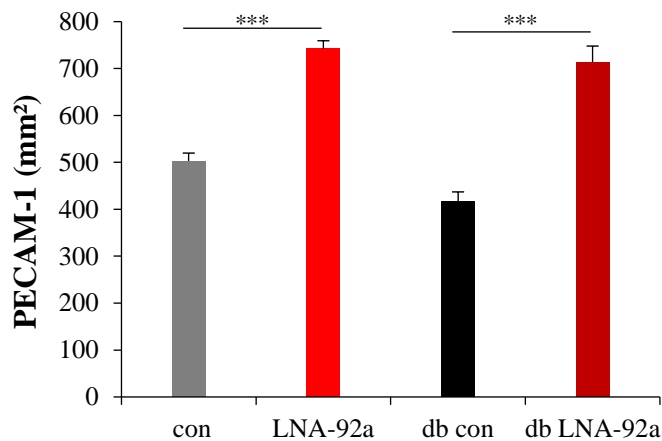
3.2. Microscopic assessment of capillary network

Figure 19: PECAM-1/ NG2 stainings

A) con, B) LNA-92a, C) db con, D) db LNA. Representative pictures taken in confocal microscopy for NG2 (green color) and PECAM-1 (red color) show an increase in capillary density in both LNA-92a treated groups. Capillary rarefaction is particularly pronounced in the db control group. DAPI was utilized as nucleic stain (scale bar = 25 μ m).

Neovascularization was quantified in histological analysis. PECAM-1/ NG2 stain showed an increase in density in the LNA-92a (PECAM-1: LNA-92a $742.8 \pm 16.4/ \text{mm}^2$ and NG2: $596.4 \pm 17.3/ \text{mm}^2$) group and the db LNA-92a group (PECAM-1: LNA-92a $713.9 \pm 34.1/ \text{mm}^2$ and NG2: $515.1 \pm 22.1/ \text{mm}^2$). Interestingly, db LNA-92a treated hearts show a dense microcirculatory network. A distinct capillary rarefaction is detected in both control groups (con PECAM-1: LNA-92a $502.9 \pm 16.8/ \text{mm}^2$ and NG2: $382.7 \pm 20.2/ \text{mm}^2$ and for db con PECAM-1: LNA-92a $416.9 \pm 20.1/ \text{mm}^2$ and NG2: $353.5 \pm 24.4/ \text{mm}^2$). Regarding the relative efficacy of the PECAM-1 gain after miR-92a inhibition, this results in a gain of 48 % in the wildtype and 71 % in the diabetic cohorts compared to their controls. For NG2 it is a gain of 55 % in the wildtype and 46 % in diabetics.

A



B

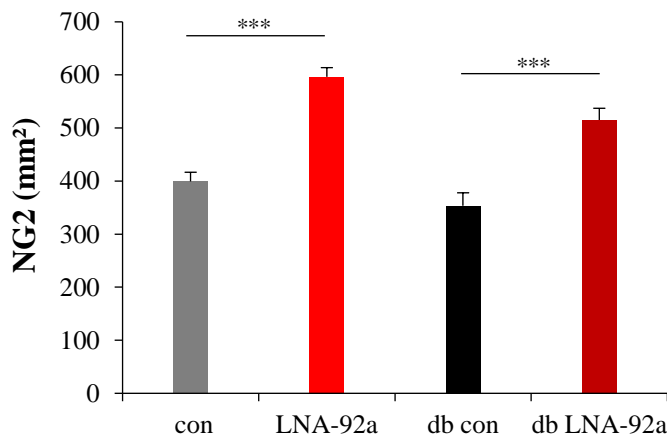


Figure 20: Assessment of capillary density in the stent model

A) Analysis of PECAM-1 and B) of NG2 positive signals in fluorescence microscopy show increase of capillary density after LNA-92a treatment. (Mean ± SEM, *p<0.001)**

3.3. Collateral and Rentrop classification

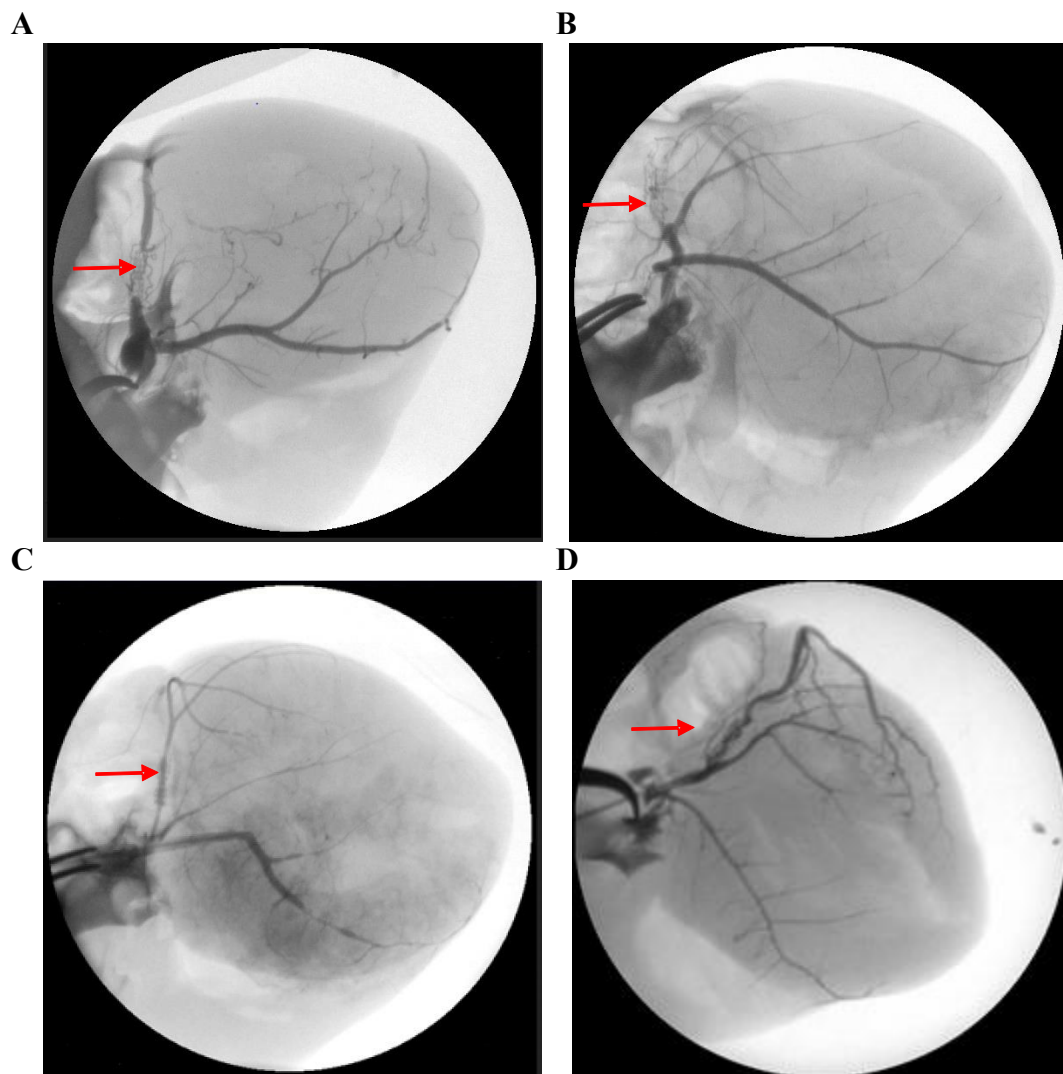


Figure 21: Post mortem angiograms

A) Capillary filling is poor in the wildtype con animal in the ischemic region distally from the implanted stent (red arrow). Even more pronounced capillary regression is seen in the db con heart (C). B) LNA-92a treated heart shows a developed capillary network. D) Contrast agent application reveals high quantity and quality in the db LNA-92a group.

Collateralization was obtained in post mortem angiograms using contrast agent, showing an increase in vessel formation in the LNA-92a and db LNA-92a group. While amount of collaterals is poor in the control group and the db con, numbers increase after LNA-92a administration. The most interesting aspect of figure 22 A, is the striking outcome of collateralization in the db LNA-92a. Amount of collaterals is around 75 % higher in this group in comparison to its control group. High Rentrop score in both treatment groups unveils filling of collaterals. Collateralization was not assessed in the 24h model due to the short timeframe. Maturity of collaterals is set out in Rentrop scoring.

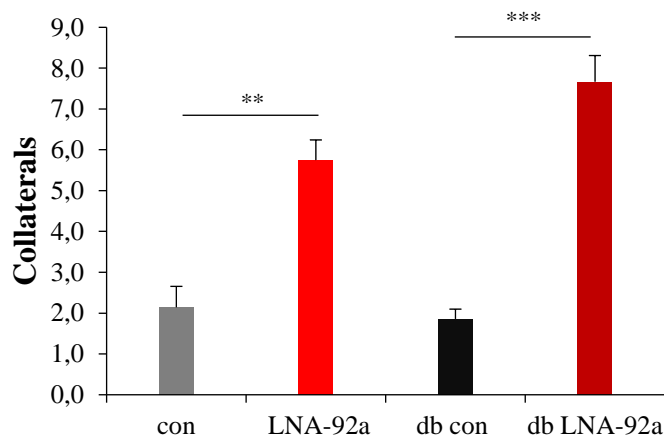
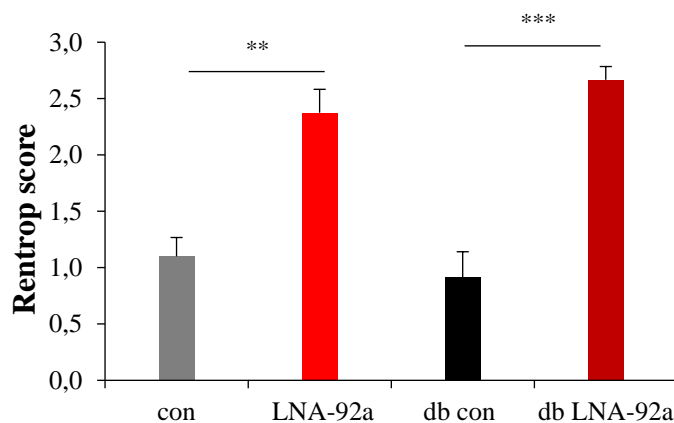
A**B**

Figure 22: Collaterals and Rentrop score

A) Amount of collaterals increases after LNA-92a treatment. Striking amounts are seen in the db LNA-92a. B) High classification in Rentrop unveils advanced capillary filling in treated animals compared to wildtype and diabetic controls. (Mean ± SEM, **p<0.01, *p<0.001)**

3.4. Assessment of apoptosis

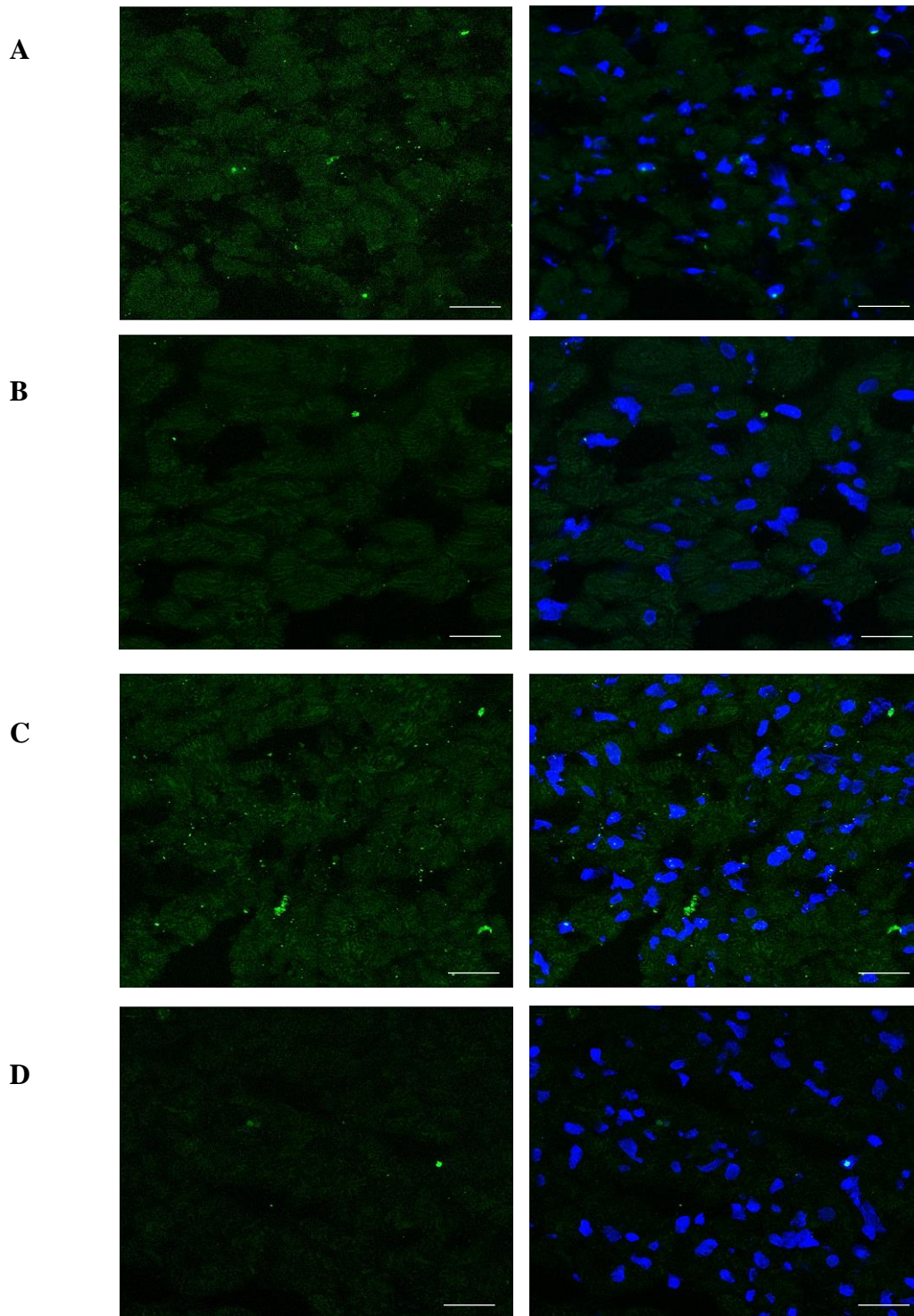


Figure 23: Representative TUNEL stainings

A) con, B) LNA-92a, C) db con, D) db LNA-92a. Representative stains taken in confocal microscopy unveil enhanced apoptosis in animals who received a scrambled LNA (A, C).

Tissue from LNA-92a treated hearts show less positive TUNEL signals (B, D) (scale bar = 25 μm) (blue = DAPI).

Apoptosis was assessed from RCX tissue using the TUNEL method. TUNEL stain gives evidence for increased apoptosis in the con group (6.3 ± 0.55 +/-hpf) and even more pronounced values (7.86 ± 0.45 +/-hpf) in the db con group. Following LNA-92a administration, a significant decrease of apoptosis is recorded in wildtype (LNA-92a: 2.64 ± 0.34 +/-hpf) and diabetic myocardia (db LNA-92a: 2.94 ± 0.35 +/-hpf). Hence, LNA-92a administration reduced the development of apoptosis by 58.1 % in wildtype pigs compared to the control group and by 62.6 % in diabetic pigs in comparison to the diabetic controls.

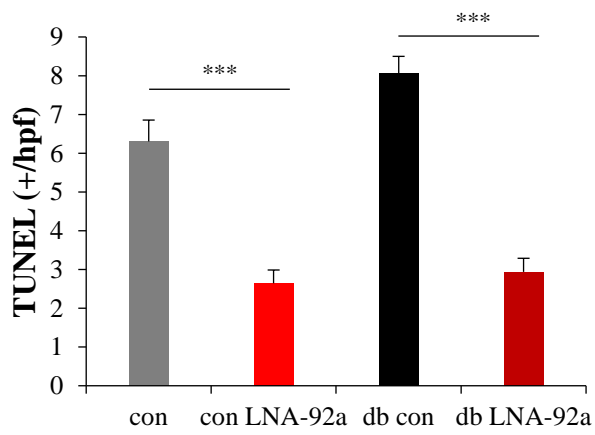


Figure 24: Apoptosis stainings

TUNEL positive cells per high power field (hpf) were counted. Increased amount of TUNEL positive signals is seen in both control groups, upon LNA-92a treatment apoptosis is reduced in wildtype and diabetic groups. (Mean \pm SEM, * $p < 0.001$)**

3.5. Sirius red stainings for fibrosis

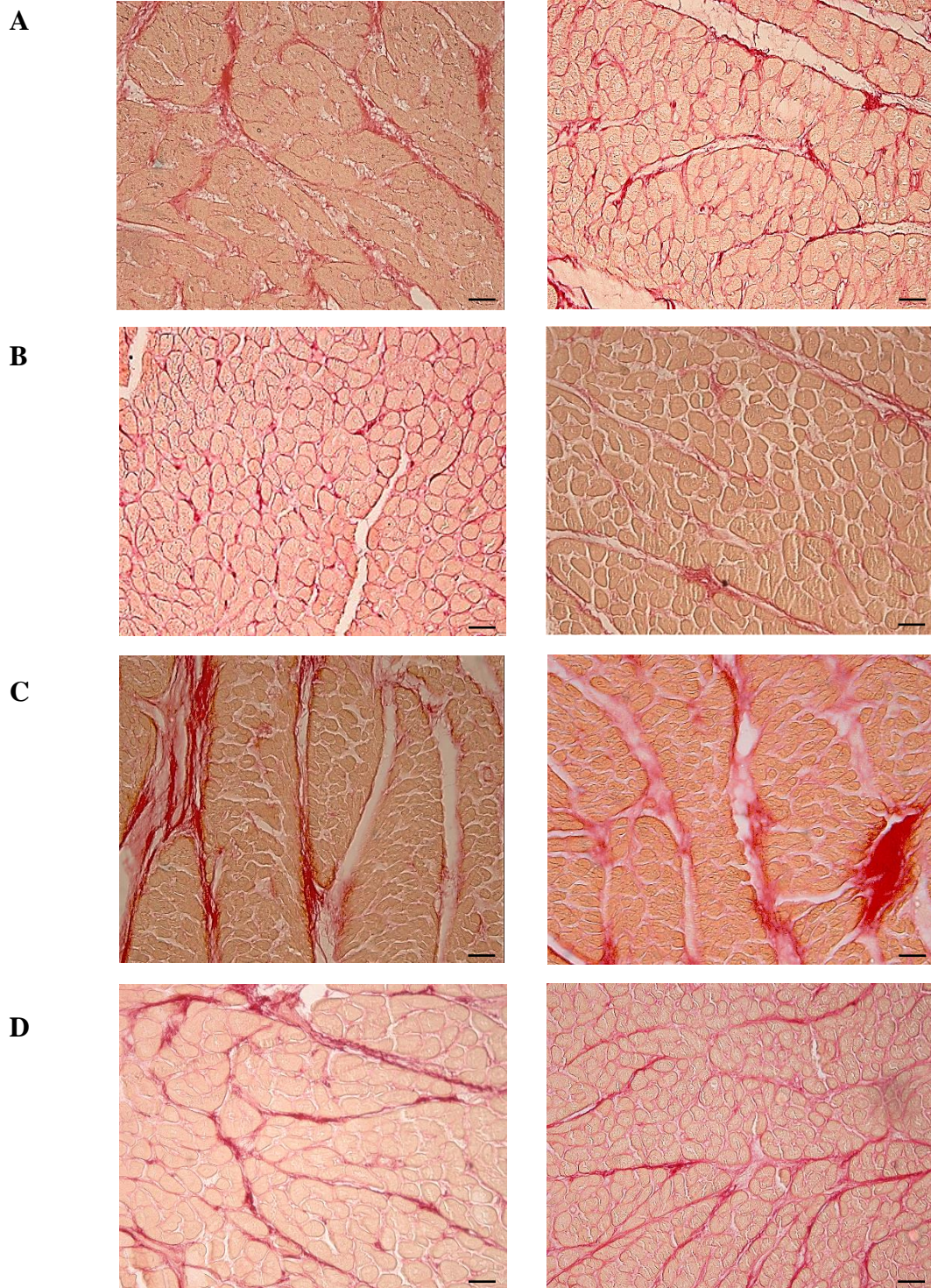


Figure 25: Fibrosis stainings

A) Control animals show increases in interstitial fibrosis in the RCX region. B) LNA-92a mitigates development of fibrosis after stent implantation in wildtype. C) Vast areas of collagen fibres stained in red color indicate a remodelling process in favor of fibrotic tissue in diabetic control pigs. D) As seen LNA-92a treated wildtype pigs, LNA-92a reduces fibrosis also in the transgenic diabetic group. (scale bar = 50 μ m)

Fibrosis development increases in the onset of DM. Db control animals have significantly enhanced interstitial fibrosis (16.8 ± 0.4 %) compared to the wildtype control group (12.75 ± 0.5 %). LNA-92a application could reduce the development of fibrosis in the LNA-92a group as well as in the db LNA-92a animals (LNA-92a: 8.6 ± 0.4 %; db LNA-92a: 12.11 ± 0.4 %). The percentage efficacy of mitigating fibrosis was higher in comparison to both wildtype groups than in both diabetic groups (reduction of 47.5 % between the LNA-92a group and the con group in wildtype and in diabetics 39.2 % reduced in the db LNA-92a animals compared to the db con). Since fibrosis is a longtime event upon ischemia, it was not detected in the 24h model.

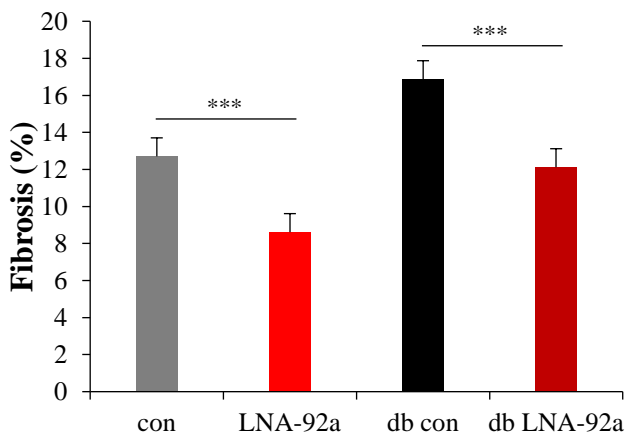


Figure 26: Development of fibrosis

Pronounced fibrosis is seen in untreated diabetic hearts. Upon LNA-92a treatment, development of fibrosis is reduced in the wildtype and diabetic pigs. (Mean \pm SEM, *** $p < 0.001$)

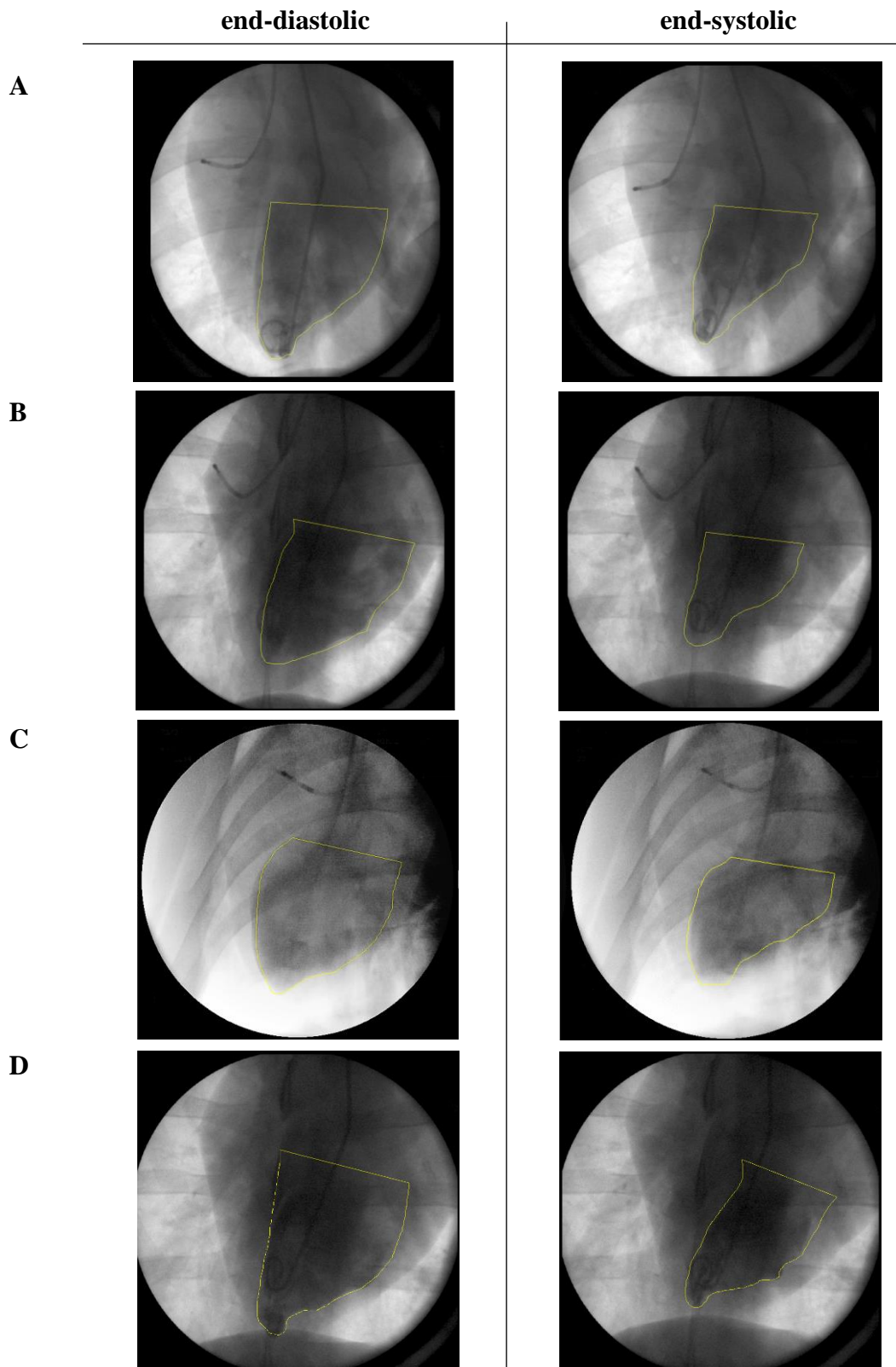
3.6. Global heart function data

Figure 27: Angiograms taken on day 56 of the stent model

EF is reduced in the con (A) and db con (C). After LNA-92a injection, EF increases in the wildtype (B) and diabetic (D) pigs.

Global heart function was obtained on day 0, 28 and 56 as LVEDP and EF by placing a pressure-tip catheter in the LV. EF was determined planimetrically from angiograms with Image J.

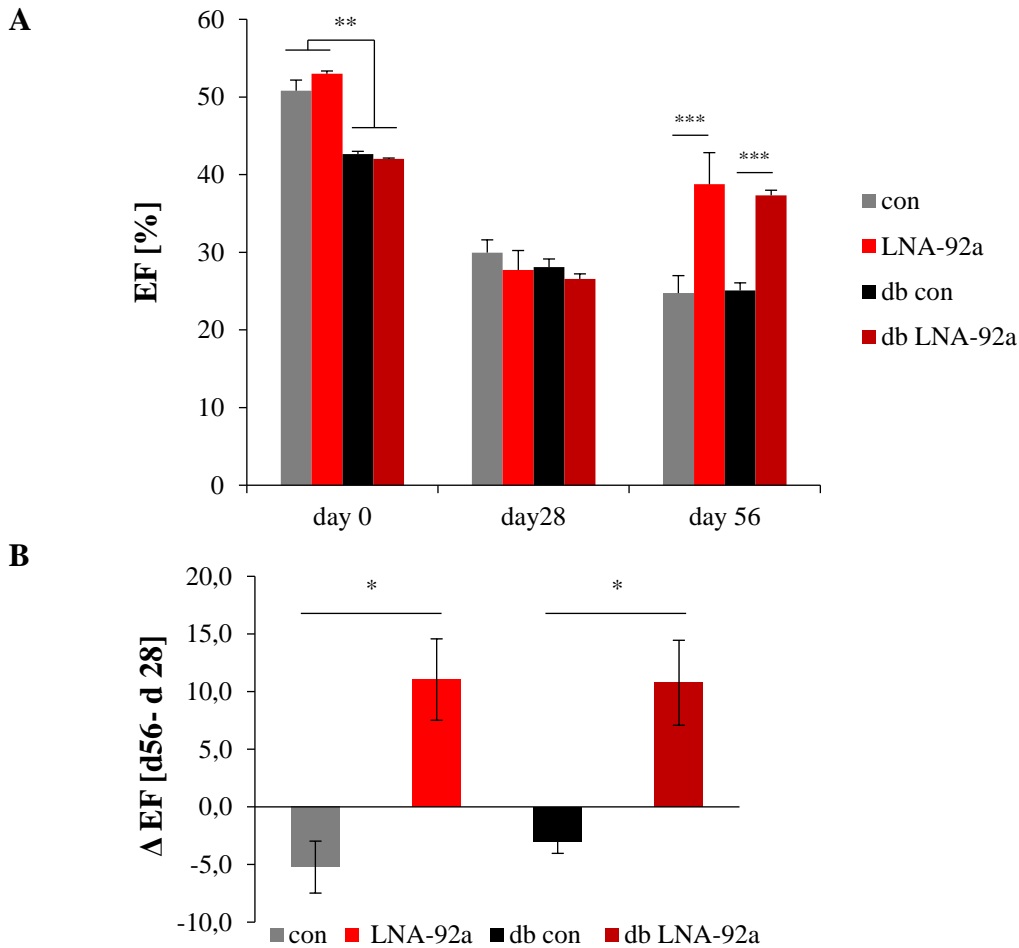
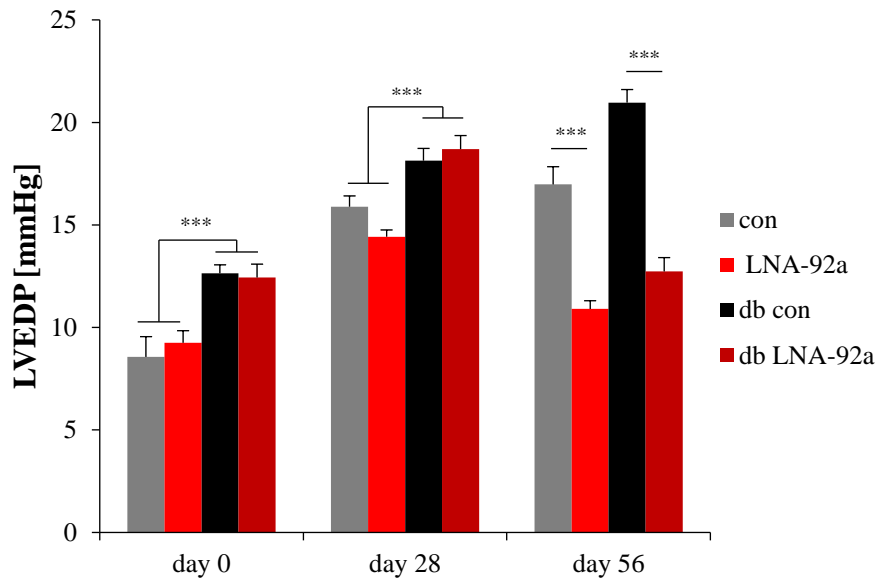


Figure 28: Improvement of EF

A) Cardiac performance assessed as EF improves after regional catheter based LNA-92a administration. B) Delta EF reveals the extent of decrease resp. increase of EF measures from d 28 to d 56. (Mean \pm SEM, * p <0.05, ** p <0.01, * p <0.001)**

As can be seen in figure 28, baseline values (d 0) of EF in diabetic pigs are 17 % lower on average compared to wildtype pigs. Twenty-eight days after stent implantation, all groups consistently show a decrease of EF compared to day 0. Notably, EF significantly increases on day 56 in both groups, the LNA-92a and the db LNA-92a treated group, whereas values further decline in both control groups. These findings are depicted as delta EF. While EF further declined in the control groups, cardiac output is increased in the treatment groups to a similar extent.

A



B

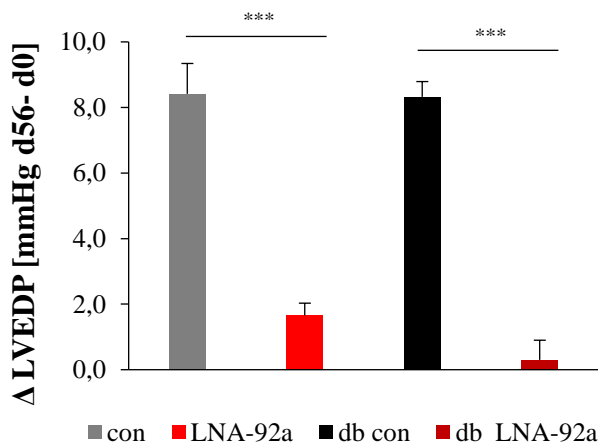


Figure 29: LVEDP measurements

A) LVEDP is a measure for left ventricular pressure. Treatment via LNA-92a application had a mitigating effect on cardiac pressure. B) Delta LVEDP reveals the extent of decrease resp. increase of LVEDP measures. (Mean ± SEM, *p<0.001)**

LVEDP increased from day 0 to day 28 from 8.6 ± 1.0 to 15.9 ± 0.5 in wildtype and from 12.4 ± 0.7 to 18.9 ± 0.6 in db. Thus, LVEDP was 44 % higher in db in comparison to wt at day 0 and further increased to 52 % till day 28 due to stent implantation. On day 56, LVEDP decreased in the LNA-92a groups. Remarkably, LVEDP drastically decreased in db LNA-92a treated animals in contrast to the db control (db con: Δ LVEDP 8.3 ± 0.4 , db LNA-92a: Δ LVEDP 0.3 ± 0.6).

3.7. Regional heart function

On day 56, SES measurements were performed implanting ultrasonic crystals into the heart. SES revealed a worsening of regional cardiac contractility in both control (con, db con) groups. Functional cardiac reserve during pacing at 120 - 150 bpm was poor in alluded groups. As seen in figure 30, LNA-92a treatment significantly increases regional contractility. In treated animals, capacity of SES was high in baseline conditions and when paced at 120 resp. 150 bpm indicating a functional reserve of the myocardium.

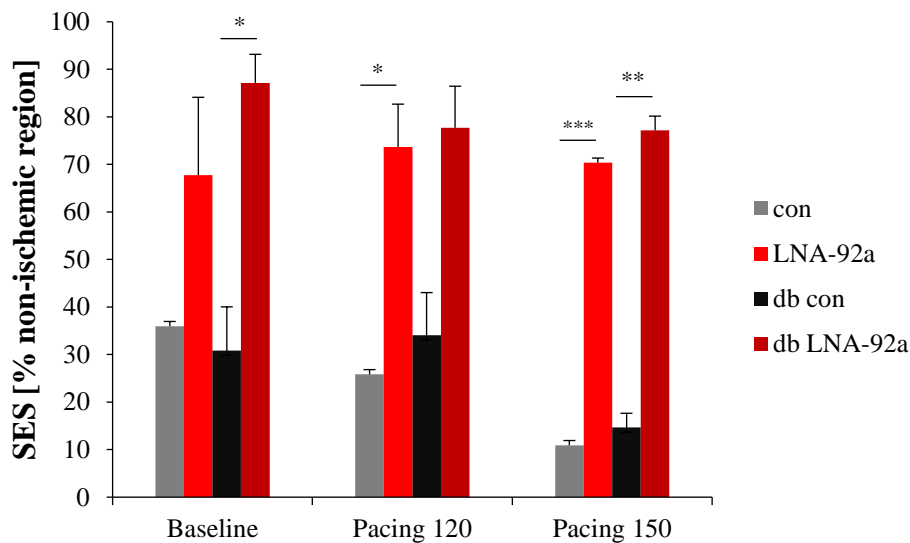


Figure 30: Subendocardial segment shortening

SES was obtained on day 56 at baseline heart rate and pacing of 120 resp 150 bpm. While capacity of contractility drops in both control groups, when paced at 120 and 150 bpm, SES does not significantly decrease when paces in treatment groups. (Mean \pm SEM, * $p < 0.05$, ** $p < 0.01$, *** $p < 0.001$)

V. DISCUSSION

1. Ameliorating hallmarks of myocardial ischemia

1.1. Mechanism of induced capillarization via miR-92a inhibition

The capacity of endothelial cells for migration and angiogenesis is a crucial prerequisite for the neof ormation of vessels. In cell culture assays, the angiogenic effect of LNA-92a application was proven and is apparently feasible even in high glucose conditions. Restoration of blood flow constitutes the basis for a recovery of the myocardium after ischemic impact. Present data unveils that LNA-92a administration is capable of enhancing capillary density in wildtype and db hearts in the chronic as well as the acute model. Indicating their maturity, NG2 staining demonstrated pericyte investment. However, Pecam-1/ NG2 stains do not evidence capillary filling and functionality. Whereas in the chronic model, the time frame allows for capillary sprouting and maturation over weeks, the 24 h period after infarction is too short. Here, most likely, preservation of pre-existing capillaries took place. Explanatory theories for increase in capillary density are either the promotion of angiogenesis (chronic model) via miR-92a inhibition due to the influence of its target genes or the protection of preexisting endothelial cells (24h model).

Integrin $\alpha 5$ is a core regulator of angiogenesis [156, 157, 125]. Previous studies substantiate its upregulation upon miR-92a inhibition and thereby identify it as a direct target of miR-92a [122, 123, 158]. Longtime pro-capillary effects in LNA-92a treated animals in this study are most likely due to integrin $\alpha 5$ level recovery. In cultured cells, integrin $\alpha 5$ expression was diminished in high glucose media [159]. In a db murine model of dermal wound healing, integrin $\alpha 5$ and Sirt-1 were upregulated after light- induced anitmiR-92a therapy, which resulted in healing-supportive effects [160]. Integrin $\alpha 5$'s upregulation might also play a crucial role in the db LNA-92a groups concerning neovascularization.

Moreover, eNOS mediates neovascularization through its involvement in the VEGF-mediated vascular signaling [161, 162]. Concomitant with eNOS' regulation by integrin $\alpha 5$ and by KLF-2, eNOS expression profile is reduced in the presence of overwhelming miR-92a levels and recovered after LNA-92a treatment by the

increase of its regulators integrin $\alpha 5$ and KLF-2 [122]. Proangiogenic features of LNA-92a application might consequently also be ascribed to eNOS in these models.

KLF-2 is a direct target of miR-92a. Overexpressed miR-92a as well as high glucose levels decrease KLF-2 expression [127, 163]. It is well known that pulsatile forward directed shear stress is an essential stimulus for a cascade of anti-thrombotic and – inflammatory effects and induces the upregulation of KLF-2 [100, 164]. In present study, improvement of vascular integrity and protection from capillary rarefaction can be explained by induction of KLF-2 expression via miR-92a inhibition. Diabetic animals might have additionally benefited from LNA-92a application since KLF-2 values are decreased by diabetes per se. Further, enhanced collateralization and the advanced maturation of collaterals prove for ameliorated hemodynamic conditions and blood flow favoring increased pulsatile shear stress which might promote KLF-2's expression [165].

Capillary regression is a hallmark seen in diabetes. Untreated DM by itself rarefies micro circulatory density in the retina and heart [166, 49]. Angiopoetin-2 (Ang-2) is believed to play a key role for capillary destabilization. During diabetes it is overexpressed and causes cell death and inhibits vascularization [167]. Clinical mechanisms for its upregulation are explained in hyperglycemia (marked by the glycated hemoglobin HbA1c) and in endothelial damage promoted by vWf which releases Ang-2 [168]. Contrary tasks compared to those of Ang-2 are attributed to Angiopoetin-1 (Ang-1); it enhances vessel stabilization, vascular sprouting and has an anti-leakage effect [169]. Ang-1 binds to Tie-2 resulting in activation of signaling pathways including PI3-kinase/AKT and ERK which in turn decreases the expression of adhesion proteins such as ICAM-1 and VCAM-1. Increased Ang-2 hampers Ang-1/Tie-2 signaling by binding to Tie-2. In cell culture assays, concentrations of Ang-1 were significantly lower when miR-92a was overexpressed in the dish [170]. Inhibition of miR-92a might lead to a balanced ratio of Ang-1 and Ang-2 thereby equilibrate vessel destructive effects.

After reperfusion duration of 24h, neovascularization cannot be assumed and is even improbable due to its duration up to 7 days [171, 172, 123]. Regarding capillary density in LNA-92a treated animals from the 24h trial, provided data argues in favor of the endothelial protection by inhibiting cellular damage after ischemia/reperfusion rather than neovascularization. The protective LNA-92a

effect might be evoked by its impact on angio-proliferative target genes as described previously.

1.2. Positive effect on fibrosis development

The development of fibrosis is a double-edged sword: it is a physiological healing event but it has a detrimental impact because it enhances progressive impairment of the heart's function due to increased tissue stiffness and loss of function. Fibrosis is a core determinant in CAD arising from ischemia and cell death. Further, chronic ischemia triggers excess inflammation promoting fibrosis [173]. In the onset of DM, fibrotic development is significantly facilitated mostly due to high AGE levels, which is a trigger for collagen crosslinking [49, 174]. After LNA-92a therapy, fibrosis is significantly reduced in all animals of both treatment groups. This reduction might be justified by the improvement of capillarization as well as the reduction of apoptosis which obviously go together [175]. Mitigated inflammation and cell infiltration might also contribute to attenuated fibrosis. KLF-4 has been reported to regulate pro-inflammatory signaling [176]. As a direct target of miR-92a, it might be the key to LNA-92a induced inflammatory mitigation.

LNA-92a application was reported of reducing not only miR-92a expression but also miR-25 levels [123]. This is achieved by miR-25's similarity to the sequence of miR-92a varying in two base pairs only. MiR-25 is a promoter of heart failure because it regulates the calcium transporting ATPase SERCA2. As a regulator of Ca²⁺ uptake, it is essential for the contractile function of the heart. Previous studies report an upregulation of miR-25 in heart failure and its inhibition reduced fibrosis in mice hearts [177]. Its inhibition might play a role in the reduction of fibrosis development in LNA-92a treated animals of this study. Like miR-92a, miR-25 is overexpressed during DM per se [178]. A potential downregulation of miR-25 via LNA-92a might be an auxiliary secondary effect for the fibrosis reduction in the db treatment group.

1.3. Reduction of apoptosis

Apoptosis, a programmed cell death, is a common pathologic consequence in CAD triggered by oxidative stress, hypoxia and deprivation of nutrition to the cells by shortage of blood flow. Besides TNF α , the cell surface receptor Fas was identified

to decisively regulate apoptosis by binding to its ligand (FasL) [179]. Besides the death ligand induced apoptosis via FasL, other pathways of programmed cell death must be distinguished, like the mitochondrial apoptosis induced channel (MAC) activation or cytochrome C related apoptosis. Further, necroptosis and ferroptosis are special forms of programmed cell death.

In oncology research, miR-92a was shown to negatively regulate tumor protein p53 involved in apoptosis [180, 181]. Hinkel et al. have already linked a reduction of apoptosis in cell culture and porcine heart tissue of acute MI upon miR-92a inhibition [123]. Other cell culture assays suggest SMAD7 as miR-92a's key target to enhanced apoptosis. With excess miR-92a presence, SMAD7 is downregulated. Its anti-apoptotic impact is in the regulation of NF- κ B. This connection was stated as miR92a/SMAD7/NF- κ B p65 pathway; after miR-92a inhibition, SMAD7 increases, performing its anti-apoptotic potential [182]. Besides SMAD7 favorable effect, reduction of apoptosis in LNA-92a treatment groups is secondarily conditioned by improved capillarization. The drop of core triggers for apoptosis may also contribute.

Differences in TUNEL positive cells were obtained in this study. All untreated animals from both models and both conditions showed increases in apoptosis indicating an impaired cardiomyocyte status compared to treated myocardia. Interestingly, TUNEL levels were less pronounced in control animals from the chronic ischemia model compared to controls undergoing MI. Causal reason might be underlying different time frames: 24h after MI there is apoptosis due to ischemia but phagocytosis of apoptotic bodies might not start yet. LNA-92a treated animals undergoing MI experience less apoptosis ab initio due to mitigation of ischemic exposure, conceivably via already mentioned pathways and target gene influence. In the chronic ischemia model, apoptotic cardiomyocyte dropout already shifted in favor of tissue replacement with fibrosis.

1.4. Stabilization of cytoskeleton

Although data is not shown, tissue from all groups and both models were stained for α -actinin to check for cytoskeletal integrity. A functioning cytoskeletal activity is pivotal for muscular myocardial contractility. As a dynamic network, the cytoskeleton enables the heart to stretch and contract with each heart beat [183].

The cytoskeleton is a delicate scaffold consisting of several proteins. Alpha-actinin is a cross-linking protein providing the connection between cytoskeletal and transmembrane receptors. Given its versatile functions, α -actinin is easily changed during ischemia. In dogs undergoing coronary ligation, drastic decreases in α -actinin as well as Z-lines percentages were obtained 3h after intervention [184]. Hitherto, nothing is reported about how miR-92a influences the cytoskeleton and there are no identified target genes directly involved in cytoskeletal regulation. However, the question if miR-92a presence influences α -actinin has already been answered. In a rat model of MI, an anti-miR-92a impregnated hydrogel sheet could enhance α -actinin levels after its implantation [185]. The improvement of cytoskeleton integrity after LNA-92a treatment is most probably due to the ameliorated capillary over all status and the myocyte protective effect after miR-92a inhibition. Being sensitive to ischemia, α -actinin increase is a marker for the cardiomyocyte protective effect of miR-92a inhibition. Improves in α -actinin density could be ranked as a secondary beneficial event arising from the myocyte protective effect rather than a direct effect of miR-92a targeting. Ameliorated cytoskeletal integrity reflects also as gain of contractile function in the SES measurement

1.5. Improving myocardial performance

Recovery and optimization of cardiac performance are indubitably major aim of cardiac interventions. Since LNA-92a application was demonstrated to entail a range of beneficial cardio protective effect, its influence and scope on hemodynamics and myocardial function is of great importance concerning a translational aspect. Macroscopically, evidence for a reduction of ischemia was given in both models in treated animals. Gain of contractile function was proven in regional segment shortening. Additionally, an enhancement of left ventricular function was worthy of note. This was given as LVEDP, a marker for heart insufficiency, and EF, the measure for left heart performance and output. Clinical studies conclude that an EF > 50 % is beneficial for the longtime prognosis of survival [186, 187]. With regard to the development of heart insufficiency as a consequence of ischemia, provided data might indicate a lowering of the risk for developing heart failure. The interplay of an improved capillary network and cytoskeletal integrity as well as reduction of fibrosis and thereby mitigation of

myocardial stiffness, attenuated inflammatory infiltration and reduced apoptosis upon LNA-92a treatment culminates in an improvement of global cardiac function.

Global heart function measurements were obtained under total intravenous anesthesia. Propofol, and especially its combination with fentanyl, exerts a negative inotropic effect which can be a disruptive factor for the assessment of heart function. Since dosage of anesthetics must be set individually to the patient's need, modulating effect of the anesthesia on the cardiac performance cannot be excluded entirely. However, measured EF and LVEDP values were approximately similar when compared within the animals from the same group. The widely used isoflurane has a traceably coronary dilative effect and is known to potentially trigger malignant hyperthermia [188]. In an anesthetic study of porcine MI induction, sevoflurane had better outcome than isoflurane which caused ventricular fibrillation in 81.3 % of the pigs and poorer overall survival [189]. However, use of propofol is the more economic approach compared to sevoflurane. Proportionally low EF measured on day 0 is due to the angulation of the C-arm and the anatomic position of the pig heart in the chest.

2. Clinical relevance of miRNA for cardiac issues and beyond

Preclinical basic research on miRNA and on their effect and efficacy is decisive for leading their way to clinical application. First clinical studies are dealing with blood analysis for circulating miRNAs as biomarkers. Prerequisites for biomarkers are an early and reliable detection combined with a high specificity addressed to a certain disease, preferably specimen for biomarker detection are gained easily and reproducibly without great endeavor, e.g. serum or urine sampling. Due to their role as posttranscriptional regulators of gene expression, their ubiquitous presence and their early alteration in diseases, many miRNAs were described as promising biomarkers in oncology and cardiology. Early cancer detection is crucial for optimal outcome after therapy. Promising data on miR-92a use as biomarker were published for the detection of small cell lung cancer and colorectal cancer [190] [191]. Analysis of circulating miRNA as biomarkers could be an attractive method also for MI and CAD detection. MiR-208, -133, -499 and -1 have been demonstrated to be markedly increased during MI [192]. MiR-208 was suggested a decent biomarker for myocardial injury [193]. In cardiology, miR-92a was

described as a biomarker for aortic valve calcification [194].

Interestingly, Fichtlscherer et al. reported reduced circulating levels of miR-92a while its expression in cardiomyocytes was enriched during CAD [195]. These findings were surprising, since the authors assumed an endothelial activation in CAD. As explicatory hypothesis, they constituted miRNA uptake into atherosclerotic lesions. Recently, significantly increased serum miR-92a values were described in the onset of Kawasaki disease in children [196], an autoimmune disease signed by vascular and coronary damage. Further, miR-92a together with miR-486 overexpression in urine samples purchased from employees hired in a mercury thermometer producing company was demonstrated as a potential biomarker for mercury poisoning [197].

Besides their merit as biomarkers, miRNA could function also as promising therapeutic targets for CAD. Several miRNAs possess amply target molecules, so their modulation is followed by far-reaching cellular modification, which underscores miRNAs' usefulness as therapeutic targets. Depending on the miRNA, different hallmarks in CAD can be affected such as hypertrophy (miR-133 [113, 198]), fibrosis (miR-21 [199]), lipid metabolism (miR-33 [200, 201]), cardiac rhythm and endothelial biology. In a wound healing model of diabetic mice, light induced activation of antimir-92a with photo labile groups, so called "cages", improved wound healing. Light induction of the antimir-92a led to a spatially confined therapeutic beneficial effect without adverse effect to other organs.

Studies in diabetic rats revealed reduced insulin levels alongside upregulation of miR-25 and miR-92a, suggesting a regulation of insulin at its mRNA level [202]. The binding side of miR-25 and miR-92a was identified to overlap with that of PTBP1, a binding molecule that stabilizes insulin mRNA for its translation.

2.1. Comparison of miR-92a inhibition to other therapeutic approaches

Besides miR-92a, miR-24 was demonstrated to be upregulated during MI [114]. In a mouse model of MI, miR-24 inhibition was capable of reducing infarction size. The effect is mediated by reduce of apoptosis and conservation of capillary networks. GATA2 and PAK4 are identified as target genes of miR-24. MiR-24 might be a promising candidate for a gene therapeutic approach, however large animal data is not available yet.

Besides miRNA, angiogenicity is also attributed to other substance groups like proteins and peptides. Cyclosporine A (an immunosuppressant drug which hampers the opening of the mitochondrial permeability-transition pore) inhibits calcineurin leading to immunosuppression on the one hand, but also promotion of angiogenesis on the other. Cyclosporin A administration led to a reduction in infarction sizes by 45 %. In a clinical study including 58 human patients presenting with MI, a bolus of 2.5 ml cyclosporine A or saline (controls) was injected prior to PCI [203]. Infarction size measured 5 days post interventionem uncovered a reduce in infarction size in the cyclosporine A injection group, troponin levels were similar in the control and cyclosporine A cohorts. Contrary findings were published in the CIRCUS- study. Outcome in almost 400 cyclosporine A injected patients was insignificantly improved after 1 year post MI compared to control patients who received saline [204]. Cyclosporin A's usefulness as a therapeutic agent remains ambivalent.

Thymosin β 4 was identified as a protein which is involved in endothelial cell migration, tube formation and angiogenesis. As a "multifunction-tool", thymosin β 4 is an anti-inflammatory, angiogenic and cardio protective agent. In pigs, outcome after MI was remarkable when thymosin β 4 was injected [110, 205]. In a porcine INS^{C94Y} model of hibernating myocardium, like taken for this study, the positive effect of thymosin β 4 was illuminated by Hinkel et al. [49]. Single dose thymosin β 4 administration via retrograde catheterization was capable of enhancing global heart function, reducing fibrosis and improving capillary rarefaction in wildtype and diabetic pigs to a similar extend like LNA-92a in this study. Thymosin β 4's profile was apparently not altered by diabetes. As a vector for thymosin β 4 delivery into the myocardial cells, a recombinant AAV 2.9 was used. AAVs offer a range of advantages as vehicles for gene therapeutic agents. Chief among these is the fact that hitherto no evidence for pathogenicity was reported. AAVs can infect various cell types due to specific tropism without evoking a cytotoxic response. However, loading capacity of AAVs is limited and outcome after AAV therapy was reported to be hampered due to neutralizing antibodies [206]. Advantage of a miR therapeutic approach compared to protein administration via AAV might be in the use of LNA instead of AAV. LNAs do not require a viral vector for cell penetration and are unaffected from immune response.

2.2. Longtime effect of miR-92a inhibition

Functionality of a single dose LNA-92a application was demonstrated for 28 days post application in the chronic ischemia model. Due to their chemical stability, LNAs are potentially persistent in the organism. Advantage of a prolonged LNA persistence are the longtime effects on angiogenesis and improvement of capillary blood supply to the ischemic region. Diabetic patients with chronic ischemia might benefit from longtime LNA-92a presence when it comes to additional acute myocardial infarction. Once new capillaries have been formed upon miR-92a inhibition, they are estimated to last given that there is resting perfusion, even when LNA-92a presence decreases. On the other hand, side effects last with longtime influence of LNA-92a. In a previous study, miR-92a expression profiles in other organs than the heart were LNA-92a dose dependent and varied with different application routes [123]. Regional retro- and antegrade catheter-based application of LNA-92a led to less excessive changes of the miR-92a expression profile than systemic administration of LNA-92a. LNA-92a application reduced miR-92a expression levels less in lung and liver compared to spleen and kidney. Data was obtained after 3 resp. 7 days, so longtime effects remain unclear. However, no micro- or macroscopic alteration was obtained in this study concerning organs like lung, spleen and kidney and liver. In a mouse model, weekly injection of LNA-21 for a time frame of 18 weeks did not cause hepatotoxicity or kidney function deterioration [199]. Despite hepatotoxicity was reported previously after LNA application [174], in primates no evidence for hepatotoxicity was obtained after LNA-122 application [134]. The LNA-122 directed against the miR-122 which is increased in hepatitis C, has already entered the clinical stage as a drug named “miravirsen” with promising outcome [207].

In this study, single dose application was sufficient to significantly improve systolic function of the heart for at least 28 days. In human patients, single dose application might not be sufficient to recover heart function and improve longtime outcome. Long time data and LNA-92a potential and side effects after multiple dose injection remain to be determined.

3. Limitations of present study

Translationality in preclinical trials implies animal models which mimic human disease and their pathways in an optimal manner. A major difficulty is to fulfill all pathologic entities arising from diseases known the contribution of comorbidities. Thereby, validity and reliability of potential effects and results together with low coefficients of variance between individual animals, are inescapable in order to carry out meaningful preclinical research.

Despite slight differences in the anatomy of coronaries, pigs' heart function and cardiac performance is similar to human. On the basis of the equivalent heart size in swine, heart catheterization can be realized like in human patients. Therefore, the pig, in comparison to other species, is a suitable candidate for preclinical research and for regional cardiac delivery of a therapeutic agent to a certain cardiac region.

Pigs in this study underwent manipulation of one vessel (RCX for the stent model and LAD for the acute infarction model) leading to an artificial impairment of one vessel. In the clinical scenario, patients presenting with unique vessel occlusion usually undergo PTCA or bypass, these interventions fail in “no-option” patients due to impaired capillary overall status and atherosclerotic narrowing. Further, more than 90 % of cardiac events and deaths are in patients older than 65 years [208]. While cardiomyocytes are highly proliferative in neonates, the capacity for cardiac regeneration shrinks with advanced age in humans and mammals [209, 88]. Only few species hold lifelong high proliferative regeneration, e.g. zebrafish. Age-dependency of cardio-vascular response is a not fulfilled factor in this experimental setup. However, animal experiments in aged adult pigs are unfeasible because of economic and technical concerns: The simplest way for aging mimicry is using an old organism which is complicated due to immense costs in large animals holding long life expectancy. Further, adult domestic pigs can weigh up to 300 kg and are therefore complicated in handling and instrumentalization for interventions. As an alternative to evade enormous gain of weight in domestic pigs, minipigs are commonly used, whose weight ranges between 30 to 50 kg. Especially the Göttingen minipig has shown its merit as swine model, also for T1DM and T2DM research. Genetic engineering allows the tailoring of animals showing premature aging and geriatric impairment. Transgenic rodent models of aging are well established and amply, presenting with

different physiologic age dependent alterations. For example, the ERCC1 mutant mouse is deficient in DNA repair promoting premature aging [210]. These models are being transferred to the pig species currently.

Despite aging, diabetes additionally aggravates cardiac remodeling and regeneration [211]. Data in this study were captured from young wildtype swine, whose regenerative capacity is assumable high. In contrary, INS^{C94Y} pigs present with capillary rarefaction and impaired heart function. Their regenerative capacity is restricted. Inclusion of diabetic animals in this study, can be seen as an approximation to the situation in “no-option patients”, where capillaries are generally atherosclerotic narrowed due to exacerbating comorbidities and poor and impeded regeneration.

Since evolution of infarction in porcine models is faster than in men, infarction duration was set for 1h in this experiment [212, 213]. In the experimental setup, LNA-92a application was achieved within the “golden hour”, which is rarely the case in the clinical human situation.

Further, prediction of present study on a potential outcome in human patients is hampered by limited animal numbers. Large animal models are restricted by excessive effort and costs compared to rodent models where throughput is substantially higher. However, the stent implantation models as well as the I/R model via balloon occlusion offer high reproducibility and standardization of ischemia induction. Thus, cardiac baseline situation prior to LNA-92a resp. scrambles LNA application can be considered as standardized within animals of one group. Major advantage of the INS^{C94Y} model compared to other diabetes models, like the STZ or pancreatectomy model, is the providing of a standardized diabetic phenotype in swine.

4. Conclusion and outlook

In all conditions -wildtype and DM, acute and chronic ischemia - LNA-92a administration had a clinically relevant cardio protective effect. How far a potential cardio protective effect in elderly and frail patients emerges, remains uncertain. Still, other comorbidities than DM, such as hypercholesterinemia, must be taken into consideration in human patients. However, modification of miR-92a expression might be a promising candidate for a new therapeutic approach because it combines core characteristics of an impactful ischemia therapy: protection of the myocardium, restoration of blood flow, strengthening of left heart performance, improvement of cardiac outcome and functionality despite presence of comorbidity.

Currently, further development on miR-92a inhibition towards clinical trials is ongoing.

VI. SUMMARY

Changing societal demographics in Western societies, characterized by prolonged life expectancy and growing numbers of patients diagnosed with DM, exacerbates the necessity for alternative strategies for CAD. Therapeutic approaches, like catheter-based angioplasty and stents, aim at restoring blood flow to the ischemic myocardium in order to protect from myocyte loss. So called “no-option” patients are not amenable for these methods due exhaustion of coronary targets and are dependent on innovations, e.g. from molecular biological origin.

MicroRNAs have gained in importance as new gene therapeutic approaches. Due to changes in its expression pattern in the onset of CAD, its amply targets and its possibility of modification *in vivo*, miR-92a proved to be a descent therapeutic approach, at least in a porcine model of hibernating myocardium and acute infarction. Besides improving microcirculation and leading symptoms of cardiac ischemia, a catheter-based administration of LNA-92a was capable of enhancing global and regional heart function. Feasibility of LNA-92a application was further proved in a diabetic model of INS^{C94Y} transgenic pigs. In a 24-hour model of acute infarction in diabetic pigs, the protective effect on endothelial cells was demonstrated.

Improved outcome after miR-92a inhibition on the one hand and its pivotal role in the development of CAD on the other hand indicate that miR-92a might emerge as novel therapeutic target for the treatment of cardio vascular disease.

VII. ZUSAMMENFASSUNG

„Kardioprotektives Potential der miR-92a Inhibition in Großtiermodellen“

Die sich wandelnde Demographie, charakterisiert durch steigende Lebenserwartung und stetig wachsende Zahlen diabetesdiagnostizierter Patienten, in westlichen Gesellschaften, verschärft die Notwendig- und Wichtigkeit alternativer Therapieansätze im Rahmen koronarer Herzkrankheiten. Gängige therapeutische Methoden, wie herzkatheterbasierte Angioplastie und Stents, zielen darauf ab eine Wiederherstellung der Blutzufuhr zum ischämischen Myokard zu erreichen, um den Verlust vitaler Myozyten möglichst gering zu halten. Allerdings sind sogenannte „no-option“ Patienten, aufgrund der Ausschöpfung gängiger Methoden auf Innovationen, z.B. aus dem molekularbiologischen Bereich, angewiesen.

Hinsichtlich ihrer Beeinflussung des Targetings von messengerRNAs, liegt es nahe, dass vor allem microRNAs als mögliche neuartige Ansätze für eine gentechnischvermittelte Angiogenese, an Bedeutung gewinnen. Aufgrund ihres veränderten Expressionsprofils im Verlauf der koronaren Herzkrankheiten, ihrer vielfältigen Targets und ihrer einfachen Modifikationsmöglichkeit *in vivo*, hat sich die miR-92a als therapeutischer Angriffspunkt zumindest im hibernierenden Schweinemyokard und akuten Herzinfarkt bewährt. So konnte in vorliegender Studie kraft regionaler katheterbasierter LNA-92a Applikation nebst einer Verbesserung der Mikrozirkulation und der vorteilhaften Beeinflussung anderer Leitsymptome chronische Myokardischämie, eine Zunahme der globalen und regionalen Herzfunktion erzielt werden. Die Wirksamkeit des Therapieansatzes im Diabetesmodel INS^{C94Y} transgener Schweine konnte bestätigt werden. Im 24 Stunden Infarktmodel in transgenen diabetischen Schweinen, wurde darüber hinaus das endothelzellprotektive Potential der LNA-92a Applikation demonstriert.

Aufgrund der verbesserten Herzleistung nach miR-92a Inhibition auf der einen Seite und aufgrund ihrer ausschlaggebenden Rolle in der Entstehung koronarer Herzkrankheiten auf der anderen, könnte sich die miR-92a als neuartiger therapeutischer Angriffspunkt für die Behandlung koronarer Herzkrankheiten erweisen.

VIII. INDEX OF TABLES AND FIGURES

1. Index of tables

Table 1: Overview on cell culture approaches for assays.....	26
Table 2: Animal groups for the stent and MI model.....	28
Table 3: Rentrop's classification scheme	36
Table 4: Staining protocol for Pecam-1/ NG2	37
Table 5: HE staining protocol.....	38
Table 6: Sirius Red staining procedure.....	39

2. Index of figures

Figure 1: Vicious circle of DM.....	5
Figure 2: Processing of miR-92a	16
Figure 3: Experimental setup for the chronic and acute ischemia model.....	33
Figure 4: Scheme of sub-endocardial segment shortening	35
Figure 5: Migration capacity of bEnd.3 cells	41
Figure 6: Representative pictures of migration assays	42
Figure 7: Rings per tube in normo and high glucose media	43
Figure 8: Ring formation assay.....	44
Figure 9: Post mortem myocardial TTC stainings.....	45
Figure 10: Infarct size	46
Figure 11: PECAM-1/ NG2 stainings.....	47
Figure 12: Assessment of capillary density in the 24h model	48
Figure 13: Representative TUNEL stainings.....	49
Figure 14: Quantification of TUNEL stainings	50
Figure 15: HE staining for inflammation.....	51
Figure 16: Angiograms (24 h post I/R).....	52
Figure 17: EF and LVEDP obtained in the 24 h model.....	53
Figure 18: Blood glucose levels measured from stent implanted pigs	54
Figure 19: PECAM-1/ NG2 stainings.....	55
Figure 20: Assessment of capillary density in the stent model.....	56
Figure 21: Post mortem angiograms	57
Figure 22: Collaterals and Rentrop score	58

Figure 23: Representative TUNEL stainings.....	59
Figure 24: Apoptosis stainings	60
Figure 25: Fibrosis stainings.....	61
Figure 26: Development of fibrosis	62
Figure 27: Angiograms taken on day 56 of the stent model.....	63
Figure 28: Improvement of EF	64
Figure 29: LVEDP measurements	65
Figure 30: Subendocardial segment shortening.....	66

IX. REFERENCES

- [1] “WHO updates fact sheet on cardiovascular diseases” (18 May 2017) | communitymedicine4asses.
- [2] World Heart Federation, “The world’s most common cause of death. Cardiovascular diseases (CVDs), global facts and figures”, p. 863, 2016.
- [3] “WHO | Cardiovascular diseases (CVDs)”, WHO, 2018.
- [4] G. Hotamisligil, “Endoplasmic reticulum stress and atherosclerosis”, *Nat. Med.*, vol. 16, no. 4, pp. 396–399, 2010.
- [5] N. G. Uren et al., “Relation between myocardial blood flow and the severity of coronary-artery stenosis”, *N. Engl. J. Med.*, vol. 330, pp. 1782-1788, 1994.
- [6] “Myocardial ischemia - Symptoms and causes - Mayo Clinic.” [Online]. Available: <https://www.mayoclinic.org/diseases-conditions/myocardial-ischemia/symptoms-causes/syc-20375417>. [Accessed: 29-Jun-2018].
- [7] P. Libby, P. M. Ridker and A. Maseri, “Inflammation and atherosclerosis”, *Circulation*, vol. 105, no. 9, pp. 1135–1143, Mar. 2002.
- [8] “Herzkrankheiten: Männer erkranken häufiger, Frauen sterben öfter daran.” [Online]. Available: <https://dgk.org/pressemitteilungen/herzkrankheiten-maenner-erkranken-haeufiger-frauen-sterben-oeffter-daran/>. [Accessed: 07-Jul-2018].
- [9] “IDF diabetes atlas - Across the globe.” [Online]. Available: <http://www.diabetesatlas.org/across-the-globe.html>. [Accessed: 30-Jun-2018].
- [10] World Health Organization, “Global report on diabetes”, *Isbn*, vol. 978, p. 88, 2016.
- [11] W. R. Rowley et al., “Diabetes 2030: Insights from yesterday, today and future trends”, *Popul. Health Manag.*, vol. 20, no. 1, pp. 6–12, 2017.
- [12] J. A. Bluestone et al., “Genetics, pathogenesis and clinical interventions in type 1 diabetes”, *Nature*, vol. 464, no. 7293, pp. 1293–1300, 2010.
- [13] C. Limbert, “Type 1 diabetes - an auto-inflammatory disease: a new concept,

-
- new therapeutical strategies”, *J. Transl. Med.*, vol. 10, no. Suppl 3, p. I12, 2012.
- [14] S. R. Babu and G. S. Eisenbarth, “Juvenile diabetes”, *Indian J. Med. Res.*, vol. 136, no. 2, pp. 179–81, Aug. 2012.
- [15] C. Ionescu-Tîrgoviște, P. A. Gagniuc and C. Guja, “Structural properties of gene promoters highlight more than two phenotypes of diabetes”, *PLoS One*, vol. 10, no. 9, pp. 1–15, 2015.
- [16] G. Serena, S. Camhi, C. Sturgeon, S. Yan and A. Fasano, “The role of gluten in celiac disease and type 1 diabetes”, *Nutrients*, vol. 7, no. 9, pp. 7143–7162, 2015.
- [17] S. Bibbò et al., “Is there a role for gut microbiota in type 1 diabetes pathogenesis?”, *Ann. Med.*, vol. 49, no. 1, pp. 11–22, 2017.
- [18] M. Rewers and J. Ludvigsson, “Environmental risk factors for type 1 diabetes”, *Lancet*, vol. 387, no. 10035, pp. 2340–2348, 2016.
- [19] G. Wilcox, “Insulin and insulin resistance”, *Clin. Biochem. Rev.*, vol. 26, no. 2, pp. 19–39, 2005.
- [20] R. A. DeFronzo, “Pathogenesis of type 2 diabetes mellitus”, *Med. Clin. North Am.*, vol. 88, no. 4, pp. 787–835, 2004.
- [21] S. Y. Zhang et al., “Overweight, resting heart rate and prediabetes/diabetes: A population-based prospective cohort study among Inner Mongolians in China”, *Sci. Rep.*, vol. 6, no. October 2015, pp. 1–6, 2016.
- [22] A. Pan et al., “Relation of active, passive and quitting smoking with incident type 2 diabetes: a systematic review and meta-analysis”, *Lancet Diabetes Endocrinol.*, vol. 510, no. 3, pp. 958–67, 2015.
- [23] C. Touma and S. Pannain, “Does lack of sleep cause diabetes?”, *Cleve. Clin. J. Med.*, vol. 78, no. 8, pp. 549–558, 2011.
- [24] W.-L. Liao and F.-J. Tsai, “Personalized medicine in Type 2 Diabetes”, *BioMedicine*, vol. 4, no. 2, p. 8, 2014.
- [25] P. Bowman et al., “Heterozygous ABCC8 mutations are a cause of MODY”, *Diabetologia*, vol. 55, no. 1, pp. 123–127, 2012.

-
- [26] D. Daneman, "Type 1 diabetes", *Lancet*, vol. 367, no. 9513, pp. 847–858, 2006.
- [27] S. Chu et al., "Maternal obesity and risk of gestational diabetes mellitus", *Diabetes Care*, vol. 30, no. 8, pp. 2070–2076, 2007.
- [28] L. Yuen, "Gestational diabetes mellitus: challenges for different ethnic groups", *World J. Diabetes*, vol. 6, no. 8, p. 1024, 2015.
- [29] M. Ashrafi et al., "Gestational diabetes mellitus and metabolic disorder among the different phenotypes of polycystic ovary syndrome", *Oman Med. J.*, vol. 32, no. 3, pp. 214–220, May 2017.
- [30] P. Damm et al., "Gestational diabetes mellitus and long-term consequences for mother and offspring: a view from Denmark", *Diabetologia*, vol. 59, no. 7, pp. 1396–1399, Jul. 2016.
- [31] J. C. Pickup, G. D. Chusney, S. M. Thomas and D. Burt, "Plasma interleukin-6, tumour necrosis factor alpha and blood cytokine production in type 2 diabetes", *Life Sci.*, vol. 67, no. 3, pp. 291–300, 2000.
- [32] A. Stirban, T. Gawlowski and M. Roden, "Vascular effects of advanced glycation endproducts: Clinical effects and molecular mechanisms", *Mol. Metab.*, vol. 3, no. 2, pp. 94–108, 2014.
- [33] D. Farbstein and A. P. Levy, "HDL dysfunction in diabetes: Causes and possible treatments", *Expert Rev. Cardiovasc. Ther.*, vol. 10, no. 3, pp. 353–361, 2012.
- [34] J.-S. Pan, M.-Z. Hong and J.-L. Ren, "Reactive oxygen species: A double-edged sword in oncogenesis", *World J. Gastroenterol.*, vol. 15, no. 14, p. 1702, 2009.
- [35] A. C. Montezano and R. M. Touyz, "Reactive oxygen species, vascular noxs, and hypertension: focus on translational and clinical research", *Antioxid. Redox Signal.*, vol. 20, no. 1, pp. 164–182, 2014.
- [36] A. J. King, "The use of animal models in diabetes research", *Br. J. Pharmacol.*, vol. 166, no. 3, pp. 877–894, Jun. 2012.
- [37] D. Dufrane et al., "Streptozotocin-induced diabetes in large animals

-
- (pigs/primates): role of GLUT2 transporter and beta-cell plasticity”, *Transplantation*, vol. 81, no. 1, pp. 36–45, Jan. 2006.
- [38] M. Andersson, R. Kruse, B. Nilsson, R. Larsson and O. Korsgren, “Original article effects of streptozotocin-induced diabetes in domestic pigs with focus on the amino acid metabolism”, *Lab. Anim.*, vol. 42, no. 3, pp. 249–254, 2009.
- [39] M. C. Deeds et al., “Single dose streptozotocin-induced diabetes: considerations for study design in islet transplantation models”, *Lab. Anim.*, vol. 45, no. 3, pp. 131–40, Jul. 2011.
- [40] J. W. Yoon et al., “Coxsackie virus B4 produces transient diabetes in nonhuman primates”, *Diabetes*, vol. 35, no. 6, pp. 712–6, Jun. 1986.
- [41] M. von Herrath and G. T. Nepom, “Animal models of human type 1 diabetes”, *Nat. Immunol.*, vol. 10, no. 2, pp. 129–132, Feb. 2009.
- [42] K. C. Stump, M. M. Swindle, C. D. Saudek and J. D. Strandberg, “Pancreatectomized swine as a model of diabetes mellitus”, *Lab. Anim. Sci.*, vol. 38, no. 4, pp. 439–43, Aug. 1988.
- [43] K. Kobayashi et al., “Development of a porcine model of type 1 diabetes by total pancreatectomy and establishment of a glucose tolerance evaluation method”, *Artif. Organs*, vol. 28, no. 11, pp. 1035–1042, 2004.
- [44] E.-G. Hong et al., “Nonobese, insulin-deficient Ins2Akita mice develop type 2 diabetes phenotypes including insulin resistance and cardiac remodeling”, *AJP Endocrinol. Metab.*, vol. 293, no. 6, pp. E1687–E1696, 2007.
- [45] M. Yoshioka, T. Kayo, T. Ikeda and A. Koizumi, “A novel locus, Mody4, distal to D7Mit189 on chromosome 7 determines early-onset NIDDM in nonobese C57BL/6 (Akita) mutant mice”, *Diabetes*, vol. 46, no. 5, pp. 887–94, May 1997.
- [46] J. Wang et al., “A mutation in the insulin 2 gene induces diabetes with severe pancreatic β -cell dysfunction in the Mody mouse”, *J. Clin. Invest.*, vol. 103, no. 1, pp. 27–37, 1999.
- [47] S. Renner et al., “Permanent neonatal diabetes in INSC94Y transgenic pigs”,

-
- Diabetes, vol. 62, no. 5, pp. 1505–1511, May 2013.
- [48] E. Wolf, C. Braun-Reichhart, E. Streckel and S. Renner, “Genetically engineered pig models for diabetes research”, *Transgenic Res.*, vol. 23, no. 1, pp. 27–38, Feb. 2014.
- [49] R. Hinkel et al., “Diabetes mellitus–induced microvascular destabilization in the myocardium”, *JACC*, vol. 69, no. 2, pp. 131–143, 2017.
- [50] G. A. Diamond et al., “Post-extrasystolic potentiation of ischemic myocardium by atrial stimulation”, *Am. Heart J.*, vol. 95, no. 2, pp. 204–209, 1978.
- [51] S. H. Rahimtoola, “The hibernating myocardium in ischaemia and congestive heart failure”, *Eur. Heart J.*, vol. 14 Suppl A, pp. 22–6, 1993.
- [52] R. A. Kloner, R. Bolli, E. Marban, L. Reinlib and E. Braunwald, “Medical and cellular implications of stunning, hibernation, and preconditioning: an NHLBI workshop”, *Circulation*, vol. 97, no. 18, pp. 1848–67, May 1998.
- [53] R. Schulz, B. D. Guth, K. Pieper, C. Martin and G. Heusch, “Recruitment of an inotropic reserve in moderately ischemic myocardium at the expense of metabolic recovery. A model of short-term hibernation”, *Circ. Res.*, vol. 70, no. 6, pp. 1282–1295, 1992.
- [54] I. L. Geft et al., “Intermittent brief periods of ischemia have a cumulative effect and may cause myocardial necrosis”, *Circulation*, vol. 66, no. 6, pp. 1150–3, 1982.
- [55] E. B. Carlson, M. J. Cowley, T. C. Wolfgang and G. W. Vetrovec, “Acute changes in global and regional rest left ventricular function after successful coronary angioplasty: Comparative results in stable and unstable angina”, *JACC*, vol. 13, no. 6, pp. 1262–1269, 1989.
- [56] K. Chatterjee et al., “Influence of direct myocardial revascularization on left ventricular asynergy and function in patients with coronary heart disease. With and without previous myocardial infarction”, *Circulation*, vol. 47, no. 2, pp. 276–86, 1973.
- [57] C.W. Akins et al., “Selection of angina-free patients with severe left

-
- ventricular dysfunction for myocardial revascularization”, *JACC*, vol. 46, no. October, 1980.
- [58] W. S. Weintraub et al., “The relationship between myocardial blood flow and contraction by myocardial layer in the canine left ventricle during ischemia” *Circ. Res.*, vol. 48, no. 3, pp. 430–438, 1981.
- [59] S. F. Vatner, “Correlation between acute reductions in myocardial blood flow and function in conscious dogs”, *Circ. Res.*, vol. 47, no. 2, pp. 201–207, 1980.
- [60] K. P. Gallagher, G. Osakada, M. Matsuzaki, W. S. Kemper and J. Ross, “Myocardial blood flow and function with critical coronary stenosis in exercising dogs”, *Am. J. Physiol.*, vol. 243, no. 5, pp. H698-707, 1982.
- [61] J. Ross, “Myocardial perfusion-contraction matching; implications for coronary heart disease and hibernation”, *Circulation*, vol.83, no.3, pp. 1076–1084, 1991.
- [62] W. Flameng et al., “Ultrastructural correlates of left ventricular contraction abnormalities in patients with chronic ischemic heart disease: determinants of reversible segmental asynergy postrevascularization surgery”, *Am. Heart J.*, vol. 102, no. 5, pp. 846–857, Nov. 1981.
- [63] P. Anversa, X. Zhang, P. Li and J. M. Capasso, “Chronic coronary artery constriction leads to moderate myocyte loss and left ventricular dysfunction and failure in rats”, *J. Clin. Invest.*, vol. 89, no. 2, pp. 618–629, 1992.
- [64] R. Kaprielian et al., “Downregulation of immunodetectable connexin43 and decreased gap junction size in the pathogenesis of chronic hibernation in the human left ventricle”, *Circulation*, vol. 97, no. 7, pp. 651–60, 1998.
- [65] T. Shimonagata et al., “Myocardium after percutaneous and the relation between recovery in left ventricular function and free fatty acid metabolism”, *JACC*, vol. 9149, no. 98, pp. 559–563.
- [66] S.H. Rahimtoola, “The hibernating myocardium”, *EXS*, vol. 76, pp. 453–462, 1996.
- [67] E. Braunwald and R. Kloner, “The stunned myocardium: prolonged,

-
- postischemic ventricular dysfunction”, *Circulation*, vol. 66, no. 6, pp. 1146–1149, 1982.
- [68] G. R. Heyndrickx et al., “Regional myocardial functional and electrophysiological alterations after brief coronary artery occlusion in conscious dogs”, *JCI*, vol. 56, pp. 978-985, October, 1975.
- [69] J. Litvak, L. E. Siderides and A. M. Vineberg, “The experimental production of coronary artery insufficiency and occlusion”, *Am. Heart J.*, vol. 53, no. 4, pp. 505–518, Apr. 1957.
- [70] E. Unger, “Experimental evaluation of coronary collateral development”, *Cardiovasc. Res.*, vol. 49, no. 3, pp. 497–506, Feb. 2001.
- [71] C. Chen et al., “Functional and structural alterations with 24-hour myocardial hibernation and recovery after reperfusion. A pig model of myocardial hibernation”, *Circulation*, vol. 94, no. 3, pp. 507–16, Aug. 1996.
- [72] G. C. Hughes, M. J. Post, M. Simons and B. H. Annex, “Translational physiology: porcine models of human coronary artery disease: implications for preclinical trials of therapeutic angiogenesis”, *J. Appl. Physiol.*, vol. 94, no. 5, pp. 1689–1701, 2003.
- [73] G. Von Degenfeld et al., “Selective pressure-regulated retroinfusion of fibroblast growth factor-2 into the coronary vein enhances regional myocardial blood flow and function in pigs with chronic myocardial ischemia”, *JACC*, vol. 42, no. 6, pp. 1120–1128, 2003.
- [74] K. Thygesen et al., “Third universal definition of myocardial infarction”, *Eur. Heart J.*, vol. 33, no. 20, pp. 2551–2567, 2012.
- [75] C. Kawai, “Pathogenesis of acute myocardial infarction; novel regulatory systems of bioactive substances in the vessel wall”, *Circulation*, vol. 90, no. 2, 1994.
- [76] R. B. Jennings and K. A. Reimer, “The cell biology of acute myocardial ischemia”, *Annu. Rev. Med.*, vol. 42, no. 1, pp. 225–246, Feb. 1991.
- [77] S. Chen and S. Li, “The Na⁺/Ca²⁺ exchanger in cardiac ischemia/reperfusion injury”, *Med. Sci. Monit.*, vol. 18, no. 11, pp. RA161-5, Nov. 2012.

-
- [78] T. Kalogeris, C. P. Baines, M. Krenz and R. J. Korthuis, “Cell biology of ischemia/reperfusion injury”, *Int. Rev. Cell Mol. Biol.*, vol. 298, pp. 229–317, 2012.
- [79] J. M. Bond, B. Herman and J. J. Lemasters, “Protection by acidotic pH against anoxia/reoxygenation injury to rat neonatal cardiac myocytes”, *Biochem. Biophys. Res. Commun.*, vol. 179, no. 2, pp. 798–803, 1991.
- [80] R. A. Chapman and J. Tunstall, “The calcium paradox of the heart”, *Prog. Biophys. Mol. Biol.*, vol. 50, no. 2, pp. 67–96, 1987.
- [81] D. B. Zorov et al., “Regulation and pharmacology of the mitochondrial permeability transition pore”, *Cardiovasc. Res.*, vol. 83, no. 2, pp. 213–225, 2009.
- [82] D. B. Zorov, M. Juhaszova and S. J. Sollott, “Mitochondrial ROS-induced ROS release: An update and review”, *Biochim. Biophys. Acta - Bioenerg.*, vol. 1757, no. 5–6, pp. 509–517, 2006.
- [83] R. A. Kloner, C. E. Ganote and R. B. Jennings, “The ‘no reflow’ phenomenon after temporary coronary occlusion in the dog”, *J. Clin. Invest.*, vol. 54, no. 6, pp. 1496–1508, 1974.
- [84] “Coronary artery disease - Diagnosis and treatment - Mayo Clinic” [Online]. Available: <https://www.mayoclinic.org/diseases-conditions/coronary-artery-disease/diagnosis-treatment/drc-20350619>. [Accessed: 02-Jul-2018].
- [85] M.A. Pfeffer and E. Braunwald, “Ventricular remodeling after myocardial infarction”, *Circulation*, vol 81. pp. 1161–1172, 1990.
- [86] J. P. M. Cleutjens, J. C. Kandala, E. Guarda, R. V. Guntaka and K. T. Weber, “Regulation of collagen degradation in the rat myocardium after infarction”, *J. Mol. Cell. Cardiol.*, vol. 27, no. 6, pp. 1281–1292, 1995.
- [87] M. R. Munz et al. , “Surgical porcine myocardial infarction model through permanent coronary occlusion”, *Comp. Med.*, vol. 61, no. 5, pp. 445–452, 2011.
- [88] O. Bergmann et al., “Dynamics of cell generation and turnover in the human heart”, *Cell*, vol. 161, no. 7, pp. 1566–1575, Jun. 2015.

-
- [89] R. J. Solaro, “Mechanisms of the Frank-Starling law of the heart: the beat goes on”, *Biophys. J.*, vol. 93, no. 12, pp. 4095–4096, 2007.
- [90] F. A. Spencer et al., “Delay to reperfusion in patients with acute myocardial infarction presenting to acute care hospitals: an international perspective”, *Eur. Heart J.*, vol. 31, no. 11, pp. 1328–1336, 2010.
- [91] B. L. Gerber et al., “Prognostic value of myocardial viability by delayed-enhanced magnetic resonance in patients with coronary artery disease and low ejection fraction: impact of revascularization therapy”, *JACC*, vol. 59, no. 9, pp. 825–835, 2012.
- [92] E. Perin and T. Willseron, “An essential guide to cardiac cell therapy”, *informa healthcare*, 2006.
- [93] R. J. Hajjar, “Potential of gene therapy as a treatment for heart failure”, *J. Clin. Invest.*, vol. 123, no. 1, 2013.
- [94] A. Birbrair et al., “Pericytes at the intersection between tissue regeneration and pathology”, *Clin. Sci.*, vol. 128, no. 2, pp. 81–93, Jan. 2015.
- [95] M. Potente, H. Gerhardt and P. Carmeliet, “Basic and therapeutic aspects of angiogenesis”, *Cell*, vol. 146, no. 6, pp. 873–887, 2011.
- [96] M. Heil and W. Schaper, “Insights into pathways of arteriogenesis”, *Curr. Pharm. Biotechnol.*, vol. 8, no. 1, pp. 35–42, Feb. 2007.
- [97] C. Kupatt et al., “Cotransfection of vascular endothelial growth factor-A and platelet-derived growth factor-B via recombinant adeno-associated virus resolves chronic ischemic malperfusion: Role of vessel maturation”, *JACC.*, vol. 56, no. 5, pp. 414–422, 2010.
- [98] L. K. Phng and H. Gerhardt, “Angiogenesis: a team effort coordinated by Notch”, *Dev. Cell*, vol. 16, no. 2, pp. 196–208, 2009.
- [99] M. Heil, I. Eitenmüller, T. Schmitz-Rixen and W. Schaper, “Arteriogenesis versus angiogenesis: similarities and differences”, *J. Cell. Mol. Med.*, vol. 10, no. 1, pp. 45–55, 2006.
- [100] D. N. Ku, D. P. Giddens, C. K. Zarins and S. Glagov, “Pulsatile flow and atherosclerosis in the human carotid bifurcation”, *Arteriosclerosis*, vol. 5, no.

-
- 3, pp. 293–302, 1985.
- [101] J. Niu et al., “Monocyte chemotactic protein (MCP)-1 promotes angiogenesis via a novel transcription factor, MCP-1-induced protein (MCPIP)”, *J. Biol. Chem.*, vol. 283, no. 21, pp. 14542–14551, 2008.
- [102] W. Schaper, “Collateral circulation. Past and present”, *Basic Res. Cardiol.*, vol. 104, no. 1, pp. 5–21, 2009.
- [103] W. Risau, “Mechanisms of angiogenesis”, *Nature*, vol. 386, no. 6626, pp. 671–674, Apr. 1997.
- [104] S. Balaji, A. King, T. M. Crombleholme and S. G. Keswani, “The Role of endothelial progenitor cells in postnatal vasculogenesis: implications for therapeutic neovascularization and wound healing”, *Adv. wound care*, vol. 2, no. 6, pp. 283–295, Jul. 2013.
- [105] M. Giacca and S. Zacchigna, “VEGF gene therapy: therapeutic angiogenesis in the clinic and beyond”, *Gene Ther.*, vol. 19, no. 6, pp. 622–629, Jun. 2012.
- [106] G. Czibik et al., “Gene therapy with hypoxia-inducible factor 1 alpha in skeletal muscle is cardioprotective in vivo”, *Life Sci.*, vol. 88, no. 11–12, pp. 543–550, Mar. 2011.
- [107] R. Hinkel et al., “Thymosin 4 is an essential paracrine factor of embryonic endothelial progenitor cell-mediated cardioprotection”, *Circulation*, vol. 117, no. 17, pp. 2232–2240, Apr. 2008.
- [108] Y.-A. Ko and K. Susztak, “Epigenomics: the science of no-longer “junk” DNA. Why study it in chronic kidney disease?”, *Semin. Nephrol.*, vol. 33, no.4, pp 354-362, 2014.
- [109] E. L. Vegter et al., “MicroRNAs in heart failure: from biomarker to target for therapy”, *Eur. J. Heart Fail.*, vol. 18, no. 5, pp. 457–468, 2016.
- [110] R. Hinkel, T. Trenkwalder and C. Kupatt, “Gene therapy for ischemic heart disease”, *Expert Opin. Biol. Ther.*, vol. 11, no. 6, pp. 723–737, Jun. 2011.
- [111] Y. Lee et al., “The nuclear RNase III Droscha initiates microRNA processing”, *Nature*, vol. 425, no. 6956, pp. 415–419, 2003.
- [112] J. Bauersachs and T. Thum, “Biogenesis and regulation of cardiovascular

-
- MicroRNAs”, *Circ. Res.*, vol. 109, no. 3, pp. 334–347, 2011.
- [113] A. Carè et al., “MicroRNA-133 controls cardiac hypertrophy”, *Nat. Med.*, vol. 13, no. 5, pp. 613–618, May 2007.
- [114] J. Fiedler et al., “MicroRNA-24 regulates vascularity after myocardial infarction”, *Circulation*, vol. 124, no. 6, pp. 720–730, 2011.
- [115] T. Thum et al., “MicroRNAs in the human heart: A clue to fetal gene reprogramming in heart failure”, *Circulation*, vol. 116, no. 3, pp. 258–267, 2007.
- [116] L. Maegdefessel, “The emerging role of microRNAs in cardiovascular disease”, *J. Intern. Med.*, vol. 276, no. 6, pp. 633–644, 2014.
- [117] F. Spallotta et al., “A nitric oxide-dependent cross-talk between class I and III histone deacetylases accelerates skin repair”, *J. Biol. Chem.*, vol. 288, no. 16, pp. 11004–12, Apr. 2013.
- [118] T. Thum, “MicroRNA therapeutics in cardiovascular medicine”, *EMBO Mol. Med.*, vol. 4, no. 1, pp. 3–14, Jan. 2012.
- [119] A. Ventura et al., “Targeted deletion reveals essential and overlapping functions of the miR-17~92 family of miRNA clusters”, *Cell*, vol. 132, no. 5, pp. 875–886, 2008.
- [120] L. He et al., “A microRNA polycistron as a potential human oncogene”, *Nature*, vol. 435, no. 7043, pp. 828–833, 2005.
- [121] M. Dews et al., “Augmentation of tumor angiogenesis by a Myc-activated microRNA cluster”, *Nat. Genet.*, vol. 38, no. 9, pp. 1060–1065, Sep. 2006.
- [122] A. Bonauer et al., “MicroRNA-92a controls angiogenesis and functional recovery of ischemic tissues in mice”, *Science*, vol. 15, no. 797, pp. 2969–2203, 2008.
- [123] R. Hinkel et al., “Inhibition of microRNA-92a protects against ischemia/reperfusion injury in a large-animal model”, *Circulation*, vol. 128, no. 10, pp. 1066–1075, 2013.
- [124] C. Ohyagi-Hara et al., “MiR-92a inhibits peritoneal dissemination of ovarian cancer cells by inhibiting integrin $\alpha 5$ expression”, *Am. J. Pathol.*, vol. 182,

-
- no. 5, pp. 1876–1889, 2013.
- [125] S. E. Francis et al., “Central roles of $\alpha 5\beta 1$ integrin and fibronectin in vascular development in mouse embryos and embryoid bodies”, *Arterioscler. Thromb. Vasc. Biol.*, vol. 22, no. 6, pp. 927–933, 2002.
- [126] Y. Wang et al., “Overexpression of SIRT1 promotes high glucose-attenuated corneal epithelial wound healing via p53 regulation of the IGFBP3/IGF-1R/AKT pathway”, *Invest. Ophthalmol. Vis. Sci.*, vol. 54, no. 5, pp. 3806–3814, 2013.
- [127] W. Wu et al., “Flow-dependent regulation of Kruppel-like factor 2 is mediated by microRNA-92a”, *Circulation*, vol. 124, no. 5, pp. 633–41, 2011.
- [128] H. Liu, G. Li, W. Zhao and Y. Hu, “Inhibition of miR-92a may protect endothelial cells after acute myocardial infarction in rats: role of KLF2/4”, *Med. Sci. Monit.*, vol. 22, pp. 2451–62, Jul. 2016.
- [129] G. Zhou et al., “Endothelial Kruppel-like factor 4 protects against atherothrombosis in mice”, *J. Clin. Invest.*, vol. 122, no. 12, pp. 4727–4731, 2012.
- [130] X. Loyer et al., “Inhibition of microRNA-92a prevents endothelial dysfunction and atherosclerosis in mice”, *Circ. Res.*, vol. 114, no. 3, pp. 434–43, 2013.
- [131] R. D. Rudic et al., “Direct evidence for the importance of endothelium-derived nitric oxide in vascular remodeling”, *J. Clin. Invest.*, vol. 101, no. 4, pp. 731–736, 1998.
- [132] E. Van Rooij, “The art of MicroRNA research”, *Circ. Res.*, vol. 108, no. 2, pp. 219–234, 2011.
- [133] C. A. Stein et al., “Efficient gene silencing by delivery of locked nucleic acid antisense oligonucleotides, unassisted by transfection reagents”, *Nucleic Acids Res.*, vol. 38, no. 1, pp. 1–8, 2009.
- [134] J. Elmén et al., “LNA-mediated microRNA silencing in non-human primates”, *Nature*, vol. 452, no. 7189, pp. 896–899, Apr. 2008.
- [135] R. E. Lanford et al., “Therapeutic silencing of microRNA-122 in primates

-
- with chronic hepatitis C virus infection”, *Science*, vol. 327, no. 5962, pp. 198–201, Jan. 2010.
- [136] J. Krützfeldt et al., “Silencing of microRNAs in vivo with ‘antagomirs’”, *Nature*, vol. 438, no. 7068, pp. 685–689, Dec. 2005.
- [137] H. L. A. Janssen et al., “Treatment of HCV infection by targeting microRNA”, *N. Engl. J. Med.*, vol. 368, no. 18, pp. 1685–1694, 2013.
- [138] M. E. Visser et al., “Antisense oligonucleotides for the treatment of dyslipidaemia”, *Eur. Heart J.*, vol. 33, no. 12, pp. 1451–1458, 2012.
- [139] M. Feola and L. Wiener, “A method of coronary retroperfusion for the treatment of acute myocardial ischemia”, *Cardiovasc Dis*, vol. 5, no. 3, pp. 235–243, 1978.
- [140] P. Raake et al., “Myocardial gene transfer by selective pressure-regulated retroinfusion of coronary veins: comparison with surgical and percutaneous intramyocardial gene delivery”, *JACC*, vol. 44, no. 5, pp. 1124–1129, Sep. 2004.
- [141] R. Hinkel and C. Kupatt, “Selective pressure-regulated retroinfusion for gene therapy application in ischemic heart disease”, Humana Press, New York, NY, pp. 249–260, 2017.
- [142] P. Boekstegers et al., “Preservation of regional myocardial function and myocardial oxygen tension during acute ischemia in pigs: comparison of selective synchronized suction and retroinfusion of coronary veins to synchronized coronary venous retroperfusion”, *JACC*, vol. 23, no. 2, pp. 459–469, Feb. 1994.
- [143] P. Boekstegers et al., “Selective suction and pressure-regulated retroinfusion: An effective and safe approach to retrograde protection against myocardial ischemia in patients undergoing normal and high risk percutaneous transluminal coronary angioplasty”, *JACC*, vol. 31, no. 7, pp. 1525–1533, 1998.
- [144] P. Boekstegers et al., “Myocardial gene transfer by selective pressure-regulated retroinfusion of coronary veins”, *Gene Ther.*, vol. 7, no. 3, pp. 232–40, 2000.

-
- [145] C. Kupatt et al., “Retroinfusion of embryonic endothelial progenitor cells attenuates ischemia-reperfusion injury in pigs: role of phosphatidylinositol 3-kinase/AKT kinase”, *Circulation*, vol. 112, no. 9, pp. 117–123, 2005.
- [146] G. Hasenfuß et al., “Herzinsuffizienz Leitlinien für die Diagnose und Behandlung der akuten und chronischen Herzinsuffizienz”, *Eur. Heart J.*, vol. 33, no. 14, pp. 1787–847, 2013.
- [147] G. W. P. House and B. L. Segal, “Left ventricular end-diastolic pressure in evaluating left ventricular function”, *Clin. Cardiol.*, vol. 33, pp. 28–33, 1981.
- [148] R. F. Mould, “Pierre Curie, 1859-1906”, *Curr. Oncol.*, vol. 14, no. 2, pp. 74–82, 2007.
- [149] S. Leraand and F. Kiil, “Local dimensional changes of the myocardium measured by ultrasonic technique”, *Scand. J. Clin. Lab. Invest.*, vol. 24, no. 4, pp. 361–371, 1969.
- [150] K. Rentrop, M. Cohen, H. Blanke and R. A. Phillips, “Changes in collateral channel filling immediately after controlled coronary artery occlusion by an angioplasty balloon in human subjects”, *JACC*, vol. 5, no. 3, pp. 587–592, 1985.
- [151] H.-C. Lin et al., “Histopathological assessment of inflammation and expression of inflammatory markers in patients with ketamine-induced cystitis”, *Mol. Med. Rep.*, vol. 11, no. 4, pp. 2421–8, Apr. 2015.
- [152] M. Gyöngyösi et al., “Myocardial fibrosis: biomedical research from bench to bedside”, *Eur. J. Heart Fail.*, vol. 19, no. 2, pp. 177–191, Feb. 2017.
- [153] J. Asbun and F. J. Villarreal, “The pathogenesis of myocardial fibrosis in the setting of diabetic cardiomyopathy”, *JACC*, vol. 47, no. 4, pp. 693–700, 2006.
- [154] M. Mulisch and U. Welsch, “Romeis - Mikroskopische Technik”, *Spektrum*, vol. 18, 2010.
- [155] S. L. Puhl, “The effect of adenosine-A1-receptor activation and endurance training on cardiac remodeling”, dissertation, p. 75, Universität des Saarlandes, 2012.

-
- [156] S. Lakshmikanthan et al., “Rap1 promotes VEGFR2 activation and angiogenesis by a mechanism involving integrin $\alpha v\beta_3$ ”, *Blood*, vol. 118, no. 7, pp. 2015–26, Aug. 2011.
- [157] B. P. Eliceiri and D. A. Cheresh, “The role of alphav integrins during angiogenesis”, *Mol. Med.*, vol. 4, no. 12, pp. 741–50, Dec. 1998.
- [158] A. Bonauer, “Die Bedeutung von microRNAs für die Funktion von Endothelzellen”, dissertation, Goethe Universität, Frankfurt, 2008.
- [159] M. E. S. Almeida et al., “Hyperglycemia reduces integrin subunits alpha v and alpha 5 on the surface of dermal fibroblasts contributing to deficient migration”, *Mol. Cell. Biochem.*, vol. 421, no. 1–2, pp. 19–28, Oct. 2016.
- [160] T. Lucas et al., “Light-inducible antimicroRNA-92a as a therapeutic strategy to promote skin repair in healing-impaired diabetic mice”, *Nat. Commun.*, vol. 8, no. May, 2017.
- [161] S. Ahmad et al., “Direct evidence for endothelial vascular endothelial growth factor receptor-1 function in nitric oxide-mediated angiogenesis”, *Circ. Res.*, vol. 99, no. 7, pp. 715–22, Sep. 2006.
- [162] C. Kupatt et al., “Endothelial nitric oxide synthase overexpression provides a functionally relevant angiogenic switch in hibernating pig myocardium”, *JACC*, vol. 49, no. 14, pp. 1575-1584, 2007
- [163] H. Y. Lee et al., “Krüppel-like factor 2 suppression by high glucose as a possible mechanism of diabetic vasculopathy”, *Korean Circ. J.*, vol. 42, no. 4, pp. 239–245, 2012.
- [164] N. Wang et al., “Shear stress regulation of Krüppel-like factor 2 expression is flow pattern-specific”, *Biochem. Biophys. Res. Commun.*, vol. 341, no. 4, pp. 1244–1251, Mar. 2006.
- [165] L. Nayak, Z. Lin and M. K. Jain, “‘Go with the flow’: how Krüppel-like factor 2 regulates the vasoprotective effects of shear stress”, *Antioxid. Redox Signal.*, vol. 15, no. 5, pp. 1449–61, 2011.
- [166] J. Amin, M. Sharif and M. Yasmin, “A review on recent developments for detection of diabetic retinopathy”, *Scientifica*, vol. 2016, p. 6838976, 2016.

-
- [167] H. S. Lim, G. Y. Lip and A. D. Blann, “Angiopoietin-1 and angiopoietin-2 in diabetes mellitus: relationship to VEGF, glycaemic control, endothelial damage/dysfunction and atherosclerosis”, *Atherosclerosis*, vol. 180, no. 1, pp. 113–118, May 2005.
- [168] T. A. J. Mckinnon et al., “Von Willebrand factor binds to the endothelial growth factor angiopoietin-2 both within endothelial cells and upon release from weibel palade bodies”, *Blood*, vol. 118, no. 21, 2011.
- [169] G. Thurston et al., “The complex role of angiopoietin-2 in the angiopoietin – Tie signaling pathway”, *Cold Spring Harb Perspect Med*, vol. 2, no. 9, pp. 1–14, 2013.
- [170] N. Kalinina et al., “MiR-92a regulates angiogenic activity of adipose-derived mesenchymal stromal cells”, *Exp. Cell Res.*, vol. 339, pp. 61–66, 2015.
- [171] C. Kupatt et al., “Embryonic endothelial progenitor cells expressing a broad range of proangiogenic and remodeling factors enhance vascularization and tissue recovery in acute and chronic ischemia”, *FASEB J.*, vol. 21, pp. 1–21, 2005.
- [172] J. Cleutjens et al., “The infarcted myocardium Simply dead tissue, or a lively target for therapeutic interventions”, *Cardiovasc. Res.*, vol. 44, no. 2, pp. 232–241, Nov. 1999.
- [173] M. Mack, “Inflammation and fibrosis”, *Matrix Biol.*, vol. 68–69, pp. 106–121, Aug. 2018.
- [174] E. E. Swayze et al., “Antisense oligonucleotides containing locked nucleic acid improve potency but cause significant hepatotoxicity in animals”, *Nucleic Acids Res.*, vol. 35, no. 2, pp. 687–700, 2007.
- [175] A. Johnson and L. A. DiPietro, “Apoptosis and angiogenesis: an evolving mechanism for fibrosis”, *FASEB J.*, vol. 27, no. 10, pp. 3893–901, Oct. 2013.
- [176] X. Luo et al., “Krüppel-like factor 4 is a regulator of proinflammatory signaling in fibroblast-like synoviocytes through increased IL-6 expression”, *Mediators Inflamm.*, vol. 2016, Jun. 2016.
- [177] C. Wahlquist et al., “Inhibition of miR-25 improves cardiac contractility in

-
- the failing heart”, *Nature*, vol. 508, no. 7497, pp. 531–535, Apr. 2014.
- [178] L. B. Nielsen et al., “Circulating levels of MicroRNA from children with newly diagnosed type 1 diabetes and healthy controls: Evidence that miR-25 associates to residual beta-cell function and glycaemic control during disease progression”, *Exp. Diabetes Res.*, vol. 2012, 2012.
- [179] P. Lee et al., “Fas pathway is a critical mediator of cardiac myocyte death and MI during ischemia-reperfusion in vivo”, *Am. J. Physiol. - Hear. Circ. Physiol.*, vol. 284, no. 2, pp. H456–H463, 2003.
- [180] J. Abdi, N. Rastgoo, L. Li, W. Chen and H. Chang, “Role of tumor suppressor p53 and micro-RNA interplay in multiple myeloma pathogenesis”, *J. Hematol. Oncol.*, vol. 10, no. 1, pp. 1–11, 2017.
- [181] V. Olive et al., “A component of the mir-17-92 polycistronic oncomir promotes oncogene-dependent apoptosis”, *Elife*, vol. 2013, no. 2, pp. 2009–2011, 2013.
- [182] B. Zhang et al., “MicroRNA-92a inhibition attenuates hypoxia/reoxygenation-induced myocardiocyte apoptosis by targeting Smad7”, *PLoS One*, vol. 9, no. 6, pp. 5–12, 2014.
- [183] V. Sequeira et al., “The physiological role of cardiac cytoskeleton and its alterations in heart failure”, *Biochim. Biophys. Acta - Biomembr.*, vol. 1838, no. 2, pp. 700–722, Feb. 2014.
- [184] H. Sashida, K. Uchida and Y. Abiko, “Changes in cardiac ultrastructure and myofibrillar proteins during ischemia in dogs, with special reference to changes in Z lines”, *J. Mol. Cell. Cardiol.*, vol. 16, no. 12, pp. 1161–1172, Dec. 1984.
- [185] M. Fujita et al., “Antagomir-92a impregnated gelatin hydrogel microsphere sheet enhances cardiac regeneration after myocardial infarction in rats”, *Regen. Ther.*, vol. 5, pp. 9–16, Dec. 2016.
- [186] M. Kruk et al., “Predictors of outcome and the lack of effect of percutaneous coronary intervention across the risk strata in patients with persistent total occlusion after myocardial infarction. Results from the OAT (occluded artery trial) study”, *JACC Cardiovasc. Interv.*, vol. 1, no. 5, pp. 511–520,

2008.

- [187] R. Desk, L. William and K. Health, “Left ventricular end-systolic volume as the major determinant of survival after recovery from myocardial infarction”, *Circulation*, vol. 76, pp. 44–51, 1987.
- [188] H. Rosenberg et al., “Malignant hyperthermia”, *Orphanet J. Rare Dis.*, vol. 2, no. 1, pp. 1–14, 2007.
- [189] J. R. Altónaga et al., “Ventricular arrhythmias and mortality associated with isoflurane and sevoflurane in a porcine model of myocardial infarction”, *J. Am. Assoc. Lab. Anim. Sci.*, vol. 50, no. 1, pp. 73–78, 2011.
- [190] A. R. Ranade et al., “MicroRNA 92a-2*: A biomarker predictive for chemoresistance and prognostic for survival in patients with small cell lung cancer”, *J. Thorac. Oncol.*, vol. 5, no. 8, pp. 1273–1278, 2010.
- [191] X. Yang et al., “MicroRNA-92a as a potential biomarker in diagnosis of colorectal cancer: A systematic review and meta-analysis”, *PLoS One*, vol. 9, no. 2, pp. 1–7, 2014.
- [192] H. Yan et al., “miRNAs as biomarkers for diagnosis of heart failure: A systematic review and meta-analysis”, *Medicine (Baltimore)*, vol. 96, no. 22, p. e6825, 2017.
- [193] X. Ji, R. et al., “Plasma miR-208 as a biomarker of myocardial injury”, *Clin. Chem.*, vol. 55, no. 11, pp. 1944–9, Nov. 2009.
- [194] J. Nader et al., “miR-92a: a novel potential biomarker of rapid aortic valve calcification” *J. Heart Valve Dis.*, vol. 26, no. 3, pp. 327–333, 2017.
- [195] S. Fichtlscherer et al., “Circulating microRNAs in patients with coronary artery disease”, *Circ. Res.*, vol. 107, no. 5, pp. 677–684, 2010.
- [196] X. Rong et al., “Serum miR-92a-3p as a new potential biomarker for diagnosis of Kawasaki disease with coronary artery lesions”, *J. Cardiovasc. Transl. Res.*, vol. 10, no. 1, pp. 1–8, 2017.
- [197] E. Ding et al., “MiR-92a and miR-486 are potential diagnostic biomarkers for mercury poisoning and jointly sustain NF- κ B activity in mercury toxicity”, *Sci. Rep.*, vol. 7, no. 1, p. 15980, Dec. 2017.

-
- [198] Maha Abdellatif, “The role of miR-133 in cardiac hypertrophy uncovered”, *Cardiovasc. Res.*, vol. 106, no. 1, pp. 16–18, 2011.
- [199] T. Seeger et al., “Long-Term inhibition of miR-21 leads to reduction of obesity in db/db mice”, *Obesity*, vol. 22, no. 11, pp. 2352–2360, 2014.
- [200] S. H. Najafi-Shoushtari et al., “MicroRNA-33 and the SREBP host genes cooperate to control cholesterol homeostasis”, *Science*, vol. 328, no. 5985, pp. 1566–1569, Jun. 2010.
- [201] K. J. Rayner et al., “MiR-33 contributes to the regulation of cholesterol homeostasis”, *Science*, vol. 328, no. 5985, pp. 1570–3, Jun. 2010.
- [202] D. S. Karolina et al., “MiR-25 and miR-92a regulate insulin biosynthesis in rats”, *RNA Biol.*, vol. 10, no. 8, pp. 1365–1378, 2013.
- [203] C. Piot et al., “Effect of cyclosporine on reperfusion injury in acute myocardial infarction”, *N. Engl. J. Med.*, vol. 359, no. 5, pp. 473–481, Jul. 2008.
- [204] T.-T. Cung et al., “Cyclosporine before PCI in patients with acute myocardial infarction”, *N. Engl. J. Med.*, vol. 373, no. 11, pp. 1021–1031, Sep. 2015.
- [205] R. Hinkel, T. Trenkwalder and C. Kupatt, “Molecular and cellular mechanisms of thymosin β 4-mediated cardioprotection”, *Ann. N. Y. Acad. Sci.*, vol. 1269, no. 1, pp. 102–109, 2012.
- [206] W. Xiao et al., “Impact of neutralizing antibodies against AAV is a key consideration in gene transfer to nonhuman primates”, *Nat. Med.*, vol. 24, 2018.
- [207] R. Titze-de-Almeida et al., “The race of 10 synthetic RNAi-based drugs to the pharmaceutical market”, *Pharm. Res.*, vol. 34, no. 7, pp. 1339–1363, 2017.
- [208] J. B. Strait and E. G. Lakatta, “Aging-associated cardiovascular changes and their relationship to heart failure”, *Heart Fail. Clin.*, vol. 8, no. 1, pp. 143–164, 2012.
- [209] B. J. Haubner, T. Schuetz and J. M. Penninger, “Cardiac regeneration in a newborn: what does this mean for future cardiac repair research?”, *Expert*

-
- Rev. Cardiovasc. Ther., vol. 16, no. 3, pp. 155–157, 2018.
- [210] W. P. Vermeij et al., “Restricted diet delays accelerated ageing and genomic stress in DNA-repair-deficient mice”, *Nature*, vol. 537, no. 7620, pp. 427–431, 2016.
- [211] G. Spinetti et al., “Diabetes and vessel wall remodelling: From mechanistic insights to regenerative therapies”, *Cardiovasc. Res.*, vol. 78, no. 2, pp. 265–273, 2008.
- [212] E. Hedström et al., “Infarct evolution in man studied in patients with first-time coronary occlusion in comparison to different species - implications for assessment of myocardial salvage”, *J. Cardiovasc. Magn. Reson.*, vol. 11, no. 1, p. 38, Sep. 2009.
- [213] C. R. Mandel, “Untersuchungen zum Einfluss von Erythropoietin auf die myokardiale Funktion des ischämischen Schweineherzens”, dissertation, LMU, Munich, 2005.

X. ACKNOWLEDGEMENT

I would like to thank Univ.-Prof. Dr. Eckhard Wolf for being my veterinary supervisor and for accepting this external thesis at the veterinary faculty and further for providing us with the diabetic transgenic pig line.

I would like to express my sincere thanks to Prof. Dr. Rabea Hinkel for being my mentor and supervisor. Throughout the period I spent working on this thesis, she was supporting me and advising me with her profound experience and expertise. I have greatly benefited from her surgical skills. Thanks to her, I have had the opportunity to realize this work. Thank you for being a patient, encouraging and illuminating supervisor.

Next, I have had the support of Prof. Dr. Christian Kupatt during the work in his group at the Klinikum rechts der Isar. Being a reputable scientist, his advice and suggestions have always been illuminating and expedient. Thanks for being my mentor.

The people in Prof. Kupatt's group have encouraged me during my time as a doctoral candidate in the lab. I would like to thank Dr. Andrea Bähr, Dr. Tarik Bozoglu, Dr. Tilman Ziegler, Farah Abdel Rahman, Anja Wolf, Konstantin Tsekos and Morad Asadi for being loyal and supportive coworkers. I would like to emphasize my gratefulness for Dr. Andrea Bähr's support during most of the surgeries and Anja Wolf's expert help on the cell culture experiments. It was great sharing the laboratory with all of you.

I would like to thank Univ.-Prof. Dr. Karl-Ludwig Laugwitz and Prof. Dr. Alessandra Moretti for giving me the opportunity to work in their department and to use their lab devices.

I am deeply grateful for my parents and sister for always supporting me. They have always been there for me, supporting me in the best possible way through moral and emotional encouragement. Without them, completion of this thesis would not have been possible. Thank you for being in my life!

I can no other answer make, but, thanks, and thanks.

(William Shakespeare)